ROYAUME DU MAROC
Université Mohammed V - RABAT -
جامعة محمد الخامس – الرباط –
Faculté des sciences
كلية العلوم

DOCTORAL STUDIES CENTER- SCIENCE AND TECHNOLOGY

Order N° : 3715

THESIS

In order to obtain the **: *DOCTORATE***

Research structure **:** High Energy Physics-Modeling and Simulation Team
Discipline **:** Physics
Speciality **:** Medical Physics

Presented and defended on 03/12/2022 by :

Sanae DOUAMA

Medical physics surveys in Morocco
Establishment of diagnostic reference levels
Study of breast cancer screening optimization parameters
Optimization of IMRT treatment techniques

Jury

Abdelkader BOULEZHAR	PES, Hassan II University, Faculty of Sciences, Ain Chock, Casablanca	President
Lalla Btissam DRISSI	PES, Mohammed V University, Faculty of Sciences, Rabat	Reporter/Examiner
Youssef ELMERABET	PES, Ibn Tofail University, Faculty of Sciences, Kenitra	Reporter/Examiner
Mohammed CHERRAJ	PH, Mohammed V University, Faculty of Sciences, Rabat	Reporter/Examiner
Wissal IRAQI HOUSSAINI	PH, Regional Center for Education and Training Professions, Meknes	Reporter/Examiner
Farida BENTAYEB	PES, Mohammed V University, Faculty of Sciences, Rabat	Invited
Mina OUAHMAN	PH, Mohammed V University, Faculty of Sciences, Rabat	Invited
Youssef BOUZEKRAOUI	PA, Hassan I University, Higher Institute of Health Sciences, Settat	Invited
Rachid AHL LAAMARA	PH, Mohammed V University, Faculty of Sciences, Rabat	Supervisor

Year : 2021-2022

Dedication

I dedicate this milestone in my life to the memory of my deceased parents. I hope that, from the world that is theirs now, they appreciate this humble gesture as a sign of gratitude from one of their daughters who has always prayed for the salvation of their souls. May Almighty God have them in his holy mercy!.

Acknowledgements

I am deeply thankful to God, the Almighty, for giving me the audacity to overcome all the difficulties and for having the goodness to surround me with great people who have, each in their own way, and at different stages of my journey (life), contributed in one way or another to the realization of my doctoral thesis.

The work presented in this thesis was carried out in the High Energy Physics, Modeling and Simulation Laboratory **(LPHE-MS)**; of the physics department of the **Faculty of Sciences of Rabat.**

I extend my sincere thanks to **Mr. El Hassan Saidi, Professor** of Higher Education, Director of this Research structure who gave me the opportunity to do my thesis in their laboratory.
A thank you is not enough to show you all my gratitude.

A part of this work is done in the frame by the research project **(RASQUAM)**; "Radiology as a Steward for Quality in Moroccan HealthCare"; between The Flemish Interuniversity Council (VLIR-UOS) and **KU Leuven University** and **Mohammed V University of Rabat**. The authors extend their sincere thanks to VLIR-UOS for its support, to **Professor Hilde Bosmans** and her research team as well as **Dr. Lesley Cockmartin** for their scientific endorsement, their collaboration and encouragement.

At the time of presenting this work, I appreciate the support and assistance I have received in the accomplishment of my task, without which many obstacles would have been insurmountable. I am deeply grateful to all those who have helped and supported me.

First I would like to thank very much **Mr. Rachid Ahl Laamara, Professor** of Higher Education at the Faculty of Sciences, Rabat for his supervision, his encouragement, his many advices and his unfailing support. Receive Professor my great thanks.

I would like to thank **Mr Abdelkader Boulezhar, Professor** of Higher Education at the Faculty of Sciences Ain Chock, Casablanca, who honored me by being the president of my thesis Jury. Please accept, Sir, the assurance of my deep respect.

I would like to express my grateful thanks to **Mrs. Farida Bentayeb, Professor** of Higher Education at the Faculty of Sciences of Rabat, for the confidence she has given me since my first steps in a dynamic and friendly group, until the writing of this manuscript and also for having directed this thesis and for having allowed me to carry it out in the best conditions. I thank her for all the patience and the availability that she has shown to me. For her invaluable help, her fruitful ideas, her patience and her perseverance in the follow-up of my work and her precious advice and also for being always there to encourage and support me. A thank you is not enough to show you all my gratitude.

I would like to thank **Mrs. Lalla Btissam Drissi, Professor** of Higher Education at the Faculty of Sciences of Rabat, for the interest she has shown in this research work by committing to being a reporter and for agreeing to judge this work as an examiner. May she find here the testimony of my sincere thanks.

Also, I would like to thank **Mr. Mr Mohammed Cherraj, Professor** of Higher Education at the Faculty of Sciences of Rabat, for the honor of being a member of the jury and who was kind enough to be a reporter and to have agreed to judge this work as a reviewer. I'm extremely grateful to him for the interest he has shown in this research work by committing to be a reporter and for agreeing to judge this work as an examiner. May he find here the testimony of my heartfelt thanks.

I would like to thank **Mrs. Wissal Iraqi Houssaini, Professor** at Regional Center for Education and Training Professions, Meknes, for the interest she has shown in this research work by committing to be a reporter and for agreeing to judge this work as an examiner. Let her find here the expression of my deep consideration.

I would like to thank **Mr Youssef ELMERABET, Professor** at the Kenitra Faculty of Science, who was kind enough to be a reporter and for agreeing to judge this work as an examiner. Please accept, Sir, the assurance of my deep respect

I would also like to thank **Mrs Mina Ouahman, Professor** at the Faculty of Sciences of Rabat, who was kind enough to continue and co-supervise the work that I undertook with Professor Bentayeb. I thank Professor Ouahman for her help, her availability. Rest assured, Professor, of my deepest gratitude.

I would like to thank **Mr. Youssef Bouzekraaoui, Professor** at Higher Institute of Health de Settat, for his invaluable help and the fruitful discussions which permitted me to improve my work. I also thank him for his availability and his scientific support.

I would like to thank **Dr. Moulay Ali Youssoufi** and **Mr. Bougtib**, members of the medical physics team, for encouraging me and giving me the necessary help to develop and improve my work. I am very grateful to them.

A big thank you to the team of medical physics under the direction of Professor Farida Bentayeb for their coordination, help and discussion and for the spirit of teamwork which was very important to succeed in the work in this field.
I also wish to thank all the members of the Laboratory of High Energy Physics-Modeling and Simulation, professors, researchers, doctors and doctoral students with whom I had the chance to work, discuss and exchange scientific knowledge.

Thank you to my extended family, thank you for your continued support and assistance. Thank you for having made me want to go always further... my sincere thanks to my husband **Lahoucine Zaama**, you have always been there for me, thank you is not enough to show you all my gratitude.

LISTE OF TABLES

LISTE OF FIGURES

List of Abbreviations

AAA	Analytical Anisotropic Algorithm
AEC	Automatic Exposure Control
ALARA	As Low As Reasonnably Achievable
AP	Anterior Posterior
BSF	Backscattering Factor
BVD	Breast Volume Density
CC	Cranio-Caudal
CBT	Compressed Breast Thickness
CRT	Conformal Radiation Therapy
CT	Computed Tomography
CTV	Clinical Target Volume
DD	Dose Difference
DICOM	Digital Imaging and Communications in Medicine
DRLs	Diagnostic Reference Levels
DRR	Digitally Reconstructed Radiographs
DTA	Distance-to-Tolerance Criteria
DTC	Differentiated Thyroid Carcinomas
ED	Effective Dose
EPID	Electronic Portal Imaging Device
ESD	Entrance Skin Dose
EU RP	European Radiation Protection
FSD	Focus Skin Distance
GTV	Gross Tumor Volume
HN	Head and Neck
IAEA	The International Atomic Energy Agency
ICRP	International Commission on Radiological Protection
ICRU	International Commission on Radiation Units
IGRT	Image-Guided Radiation Therapy
IM	Internal Margin
IMRT	Intensity-Modulated Radiation Therapy
IR	Ionizing Radiation
Kc	Collisional Kerma

KERMA	Kinetic Energy Released per unit Mass
Kr	Radiative Kerma
MED	Medical Exposure Directive
MLC	Multileaf Collimator
MLO	Medio Lateral Oblique
MRI	Magnetic Resonance Imaging
NTCP	Normal Tissue Complication Probability
OAR	Organs At Risk
PA	Posterior Anterior
PET	Positron Emission Tomography
PET	Positron Emission Tomography
PSA	Prostate Specific Antigen
PTV	Planning Target Volume
QA	Quality Assurance
RASQUAM	Radiology as a Steward for Quality in Moroccan Health Care
RT	Radiotherapy treatment
SM	Setup Margin
SPECT	Single Photon Emission Computed Tomography
TCP	Tumour Control Probability
TPS	Treatment Planning Software
UK	United Kingdom
USA	United States of America
VBD	Volumetric Breast Density
VDG	Volumetric Density Grade
WR	Radiation Weighting factor

Abstract

This thesis work is based on three investigations in medical physics in Morocco, in radiology, mammography and radiotherapy and is therefore divided into three main parts.

The first represents a dosimetric study whose objective is to promote quality assurance activities in conventional radiology and to prepare the deployment of a system for managing the dose received by patients in order to calculate local diagnostic reference levels (DRL). The results obtained showed a concordance with the international recommendations.

For the second part, we selected parameters from a combined analysis of breast compression, breast morphometry and volumetric breast density, in order to apply these investigations to a Moroccan population. The objective was to justify the use of international standards for our screening program, as these are not yet developed in our country. The results show a correlation between compression force and breast density. Volumetric breast density (VBD) decreased with compressed breast thickness (CBT) and age. The overall analysis and the comparison of the mammographic parameters showed a good similarity between the Moroccan population and the population of previous studies.

In the third part, we investigated dose verification as a quality assurance (QA) performance measure of conventional intensity-modulated radiotherapy (IMRT) technique. Comparison between 2D and 3D of the dose delivered and planned for a complex geometry was considered. Ten complex intensity-modulated radiotherapy (IMRT) plans (80 beams) for two different pathologies were calculated using the Eclipse Treatment Planning System (TPS). We also estimated the planning target volume (PTV) margins of error, for the same intensity-modulated radiotherapy (IMRT) treatment technique and for two different locations using electronic portal imaging (EPID) device. This study was conducted to assess setup errors for IMRT-treated patients and to determine the specific optimal PTV margin. Configuration data were collected from 40 IMRT-treated patients, 20 head and neck (HN) cancer patients, and 20 prostate cancer patients.

Keywords: Dose, Radiology, X-ray, DRL, Digital Mammography, Volumetric Breast Density, Compression Force, Gamma Index, Octavius 4D, IMRT, QA.

Résumé

Ce travail de thèse est basé sur trois investigations en physique médicale au Maroc, dans les domaines de radiologie, mammographie et radiothérapie et est par conséquent divisé en trois parties principales.

La première représente une étude dosimétrique dont l'objectif est de promouvoir les activités d'assurance qualité en radiologie conventionnelle et pour préparer le déploiement d'un système de gestion de la dose reçue par les patients dans le but de calculer les niveaux de référence diagnostiques (NRD) locaux. Les résultats obtenus ont montré une concordance des valeurs NRD avec les recommandations internationales.

Pour la deuxième partie, nous avons sélectionné des paramètres issus d'une analyse combinée de la compression mammaire, de la morphométrie mammaire et de la densité mammaire volumétrique, afin d'appliquer ces investigations sur une population marocaine. L'objectif était de justifier l'utilisation de normes internationales pour notre programme de dépistage, celles-ci n'étant pas encore développées dans notre pays. Les résultats montrent une corrélation entre la force de compression et la densité mammaire. La densité mammaire volumétrique (DMV) a diminué avec l'épaisseur mammaire comprimée (EMC) et l'âge. L'analyse globale et la comparaison des paramètres mammographiques ont montré une bonne similitude entre la population marocaine et la population des études précédentes.

Et dans la troisième partie, nous avons étudié la vérification de la dose comme mesure de performance de l'assurance qualité (AQ) de la radiothérapie conformationnelle à modulation d'intensité (RCMI). En effectuant une comparaison entre 2D et 3D de la dose délivrée et planifiée pour une géométrie complexe. Dix plans complexes de radiothérapie à modulation d'intensité (RCMI) (80 faisceaux) pour deux pathologies différentes ont été calculés à l'aide du système de planification du traitement Eclipse (SPT). Et nous avons également estimé les marges d'erreur du volume cible de planification (VCP), pour la même technique de traitement par radiothérapie à modulation d'intensité (RCMI) et pour deux localisations différentes à l'aide d'un dispositif d'imagerie portale électronique (DIPE). Cette étude a été menée pour évaluer les erreurs de configuration pour les patients traités par RCMI et pour déterminer la marge VCP optimale spécifique. Les données de configuration ont été recueillies auprès de 40 patients traités par RCMI, 20 patients pour un cancer de la tête et du cou (TC) et 20 patients pour un cancer de la prostate.

Mots clés: Dose, Radiologie, RX, NRD, Mammographie numérique, densité mammaire volumétrique, compression force, Indice gamma, Octavius 4D, RCMI, AQ.

Contents

Introduction

Medical physics is a subfield of physics that focuses on the medical applications of physics. This term "medical physics" was first used in 1779 by the Society's Permanent Secretary General, Félix Vicq d'Azil, in the journals of the Royal Society of Medicine (1748-1794). 1779 to 1794 mark the birth of medical physics. This institution, composed of both physicians and non-medical experts, produced the journal Memoirs of Medicine and Medical Physics between 1779 and 1798 [1]. This area mainly concerns medical imaging, radiotherapy, nuclear medicine and radiation protection.

For medical imaging, there are different modalities using ionizing radiation. We can cite conventional radiology, mammography and CT imaging, which used ionizing radiation. In nuclear medicine, PET (Positron Emission Tomography) and SPECT (single photon emission computed tomography) incorporate a radioactive tracer which is injected into the patient before the exam. Scintigraphy is based on the disintegration of radioactive tracers. We can also mention MRI which is based on magnetic radiation and ultrasound systems based on ultrasound radiation.

Radiation therapy is a treatment that uses much higher doses of radiation than radiology to kill cancer cells and shrink tumours.There are two types of radiotherapy: internal and external. In the internal therapy, the radiation is provided from radioactive source placed in close proximity to the tumor. External radiotherapy treatment is founded on irradiating the tumor with external particle beams (photons, electrons, or ions, …)

The use of ionizing radiation must comply with the guidelines of international regulations Rdiation protection relies on national and international regulations, established on three fundamental principles: justification, optimization and dose limitation. These principles represent recommendations of the International Commission on Radiation Protection (ICRP).

Ionizing radiation (IR) is widely used, in radiology. Despite its medical benefits for diagnosis, they can carry induced risks and harmful effects, leading thus to certain types of cancers. For this, great vigilance must be taken into account regarding the use of this kind of radiation. This implies that measures to optimize radiological parameters and practices are necessary.

In this sense, a radiological investigations must be carried out with the aim of establishing the local diagnostic reference levels (DRL) for optimization. The general principle of ALARA radiation protection states that exposures should be kept as low as reasonably achievable by

reducing doses to patients and workers [2].

In this work, we shall concentrate on conventional radiology, mammography and radiotherapy, and we will highlight accomplishments in these three domains. In addition, our contributions as nuclear imaging studies are mentioned in the appendix to this document

Among the main objectives of the present work:

* To estimate the dose to patients in order to establish local DRLs in standard radiology. In this context, patient dose measurement campaigns were considered as the best first initiative to promote quality assurance activities in conventional radiology and to prepare for the deployment of a patient dose management system with the aim of calculating local (DRLs) in order to ensuring their adoption in national legislation and regulations concerning radiation protection.

*The glandular tissue of the breast being very radiosensitive, the study of the various parameters permitting the optimization of the administered dose were explored. It is important to exert a compressive force on the breast in order to spread the gland, reduce the thickness of the breast and thus obtain a better image of the interior of the breast.

* The main goal of radiotherapy is to deliver an adequate dose to the tumour, making it possible to block its ability to multiply while minimizing the dose delivered to surrounding healthy tissue. To meet these requirements, two optimization methods were considered: estimating of the margin error at therapeutic volumes on the one hand and and studying of the quality of IMRT treatment plans using the analysis and comparison of the γ index.

This work is composed of three chapters organized as follows: In the first chapter, we introduce the fundamental ideas of conventional radiology by stating certain radiation isotopes, the concept of dose, radiation exposure, kerma, absorbed dose, equivalent dose, effective dose, effective dose limitations, and x-ray generation.

The second chapter presents the mammography notions by giving an anatomy of the breast by defining their tissue composition. All this makes it possible to understand the objective of mammography on the visualization of these tissues in order to improve resolution and contrast with a dose as low as reasonably achievable (ALARA principle). Dedicated equipment uses automatic exposure control (AEC) mode. The latter represents an important feature that allows for consistently optimal image exposure despite variations in tissue density and thickness and the skill level of the user. Breast compression is an important parameter in mammography and must be carefully explained to the patient whose cooperation is sought.

The third chapter discusses the fundamental concepts of radiotherapy by defining external

radiotherapy and identifying target volume delimitation by citing different target volumes in radiotherapy including (Gross Tumor Volume (GTV), Clinical Target Volume (CTV), Planning Target Volume (PTV), and Organs at Risk (OAR)). Consequently, throughout this chapter, we address the treatment path, representing diagnosis, prescription, planning, verification, therapy, and post-treatment follow-up.

The fourth chapter contains our published contributions in medical physics. The first article is devoted to the collection and evaluation of the doses delivered to patients. The optimization approach is implemented through a detailed data analysis, leading thus to the establishment of local DRLs, for five exposures most commonly used in conventional radiology.

In the second article, parameters resulting from a combined analysis of breast compression, breast morphometry and volumetric breast density were selected, in order to apply these investigations to a Moroccan population at the start of new breast cancer screening. breast. The objective was to justify the use of international standards for our screening program, as these are not yet developed in our country. The results show a correlation between compression force and breast density. Volumetric breast density (VBD) decreases with compressed breast thickness (CBT) and age. The overall analysis and the comparison of the mammographic parameters showed a good similarity between the Moroccan population and the population of previous studies.

The third article investigated dose verification as a quality assurance (QA) performance measure of conventional intensity-modulated radiotherapy (IMRT), comparing the 2D and 3D techniques of the dose delivered and planned for a complex geometry. Ten complex intensity-modulated radiotherapy (IMRT) plans (80 beams) for two different pathologies were calculated using the Eclipse Treatment Planning System (TPS). And we also estimated the planning target volume (PTV) margins of error, for the same intensity-modulated radiotherapy (IMRT) treatment technique and for two different locations using a device. electronic portal imaging (EPID). This study was conducted to assess setup errors for IMRT-treated patients and to determine the specific optimal PTV margin. Configuration data were collected from 40 IMRT-treated patients, 20 head and neck (HN) cancer patients, and 20 prostate cancer patients.

Chapter I

Radiodiagnostic dosimetry

Chapter I: Radiodiagnostic dosimetry

I.1. Radiation sources

People are regularly exposed to natural background radiation as well as human-made radiation on a regular basis. Natural radioactivity originates through numerous sources naturally-occurring radioactive isotopes present in soil, water and air. Radon, a naturally-occurring gas, emerges from rock and soil is the principal source of naturally occurring radiation that people inhale via air, food and drink [3].

The production of nuclear power and the use of radiation in medicine for diagnosis and treatment are both examples of human-made sources that contribute to the radiation that people are exposed to. Medical equipment, such as X-ray machines, is currently the source of ionizing radiation that occurs most frequently as a result of human activity.

I.2. Non-ionizing radiation

Non-ionizing radiation does not have enough energy to produce charged ions when passing through matter. Near ultraviolet rays, visible light, infrared radiation, microwaves and radio waves are examples of non-ionizing radiation.. The lower the frequency, the less energy the waves carry. Most of our daily radiation (radio, mobile phone, microwave, etc.) is non-ionizing. [3] .

Non-ionizing radiation exists in various forms in our environment and in our workplace. They include, for example, electromagnetic fields from power lines (high voltage lines, railways, transformers, induction, etc.), electromagnetic radiation from mobile telephony and radio communication, as well as static magnetic fields magnetic resonance (MRI, etc.). The propagation properties of RNIs and their effects on humans vary with frequency.

I.3. Ionizing radiation

Non-ionizing radiation does not cause atomic changes, while ionizing radiation causes them. Ionizing radiation is what we're talking about though in the present work.

These radiations have sufficient energy to transform the atoms they cross into ions, that is to say remove one or more electrons from its atoms. we are talking here about X-rays, gamma rays, alpha particles, beta particles and neutrons. Radiation falls into two categories: directly ionizing radiation, consisting of charged particles (α and β radiation) and indirectly ionizing

radiation: these are electromagnetic radiation (γ and X) and neutrons [4].

Minimal quantities of ionizing radiation remain present in the surroundings at any and all times, exposing individuals to harm. Some medical practices and other activities may also expose people to radioisotopes. Exposure to ionizing radiation above safe limits has been linked to an increased risk of cancer and other genetic disorders. While a result, people shoul be carefully controled as they consume radiation dose.

Ionizing radiation is regulated by a variety of international commissions, whose responsibilities include the obligation to safeguard the wider public and employees from becoming exposed to this type of radiation.

The utilization of radiation for medical purposes estimated to account for 98% of the average dose contributions from artificial sources and 20 percent respectively of the overall population exposure. Somewhere around 3,600 million clinical radiological diagnostic tests, 37 million nuclear medicine operations, and 7.5 million radiotherapy treatments are conducted annually on a global scale [5]. Despite the source, these various types of radiation (alpha, beta, photons, and neutrons) seem to be able to penetrate the body to differing degrees (Figure I.4) and delivering a radiation dose.

I.3.1. X-Radiation

X-radiations are electromagnetic radiation (photons) such as radio waves, visible light or infrared. Their wavelengths are approximately between 0,001 nanometer (nm) and 10 nanometer, corresponding to frequencies ($\lambda=c/f=c*T$) from 3.10^{16} Hz to 3.10^{20} Hz. The energy of these photons varies from a hundred ev (electron-volt) to approximately one MeV [6].

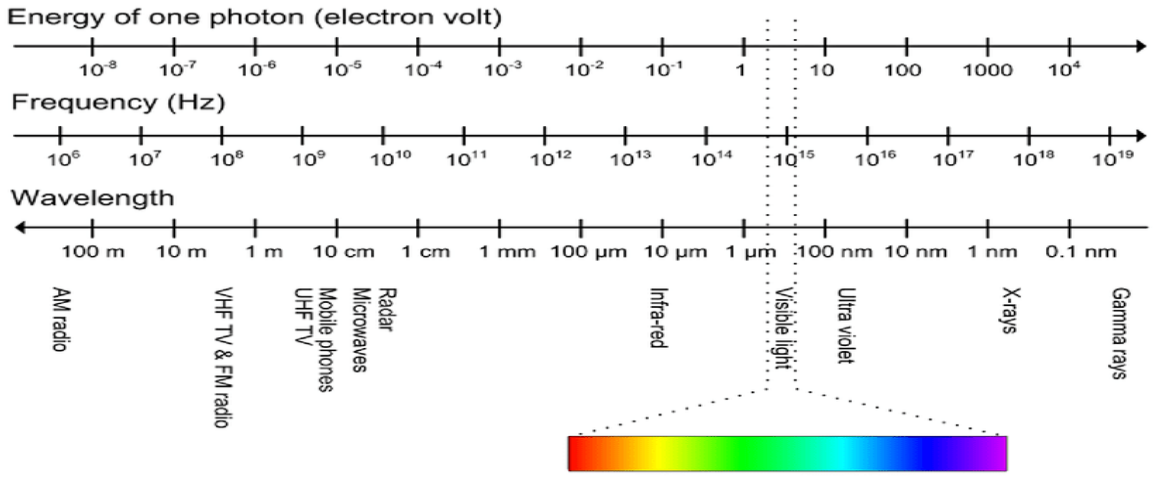

Figure I. 1. Electromagnetic spectrum showing the energy of one photon, the frequency, and wavelength [7].

X-rays can be absorbed by the matter they pass through : they are so attenuated.This property is very important because it is the basis of medical imaging using X-rays.

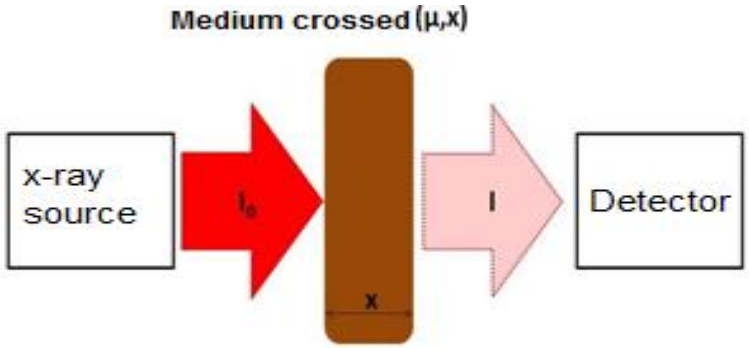

Figure I. 2. X-Ray transmission

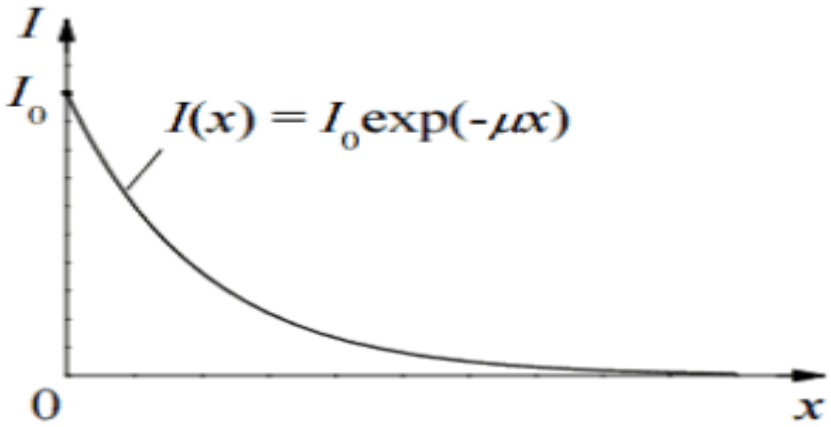

Figure I. 3. Dependence of x-radiation intensity on absorber thickness [8].

I0 and I represent respectively the intensity of the incident beam and of the transmitted beam. x is the thickness of the medium crossed μ is the linear attenuation coefficient of the medium The attenuation coefficient μ depends on the chemical composition tissues crossed. It is high for bone, medium for soft tissue, and low for fat. Bones contain salts minerals (phosphorus, calcium, magnesium) which are elements with a higher atomic number than the main constituents of soft tissues (oxygen, carbon, hydrogen, nitrogen, etc.). Consequently, their density is higher, so they absorb more Xrays.

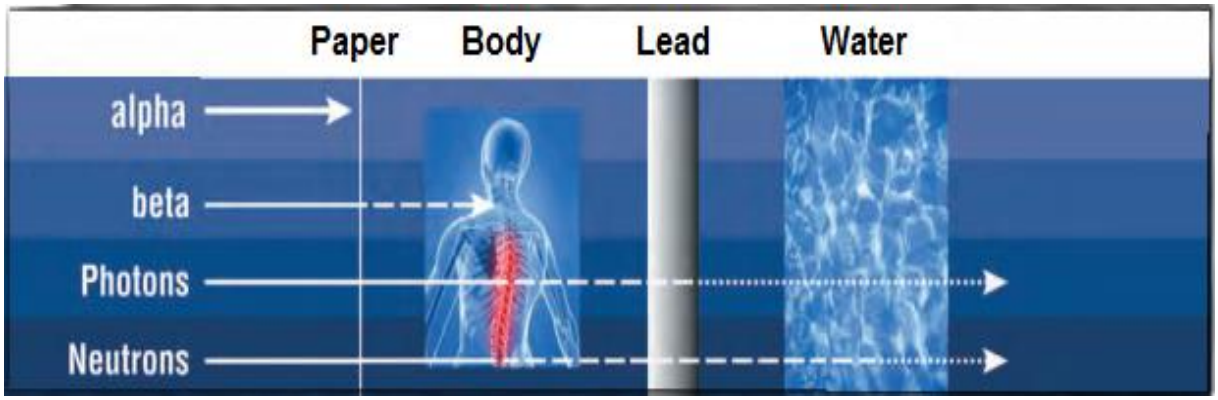

Figure I. 4. Penetration degree for different types of ionizing radiation [9]

I.3.2. X-Ray Producion

X-rays are produced in the standard way: by accelerating high-voltage electrons and allowing them to collide with a metal target selected with special specifications. X-rays are produced when electrons suddenly slow down upon hitting a metal target; These x-rays are commonly called bremsstrahlung. If the falling electrons have enough energy, they can eject an electron from the inner shell of the target metal atoms. Electrons are dropped from higher states to fill the void, by emitting X-ray photons with precise energies determined by the electron energy levels during the excitation process.

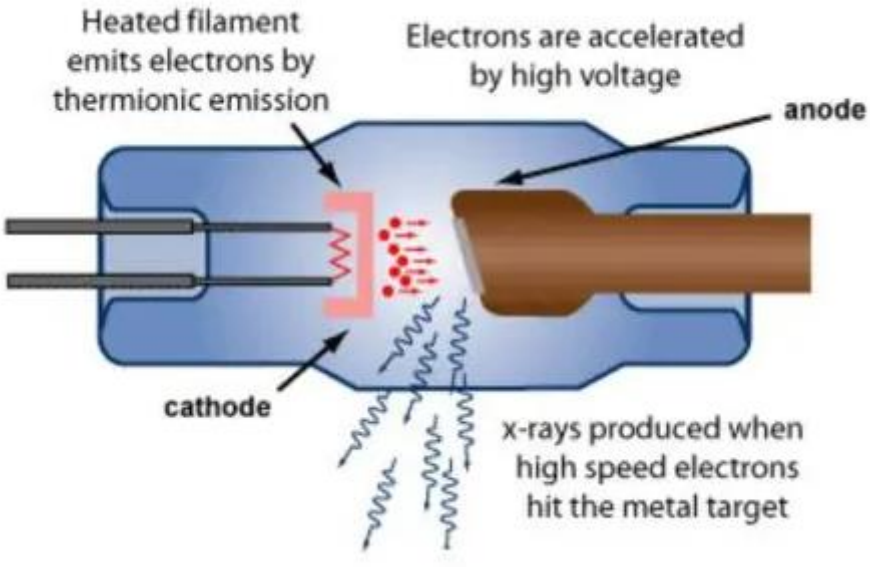

Figure I. 5. Production of X-Rays [10].

I.3.2.1. Bremsstrahlung

When the electrons of heavy elements move between lower atomic energy levels, they give

off characteristic x-rays. These x-rays can be used to identify the element. When vacancies are generated in the n=1 or K-shell of the atom and electrons drop down from above to fill the gap, a characteristic x-ray emission occurs. This emission is depicted as two sharp peaks in the picture to the left. X-rays that are created when an electron transitions from the n=2 level to the n=1 level are referred to as K-alpha x-rays, and x-rays that are produced when an electron transitions from the n=3 level to the n=1 level are referred to as K-beta x-rays.

L x-rays are the name given to transitions that occur to the n=2 shell, also known as the L-shell ((n=3→2 is L-alpha, n=4→2 is L-beta, etc.). The continuous distribution of x-rays that serves as the foundation for the two distinct peaks located on the left is referred to be "bremsstrahlung" radiation.

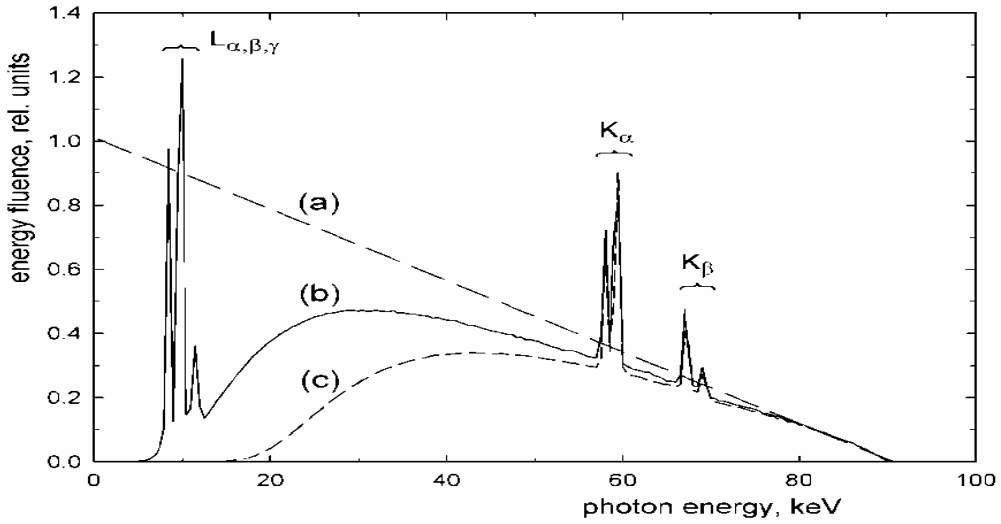

Figure I. 6. X-ray Spectrum [11].

(a) Ideal Bremsstrahlung spectrum for a tungsten anode (tube voltage 90 kV)

(b) An Actual spectrum at the beam exit port with characteristic X rays (anode angle: 20°, inherent filtration: 1 mm Be)

(c) The spectrum Filtered with an equivalent of 2.5 mm Al

I.3.2.2. Characteristic Radiation

When a fast electron collides with an atomic shell electron the electron is ejected from its orbit once KE exceeds the binding energy of the electron in that shell. The further away we are from the nucleus, the higher the binding energy for electrons in atoms, where the electrons in the K shell are as large as possible and gradually decrease for the other shells closest to the nucleus.

The scattered primary electron carries the difference in kinetic energy and binding energy of this electron in its orbit to the atom. The space in the shell is then filled with an electron from an outer shell accompanied by the emission of an X-ray photon with an energy equivalent to the difference in the binding energies of the different shells.

If a Fast Electron were to collide with an atomic shell electron, the latter may be ejected from the atomic shell if the KE of the Fast Electron was greater than the binding energy of the electron in the shell. The K shell is the region of the atom in which the binding energy is highest, and it diminishes as one moves outside (L, M, ..).

The disparity between the kinetic energy and the binding energy is carried away by the initial electron that has been scattered. The shell's vacancy is subsequently filled with an electron from an outer shell, which is followed by the emission of an X-ray photon with an energy that is comparable to the difference in the shells' respective binding energies.

X-rays differ from gamma rays in origin, as X-rays are emitted as a result of the excition of electrons from a lower energy level (closer to the nucleus) to a higher energy level (far from the nucleus).

As for gamma rays, they are emitted from the nuclei of unstable atoms in order to reach a stable state They often accompany the exit of neutrinos or alpha and beta particles (Table I.1).

Table I. 1. Characteristic Radiation

	Binding energy, keV		Energies of characteristic X rays, keV			
Element	L-shell	K-shell	Ka1	Ka2	Kb1	Kb2
W	12.10/11.54/10.21	69.53	59.32	57.98	67.24	69.07
Mo	2.87/2.63/2.52	20.00	17.48	17.37	19.61	19.97
Rh	3.41/3.15/3.00	23.22	20.22	20.07	22.72	23.17

I.4. Photoelectric effect

An incident photon ejects an electron called a photoelectron with his energy $E= h\nu$, which is ejected with a kinetic energy $Ee = h\nu - Eb$, where Eb is binding energy of ejected electron on its original electronic layer.A photon undergoes an interaction with an electron which is bound in an atom. In this interaction, the incident photon disappears completely and an energetic photoelectron is ejected by the atom from one of its bound shells.

the photoelectrons are emitted by the photoelectric effect only if the photon reaches or exceeds a treshold binding energy of the electron according to material.

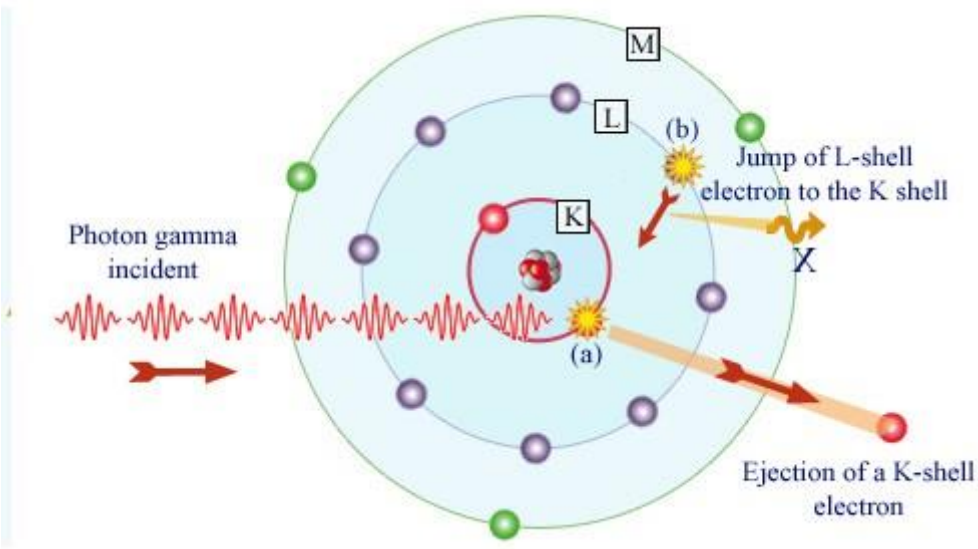

Figure I. 7. Photoelectric effect

I.5. Compton effect

The photon of frequency f collides with an electron at rest. Upon collision, the photon bounces off the electron, giving up some of its initial energy, while the electron gains momentum given by:

$$p_{\text{photon}} = \frac{E}{c} = \frac{hf}{c} = \frac{h}{\lambda}$$

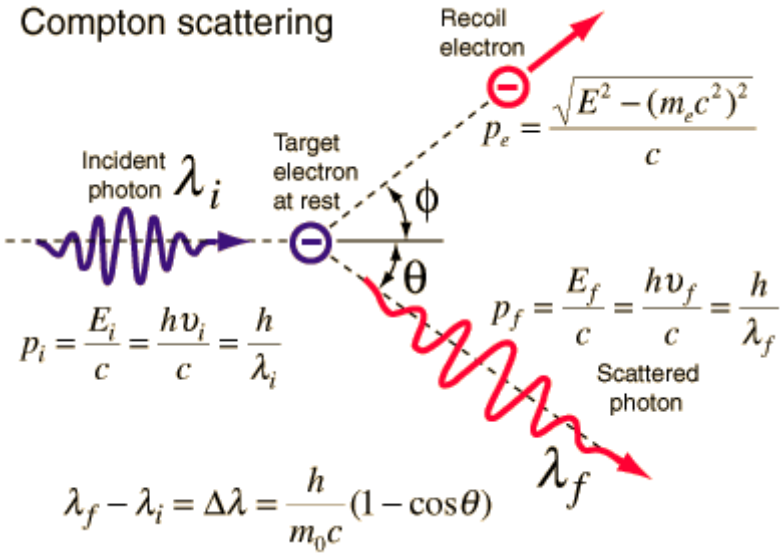

Figure I. 8. Compton effect

The incident photon is deflected by an angle Θ with respect to its original direction. This

deviation leads to a decrease in the energy of the photon. This energy must therefore result in a decrease in frequency (increase in wavelength Δ λ = λ ‘- λ). The wavelength shift increases with the scattering angle according to Compton's formula:

$$\Delta\lambda = \lambda' - \lambda = \frac{h}{m_e c}\left(1 - \cos(\theta)\right)$$

Where: λ is the initial wavelength of the photon

λ' is the wavelength after scattering,

h is Planck's constant = 6.626 x 10 -34 Js,

me is the electron rest mass (0.511 MeV)

it is the speed of light

Θ is the scattering angle.

I.6. Application of X-Ray in radiography

Radiography uses X-rays to visualize an organ or part of the body on a photosensitive detector. Its principle gives an X-ray image of the density differences of an organ. An X-ray beam produced by an X-ray tube is emitted towards the area of the human body to be examined and passes through the patient's body. As X-rays pass through matter, the detector can retain the impression and deliver the image of our internal anatomy. During an X-ray, the rays will encounter either tissues, muscles or even bones. X-rays easily pass through the body's cavities containing air, the soft tissues, but are stopped by the bones, teeth, etc. which have a higher density.

Figure I. 9. Examples of X-Ray examination in radiology (hand ,Thorax, skull)

The detector, located in front of the X-ray source and behind the subject, will therefore be

strongly exposed in relation to soft tissues, and weakly in relation to bones and dense tissues. Depending on the density of the X-rayed organ, the picture will be more or less blackened. Thus, the bony structures appear in white and the organs which, like the lungs, contain a lot of air let the rays pass and appear in black; between these two extremes, all shades of gray exist.

I.7. Dosimetric quantities

Dosimetry is the discipline that attempts to measure the effects of radiation in matter, in particular in biological tissues. Many quantities have been defined for this purpose, the main ones of which are listed below.

I.7.1. Dose concept

Ionizing radiation has the ability to pass through stuff, such as the human body, and deliver energy when it comes into contact with it. The amount of energy that is taken in by a body as a result of being exposed to radiation is referred to as the dose. The absorbed dose, the equivalent dose, and the effective dose are the three different types of radiation dosage that will be discussed in the following paragraphs. Figure 2 provides a concise overview of the relationship between these values, each of which is described in further depth in its own section.

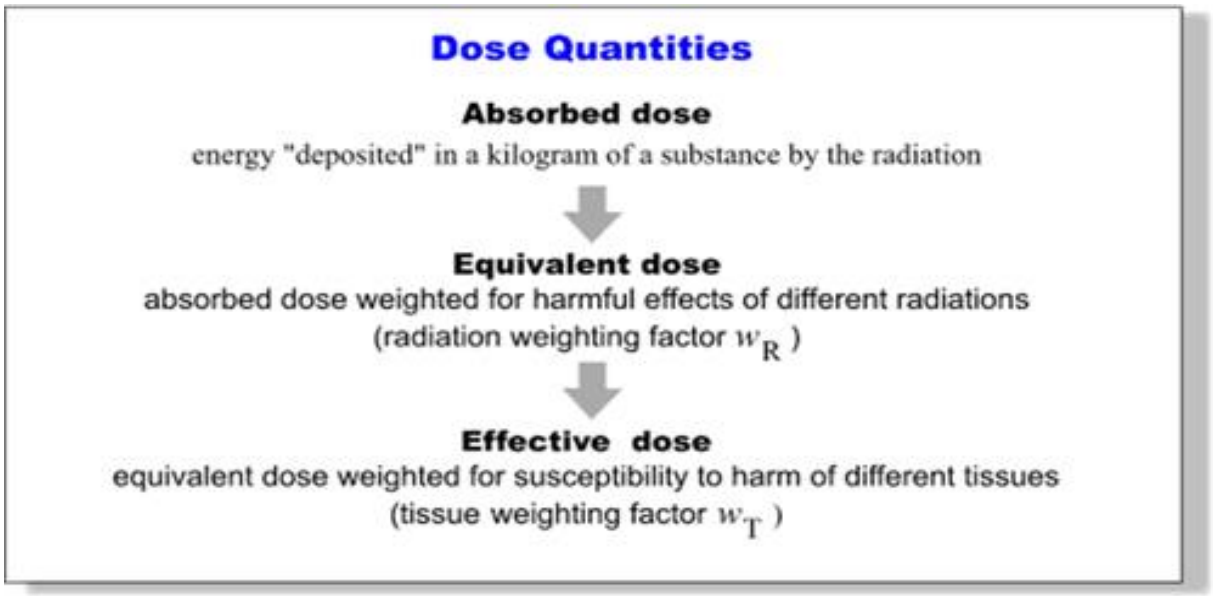

Figure I. 10. Relationship between radiation dose parameters

I.7.2. Kerma

KERMA is an acronym for Kinetic Energy Released per unit Mass. is defined for indirectly

ionizing radiation (photons and neutrons)

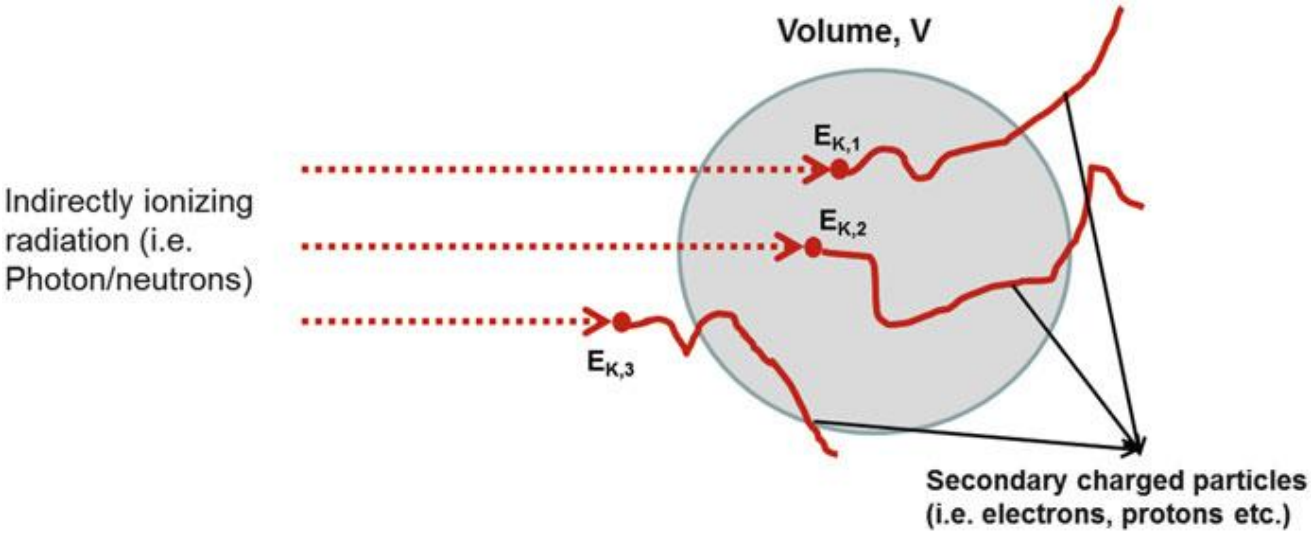

Figure I. 11. Illustration of Kerma [12].

for N particles, dEtr is the mean energy transferred from indirectly ionizing radiation to charged particles per unit mass of volume 'V', K can be written

$$K = \frac{d\bar{E}_{tr}}{dm}$$

There are two main ways that the kinetic energy that is transmitted to charged particles can be spent:

Collisional kerma is related to the part of the kinetic energy of the secondary charged particles which is spent in collisions, resulting in ionization and excitation of atoms in matter. It is the expectation value of the net energy transferred

Radiative Kerma is related to the portion of the initial kinetic energy of the secondary charged particles which is converted into photon energy.

It is possible to express the KERMA as:

$$K = K_c + K_r$$

Where, Kc is collisional KERMA and Kr are the radiative KERMA.

I.7.3. Exposure

Exposure is a quantity related to collision kerma when X or gamma ray photons interact with air. It is defined as the total charge dQ of either sign produced by X- or γ radiation in air of

mass dm. The ions must not escape the air and must be collected.

X can be presented as follows :

X= dQ/ dm

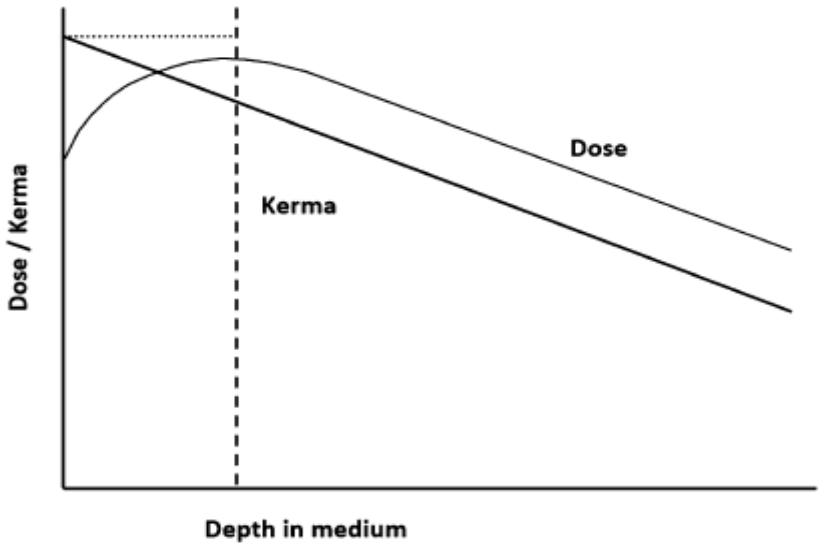

Figure I. 12. The relationship between Kerma and absorbed dose for photon and neutron radiations [12].

A cascade of electrons was caused by Photons through KERMA, so they deliver the dose and do real ionizing damage.

Most damage caused by electrons is not directly on the surface but is actually slightly deeper, which is well explained by Compton scattering which usually propels electrons forward

I.7.4. Absorbed Dose

Absorbed dose is a non-stochastic quantity applied to ionizing particles directly and indirectly. For indirectly ionizing radiation, energy is imparted to matter in a two-step process. First (resulting in KERMA), indirectly ionizing radiation transfers kinetic energy to secondary charged particles. In a second step, these charged particles transfer their energy kinetics in the middle (resulting in absorbed dose) and lose part of their energy in the form of radiative losses (Bremsstrahlung).

The absorbed dose is defined as an average energy ε transmitted by a particle ionizing to matter of mass m in a finite volume V:

$$D = \frac{d\bar{\varepsilon}}{dm}$$

The unit of absorbed dose is the joule per kg (J.kg-1). The special name for this unit is the

Gray (Gy).

I.7.5. Equivalent dose

When ionization radiation is absorbed by living organs, it can produce biological effect at different stages. As the interaction with biological materials varies according to the different types of ionizing radiation, absorbed doses of the same value do not necessarily have the same biological effects.

$Ht = WR .D$

For example, tissue damage caused by 1 Gy of alpha radiation is greater than that caused by 1 Gy of beta radiation. This is because alpha particles have a higher charge, are heavy, and transmit their energy more densely along their path. A radiation weighting factor (WR) is used in order to bring the different forms of radiation to an equivalent level of their respective biological effectiveness.

Thus, it is possible to assert that an equivalent dose corresponding to 1 Sv of alpha radiation will have the same average biological effects as an equivalent dose corresponding to 1 Sv of beta radiation. Indeed, the two types of radiation have equal energies.

I.7.6. Effective dose

It is possible that the way various tissues and organs respond biologically to a specific type of radiation varies. A weighted dose is a dose determined for each organ or tissue using the weighting variables specific to that organ or tissue. These weighted doses are then added together to obtain the overall effective dose that the body as a whole received. When determining organ and tissue weighting factors, the relative susceptibility of a body component to cancer, mortality, and the effects of heredity are taken into consideration.

$E = \Sigma Ht \times Wt$

The unit for expressing the effaective dose is the sievert (Sv).

Table I. 2. Values of the radiological weighting factors WR [13].

Radiation type and energy	Radiation weighting factor, Wr
Photons, all energies (X-ray, Gamma)	1
Electrons and muons, all energies	1
Neutrons, energy less than 10 keV	5
More than 10 to 100 keV	10
More than 100 keV to 2 MeV	20
More than 2 MeV to 20 MeV	10
More than 20 MeV	5
Alpha particles, fission fragments, heavy nuclei	20

Table I. 3. ICRP 60 and ICRP 103 weighting factors [14].

Organ	Wt	
	ICRP 60	**ICRP 103**
Gonads	0.20	0.08
Bone marrow (red)	0.12	0.12
Colon	0.12	0.12
Lung	0.12	0.12
Stomach	0.12	0.12
Bladder	0.05	0.04
Breast	0.05	0.12
Liver	0.05	0.04
Oesophagus	0.05	0.04
Thyroid	0.05	0.04
Skin	0.01	0.01
Bone surface	0.01	0.01
Brain	-	0.01
Salivary glands	-	0.01
Remainder	0.05	0.12

I.7.7. Effective Dose Limits

The regulatory limit values for workers who are exposed to ionizing radiation are set in paragraphs R.44516 to R.4451-8 of the French Labor Code 31. These articles were written in application of the dose restriction concept. These "absolute"

values are limitations that must be followed in all circumstances (with the exception of emergency conditions and long-term exposure), except for emergency situations and long-term exposure.

These "absolute" values are limits that must not be exceeded under any circumstances (with the exception of emergency situations and long-term exposures). Compliance with them is evaluated based on the doses actually received by each worker (Table I.4) [56].

Table I. 4. Exposure limit values in millisievert/year (msv over 12consecutive months) [15].

Exposer limit values in millisievert/year (mSv over 12 concecutive months)

	Body (effective dose)	Extremities: hands, forearms, feet, ankles (equivalent dose)	Skin (equivalent dose on any cm2)	Crystalline* (equivalent dose) (equivalent dose)
Workers	20 mSv	500 mSv	500 mSv	100 mSv / 20 mSv*
Young workers (between 16 and 18 years of age, subject to	6 mSv	150 mSv	150 mSv	15 mSv

subject to authorization for training purposes)				
Pregnant women	less than 1 mSv (equivalent dose to the unborn child), from the declaration of the pregnancy to the delivery			
Breastfeeding woman	prohibition to maintain them or to assign them to a position involving a risk of internal exposure			

* ELV for the lens of the eye

Starting on July 1, 2018, and continuing through June 30, 2023, the cumulative ELV for the crystalline lens has been set at 100 mSv for these 5 cumulative years; however, the dose that can be absorbed in a single year cannot be higher than 50 mSv.

The ELV for the crystalline lens will be 20 mSv averaged over a period of 12 consecutive months beginning on July 1, 2023. (This is confirmed by the new article R4451-6 of the labour code) [15].

The possibility of stochastic effects is decreased as a result of the effective dosage limits that have been imposed by the Radiation Protection Regulations. These limits are sufficient on their own to reduce the deterministic effects for practically all organs and tissues (Figure I. 13).

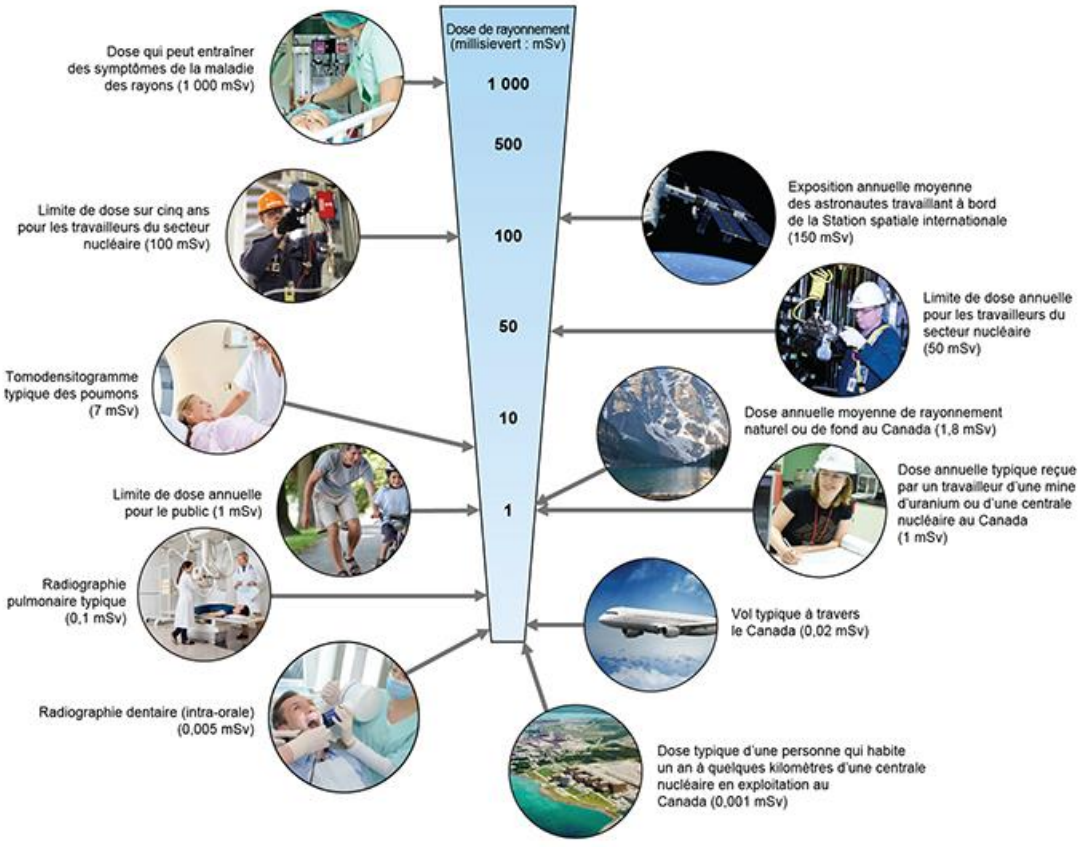

Figure I. 13. Differents effective Dose Limits [16].

I.8. Radiation protection

I.8.1 Principles

There are 3 principles of radiation protection:

I.8.1.1 Justification

Because an x-ray is a supplemental examination and not a routine examination, it is the patient's medical history and the results of the clinical examination that determine whether or not an x-ray is necessary. Before taking an x-ray, a history of the patient and a clinical examination will be performed.

I.8.1.2 Optimization

Every effort should be made to keep X-ray exposure as low as possible, given the diagnostic possible, taking into account the diagnostic needs. ALARA concept: As Low As Reasonnably Achievable must be considered.
Given the diagnostic requirements, every effort should be taken to maintain the lowest feasible level of X-ray exposure. This should be done while taking into account the requirements of the diagnostic process.

I.8.1.3 Limitation

There are three parameters to decreas the radiation doses: time, distance, and shielding materials. Existence of radiation dose limits (defined by the Health Code and the Labor Code) that must not to be exceeded. They vary according to the people in the public and workers exposed to ionizing radiation (Table I.4) [15].

There is a monitoring of the level of exposure and a medical follow-up in accordance with the principle of limiting exposure to IR.

I.8.2 Dose reference levels

The International Commission on Radiological Protection (ICRP) initially presented the idea of diagnostic reference levels (DRLs) in 1996 in its publication 73 titled "Radiation Protection and Safety in Medicine." Diagnostic radiology and diagnostic nuclear medicine each have their own unique kind of reference levels "The Commission now advises that diagnostic reference levels be used while treating patients. In a manner analogous to that of the investigative levels, these levels pertain to a readily measured quantity, "[17]. DRLs are indeed the dose stages for diagnostic practices or, throughout the particular circumstance of radiopharmaceuticals, activity levels, for typical examinations on typical diagnostic categories or on typical "phantoms," for broad categories of facility types. These levels apply to typical examinations on typical patient groups or on typical "phantoms." If excellent and typical diagnostic and technical performance methods are used, as well as if the activity levels are not surpassed, then these levels should not be exceeded for routine procedures. performance are implemented.

For a given examination, the diagnostic reference level (DRL) is evaluated. This is different from the dose limits defined by law. It is just a reference to realize the practice.
DRL= highest dose used in 75% of examinations. 75% chance of receiving less than this

dose. If you are above it, you have to do something to optimize. We must always be below the DRL.

The reference value to be considered is the 75th percentile of the doses measured for an examination on a large number of patients (Figure I.14).The dose distribution curve should be representative of the radiological practice in a country

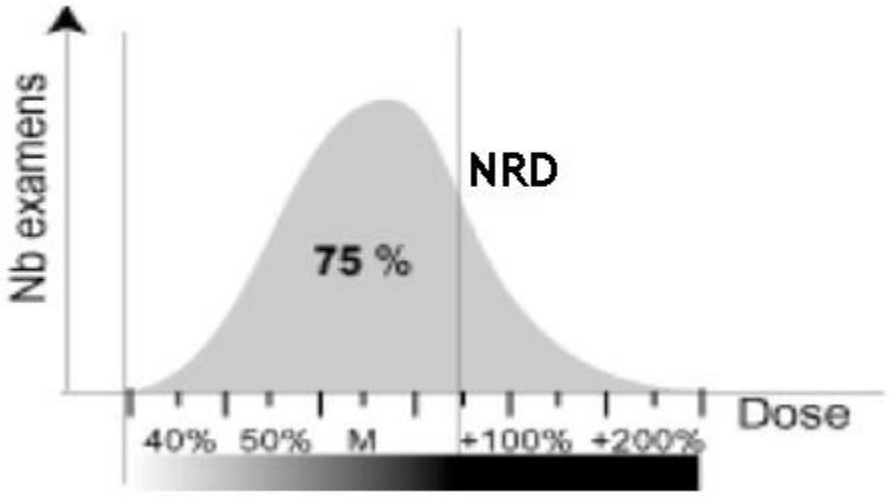

Figure I.14: the 75th percentile of the doses measured for an examination on a large number of patients[17]

Existence of radiation dosage limitations that must not be exceeded; these limits are set by the Health Code and the Labor Code respectively. They differ depending on the population of workers and members of the general public who are exposed to ionizing radiation (Table I.4) [15]. In accordance with the notion of reducing one's overall exposure to IR, there is both a monitoring of the total amount of exposure as well as a medical follow-up.
The diagnostic reference level, often known as the DRL, is assessed for a particular examination. This is not the same as the legal dose limitations that have been established. Simply using it as a reference can help you comprehend the importance of the exercise.
DRL stands for the highest dose that was administered in 75% of all examinations. There is a 75% probability that you will receive a dose that is lower than this. If you are already at that level, you need to take some steps to optimize. We are required to remain below the DRL at all times. The 75th percentile of the doses that were measured for an assessment on a large number of patients should be the reference value that is taken into consideration (Figure I.14). The dose distribution curve ought to be an accurate reflection of the radiological procedures used in a country.

Chapter II

Mammography

Chapter II: Mammography

II.1. Breast cancer

Cancer is a major public health problem. In healthy multicellular beings, a certain number of cells regularly disappear and are replaced by new cells. There must normally be a balance between cell death and cell proliferation.

Cancer, which results from an accumulation of genetic mutations after exposure to carcinogens (of chemical, physical or viral origin), is the result of anarchic cell proliferation leading to the formation of a tumor mass which attacks to surrounding healthy tissue. This tumor mass can migrate at a distance and colonize other tissues, thus leading to death in the carrier of this disease.

Breast cancer results in a malignant tumor that affects the mammary gland. the following image gives a breast anatomy containing all of its constituent tissues.

II.2. Breast anatomy

The human female breast is a well differentiated apocrine sweat gland which secretes milk during lactation. The two breasts lie anterior to the right and left pectoral muscles, extending from the sternumlaterally to the mid-axillary line.

Each breast consists of a thin outer layer of skin, beneath which is a subdermal layer of adipose tissue from several millimeters to about one centimetre thick. Beneath the fat layer lies the supportive connective tissue stroma, which contains blood vessels, lymph channels and variable amounts of adipose tissue. The stroma also contains the glandular tissue, consisting of 15 or 20 lobes which subdivide into milk forming lobules and drain via an extensive ductal system through the external centrally positioned nipple.

Most breast cancers occur centrally and laterally, in proportion to the relative amounts of glandular tissue in these areas, and it is important to choose the mammographic views which best evaluate these areas.

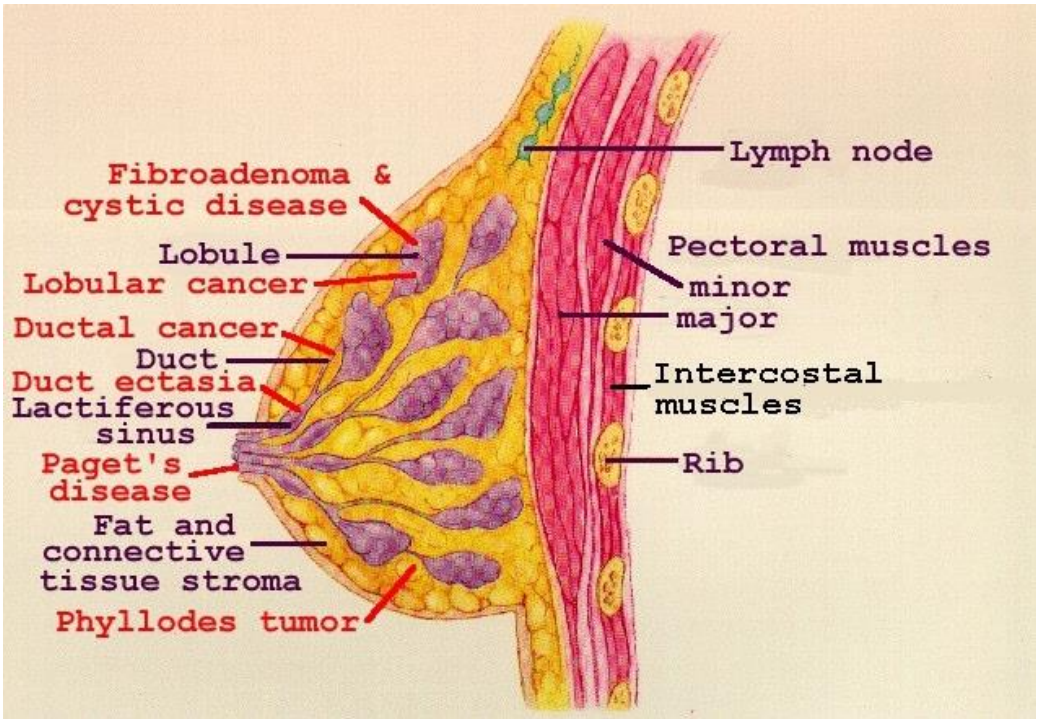

Figure II. 1. Understanding Breast Reconstruction [18].

II.3. Objective of mammography

Early diagnosis and treatment of breast cancer has a very good prognosis in terms of survival; however, the more advanced the disease, the more difficult it is to eradicate. This is why screening for this cancer by mammography is essential.

Mammography is an x-ray imaging method used to examine the breast for the early detection of cancer and other breast diseases. It is used as both a diagnostic and screening tool

Mammography, which combines specialized X-ray equipment with techniques for positioning breasts, is used both for the screening of women who have no signs or symptoms of breast cancer as well as for the diagnosis of lumps or tissues to determine whether they are cancerous. Before mammography physicians had relied on physical exams and surgical biopsies. However, physical exams could not detect emerging tumors and biopsies (of lumps that could be detected by physical examination) were expensive, invasive, potentially disfiguring, and sometimes inaccurate. Mammography has made large-scale screening feasible and diagnosis through biopsy less invasive and more accurate, while delivering the smallest dose of radiation possible.

II.4. Mammography equipment

Mammography requires specialized equipment using low-energy x-ray beams because of the

high photosensibility of the breast tissues.To visualize small details, adequate compression is required to to achieve high contrast of the subject in orther to detect early carcinoma masses.
The choice of the anode and the filter depends on the thickness of the breast and also on its density. There are different couples for mammography: Mo/Mo, Mo/Rh, Rh/Rh, Rh/Al, W/Al, W/Rh W/Ag. Depending on the thickness of the compressed breast, we will rather use molybdenum for low thicknesses and tungsten for thick and dense breasts, because its beam is more energetic. For breasts of average composition, the other couples can be used according to their atomic number. The choice of the anode/filter will have a direct link on the contrast.
After the production of X-rays, the diaphragm beam irradiates the breast located between a compression plate and the detection system (Figure II.2). In the case of an installation with a detector in the form of a screen-film couple, there is still an automatic cell whose function is to determine the duration of the irradiation so that the darkening of the film is constant. For a digital installation, no cell is useful since exposure control can be carried out directly by the detector.

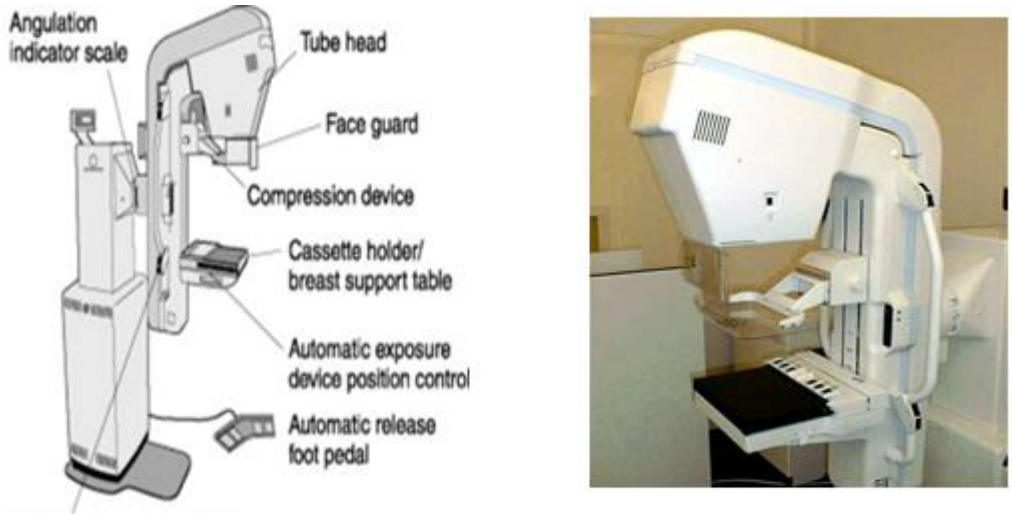

Figure II. 3. Mammography system [19].

II.5. Automatic Exposure Control (AEC)

Automatic exposure control (AEC) is an important feature in mammography. It enables consistently optimal image exposure despite variations in tissue density and thickness, and user skill level.
Mammography systems should have AEC systems that terminate x-ray emission. By automatically compensating for variance in Kvp setting and patient anatomy, AEC systems should help to provide uniform, reproducible high image quality, thereby decreasing the

number of retakes and reducing radiation exposure to the patient. The performance of the AEC is very important from both image quality and radiation safety perspectives.

II.6. Compression device

Each breast is compressed between the mammography detector and a compression paddle plate to reduce the thickness that the X-rays will pass through (Figure II.3).

This compression will spread the tissue of the breast thus avoiding the overlapping of the structures, and it will also limit the movement which could blur the x-ray image.

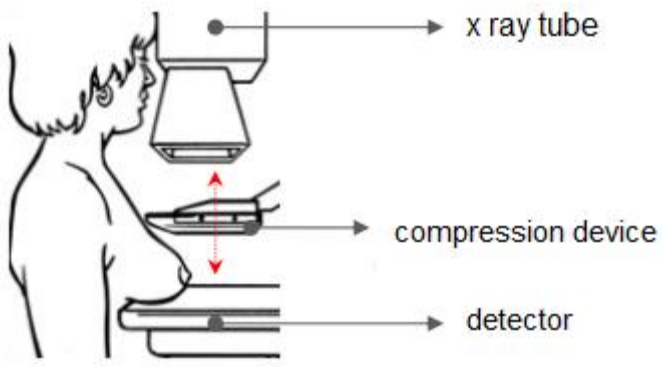

Figure II. 4. Breast screening [20].

In the mammography examination, each breast is x-rayed from the front and from the side to visualize the entire mammary gland. These views are: CC (Cranio-Caudal, vertical view), MLO (Medio Lateral Oblique, usually a 45 degree view or 90 degree view). For example in the image below, Two-view screening mammograms in, A, craniocaudal (CC) and, B, mediolateral oblique (MLO) views show fine linear calcifications located centrally in left breast (arrow). Calcifications are more clearly visible on spot magnification views (insets). Stereotactic vacuum-assisted core needle biopsy (9 gauge) revealed high-grade ductal carcinoma in situ [22] .

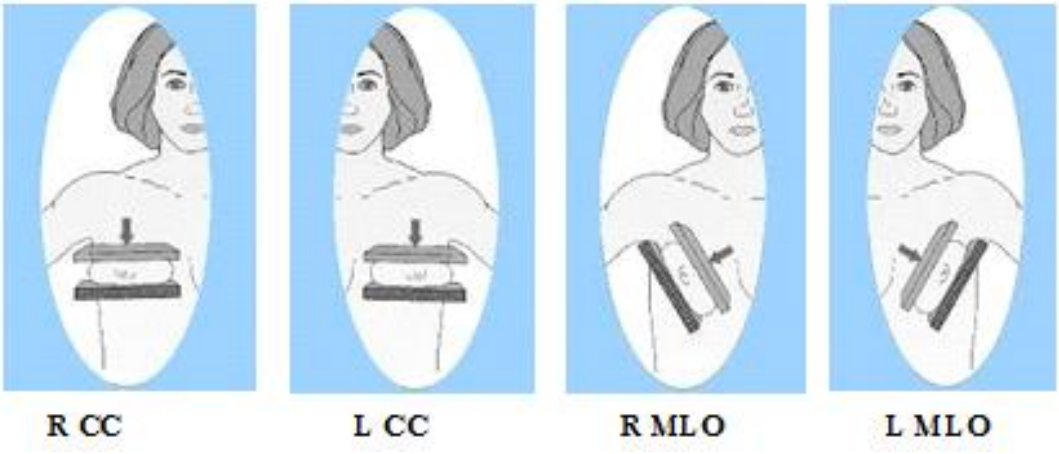

Figure II. 5. CC and MLO views in mammography [21].

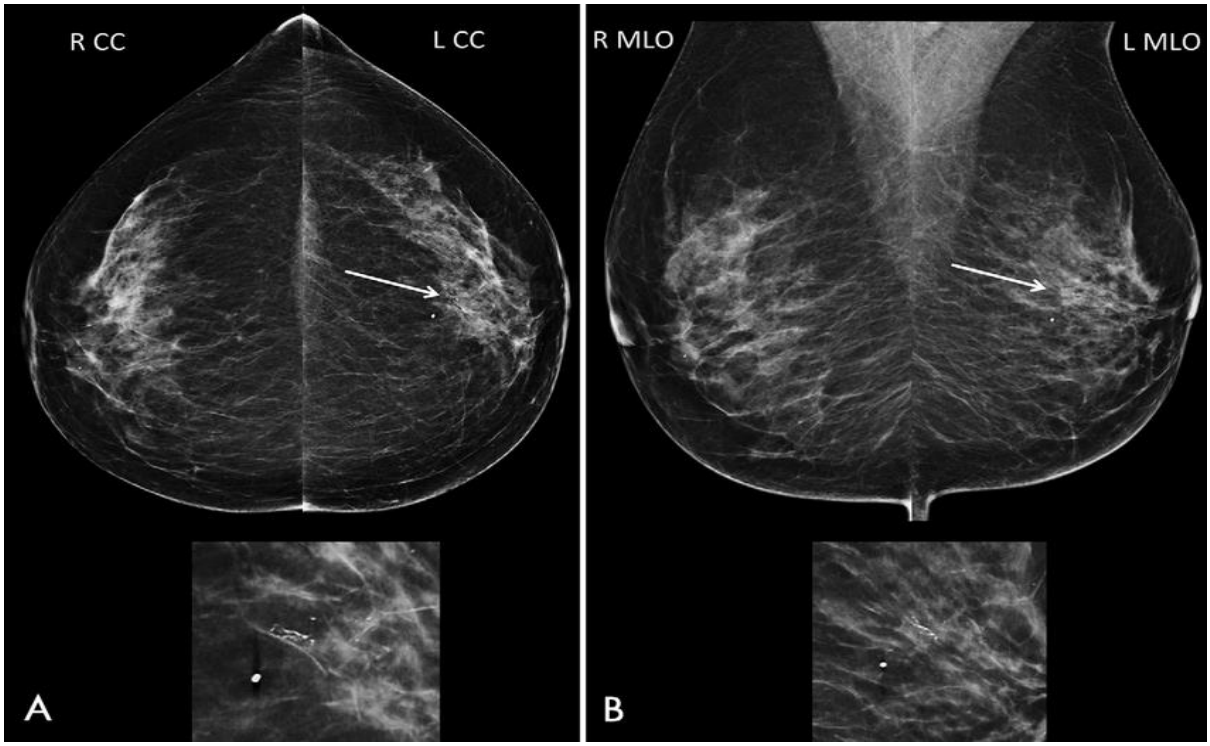

Figure II.5: MLO and CC views of a right and left breast of a patient [22].

Chapter III

Radiotherapy

Chapter III: Radiotherapy

III.1. Introduction

The main purpose of radiotherapy is the treatment of tumors. All cells are sensitive to radiation and all can be destroyed if given a sufficient dose. Tumor cells are not inherently more sensitive than healthy cells. However, their ability to repair the damage caused by radiation is less than that of healthy tissue. The aim of radiotherapy is therefore to deliver a dose to the tumor that destroys it, without producing significant side effects (complications) in healthy tissue. The limitations of radiotherapy are related to the fact that there is no dose that ensures tumor sterilization without any risk of serious complications.

III.2. In external radiation therapy:

the radiation source is located outside the patient, at a distance of about 1 meter. A collimator limits the radiation beam to the area to be treated (Figure III.1). As a general rule, the tissues at the entrance to the beam receive the most radiation. Tissues outside the field are irradiated, at a reduced dose, by radiation scattered in the patient.

The main objective of radiotherapy is to deliver a curative and homogeneous dose to cancer cells and subsequently to allow local control of the disease.

The challenge is to protect as much as possible the organs at risk and the surrounding healthy tissues of the irradiated tumor area.

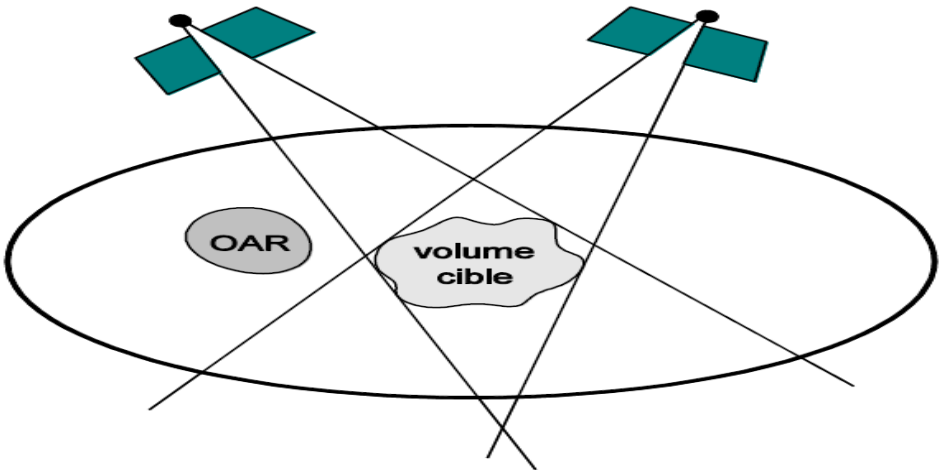

Figure III. 1. General situation in radiotherapy.

III.3. Examples of cancerous diseases

Many cancers can benefit from treatment with radiotherapy, such as prostate cancer and Head and Neck cancer.

III.3.1. Head and Neck cancer

Head and neck cancer is a cancer that affects the entire ORL sphere, from the base of the skull to the base of the neck. It represents a set of cancers forming in the upper aerodigestive tract (lips, tongue, mouth, throat, larynx), salivary glands, nasopharynx (area connecting the nose and the upper part of the throat) or the sinuses and the pit nasal.

Since most head and neck cancers originate in the squamous cells that form the lining of these passageways and cavities, they are called squamous cell carcinomas, also known as squamous cell carcinomas

Diagnostic:

Head and neck cancer is suspected if symptoms persist for more than 3 weeks, such as a lump in the neck, sore tongue, bleeding, white or red spots in the mouth, sore throat, painful swallowing, persistent hoarseness, and nosebleeds. Direct observation and palpation of suspicious lesions should be supplemented by examination of the mouth, nose, throat and upper respiratory tract using a flexible, lighted tube called an endoscope.

A diagnosis of cancer must be confirmed by microscopic analysis of cancerous tissue samples. to determine the shape and size of the tumour, as well as to check whether the cancer has spread to other parts of the body.

Clinical workup

All patients underwent a full oncological workup as Imaging consisted of computed tomography (CT) and/or magnetic resonance imaging of the head and neck, chest radiography or CT (chest CT in case of suspicious low cervical lymph nodes or suspicious bilateral cervical lymph nodes), and positron emission tomography (PET)–CT for unknown primary tumors.

Treatment

External radiation therapy involves producing radiation from an external source and directing it to the area of the head and neck where the tumor is, and in some cases, to nearby lymph vessels and lymph nodes. A mask is used to support the patient's head and keep him still while the treatment is being administered. Once the mask is put on the patient's head and neck, it is attached to the table on which the patient lies.

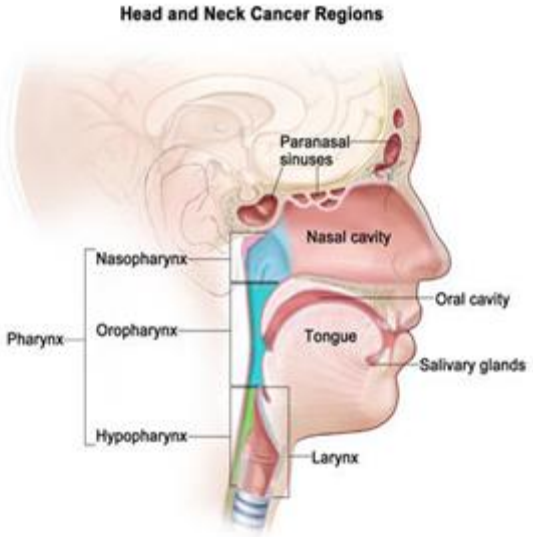

Figure III. 2. Anatomy of Head and neck [23].

Figure III. 3. Mask used in Head and Neck cancer [24].

III.3.2. Prostate cancer

The prostate is a gland of the male reproductive system. it is located just below the bladder (the organ that collects and empties urine) and in front of the rectum (the lower part of the intestine). It is about the size of a walnut and surrounds part of the urethra (the tube that empties urine from the bladder). The prostate produces fluid that is part of semen.

The tumor is initially limited to the prostate. Over time, the tumor grows and may extend beyond the prostate capsule. Cancer cells can detach from the tumor and use the blood vessels or the lymphatic vessels to invade other parts of the body: the lymph nodes located

near the prostate, the bones, the liver and the lungs.

Diagnostic

During a consultation, the doctor asks the patient about the personal and family history. He also asks about any symptoms they may experience, such as problems with urination or the presence of blood in the urine. Also the doctor performs a clinical examination.

The digital rectal examination is an examination carried out by the attending physician and the urologist to identify a suspicious size or an abnormality in the consistency of the prostate. However, such anomalies are not systematically indicative of a tumor and their absence does not exclude a risk of cancer. Rectal examination alone therefore does not confirm the presence of a cancerous abnormality.

The PSA assay consists of measuring the concentration in the blood of a protein synthesized by the prostate (prostate specific antigen). Its rate increases in case of cancer but also infection or adenoma of the prostate.

Clinical workup

It helps to see if the cancer has already spread to the lymph nodes or other organs. relevant examinations can be carried out such as:

Magnetic resonance imaging (MRI) and/or CT scan of the prostate and pelvic region to visualize the prostate and its contours, assess its possible extension into the pelvis and check whether the lymph nodes are affected.

A scintigraphy to check the absence or presence of bone metastases.

Treatment

During external beam radiation therapy, the patient lies on a table while a machine moves around their body, directing high-powered beams of energy, such as X-rays or protons, at their prostate cancer

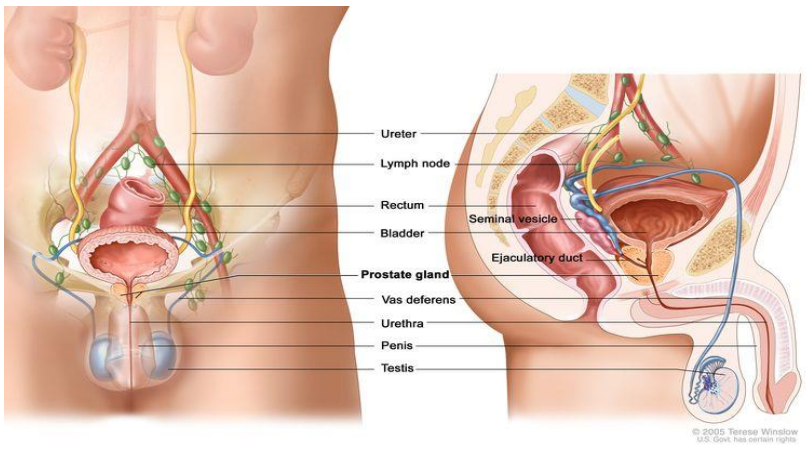

Figure III. 4. Anatomy of the prostate and other organs [25] .

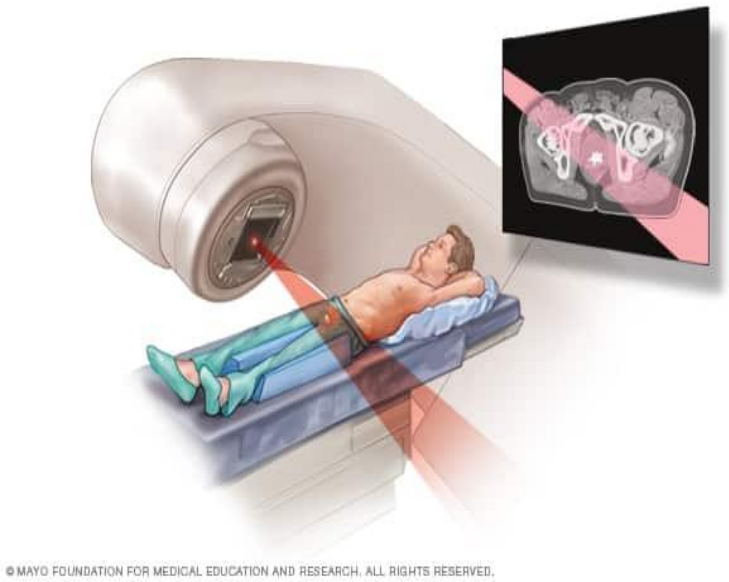

Figure III. 5. External beam radiation for cancer [26].

III.4. Course of treatment

The treatment of a patient proceeds as follows:

Diagnosis: First, the radiation oncologist diagnoses the disease by means of various tests on the patient.

Prescription: Depending on the diagnosis, the radiation oncologist prescribes the treatment. The prescription contains the type of radiotherapy, the determination of the irradiation volumes, the dose to be delivered to the target volume, the fractionation...

Planning: Based on the parameters of the prescription, the physicist decides on the treatment planning. This involves determining the orientation of the beams, the energy of the radiation, etc. The dosimetrist produces the treatment plan using treatment planning software (TPS), which is then validated by the radiation oncologist and the physicist.

Verification: After the treatment plan has been approved, the physicist prepares the necessary data set for the facility with which the treatment will be performed. The physicist verifies the data and authorizes the start of the treatment. The verification phase includes a dose calculation independent of the TPS to prevent failure of the TPS. A beam orientation check is then performed using the simulator. This installation reproduces the exact geometric conditions of the treatment installation. An X-ray image of each field is taken. These reference images are then used to validate the patient's position on the treatment system.

Treatment: The patient is treated with a series of irradiations of about two Gray to the tumor per day. The frequency and dose per session may vary depending on the treatment protocol

chosen. At the first session, the patient's positioning is checked by making a radiographic image (at high energy with the treatment installation) of each irradiation field and comparing them with the reference images obtained in the simulator. Finally, some centers carry out direct dosimetry at the entrance and exit of each field (in-vivo dosimetry) in order to compare it with a forecast dosimetry. This measurement is the only direct control of the dose delivered to the patient.

Follow-up after treatment: In order to improve the quality of treatment, it is essential to follow up patients after the end of treatment. This allows statistics to be developed which can then be used to optimize the various treatment parameters.

III.5. Medical imaging modalities for treatment

Simulation is usually the first step in external beam radiation therapy. The simulation helps to plan the radiotherapy treatment. we are talking about computed tomography (CT) to do the simulation, and a magnetic resonance imaging (MRI) examination which is often carried out in the presence of a tumor.

III.5.1. CT Scan

The most frequently used type of simulator is a CT (computed tomography) simulator. Its purpose is to define the positioning of the patient throughout his treatment. thus being able to virtually reconstruct the body in 3D in order to more precisely delimit the areas to be treated and those to be protected. This examination is not carried out for the purpose of diagnosis and will therefore not give rise to any interpretation. It is replaced by the virtual simulation of the fields using the construction of the DRR (reconstructed radiological image). The DRRs are therefore the digital equivalents of the reference films produced during the classical simulation.

A DRR is constructed using three-dimensional information from the CT. The reconstruction software takes into account the divergence of the beam and the position of the virtual source to build the projected image by integrating the CT number of each voxel crossed during the projection. A scaling of gray levels completes the reconstruction to produce the reference image of each field.

CT is based on two complementary systems:

The acquisition system is composed of an X-ray source and a detector. It provides the data necessary for the reconstruction of the image.

The signal processing system reconstructs a 2D or 3D image, from the acquired data, using

reconstruction methods adapted to the acquisition geometry.

CT sections give detailed three-dimensional information on the distribution of tissue densities. These sections are transferred to the treatment planning system (TPS)

III.5.2 Magnetic Resonance Imaging

Magnetic resonance imaging (MRI) is a test that provides two- or three-dimensional views of the inside of the body. MRI gives information about lesions that are not visible on standard X-rays, ultrasound or CT scans.

In the MRI examination, patients lie on a motorized table, which is moved through the narrow interior of a wide tube scanner, which produces a strong magnetic field. Normally, the protons (positively charged parts of an atom) of the tissues are placed randomly. But when they're surrounded by a strong magnetic field, as happens in an MRI scanner, they orient themselves parallel to the magnetic field. The scanner then emits a pulse of radio waves, which momentarily displaces the protons from the line. As the protons align themselves with the magnetic field again, they release energy (called signals). Signal strength varies with tissue. The MRI scanner records these signals. A computer is used to analyze the signals and produce the images.

III.6. Patient positioning

During the radiotherapy treatment, several imaging examinations of the patient are carried out in order to plan his treatment. To take these images, the patient is in a lying position, on a table equivalent to that which will be used for his treatment. The position in which the person finds himself will therefore serve as a reference for the rest of the process.

At the time of installation in the treatment room, the objective will be to find this position, so that the theoretical planning makes sense.

The alignment of the patient is carried out with the help of a system of three fixed laser sheets, via the marks they draw on the skin. This system allows, among other things, to visualize the

entry points of the beams when these are perpendicular or parallel to the table. The meeting point of the lasers is the isocenter and must merge with the center of the tumor.

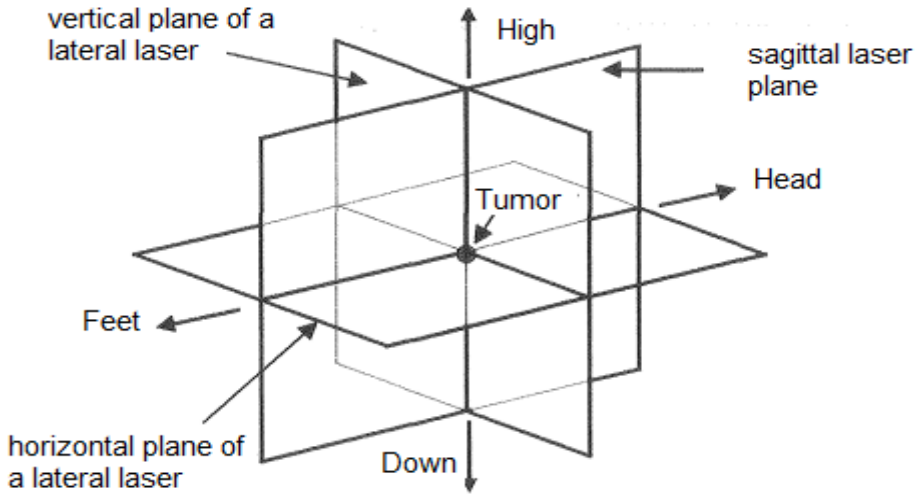

Figure III. 6. Laser beam system [27].

III.7. Target volume delineation

When treating a patient with radiation therapy, the radiation oncologist prescribes a dose to a volume to be treated* and to organs at risk. If the radiation techniques were perfect, it would be possible to irradiate the volume to be treated with the prescribed dose in a homogeneous way without irradiating the adjacent tissues. Unfortunately, this situation does not exist, healthy tissue is always irradiated. They can be massively irradiated if they are close to the volume to be irradiated, and the dose delivered to these tissues may be close to their tolerance limit.

The procedure for determining the volumes to be treated consists of several distinct steps. The volumes are defined according to the known location of the tumor and its possible extensions, but also according to the possible variations between planning and treatment, as well as patient movements and inaccuracies in placement.

Two volumes should be defined prior to treatment planning:

III.7.1. Gross Tumor Volume (GTV):

The GTV almost always corresponds to the parts of the malignant growth where the density of tumor cells is greatest. Thus, it is necessary to deliv er an adequate dose to the GTV to achieve the goal of radical radiotherapy.

III.7.2. Clinical Target Volume (CTV):

The CTV is a volume of tissue that contains the GTV and/or sub-clinical malignant lesions

that need to be destroyed. This volume must be treated adequately to achieve the goal of radical therapy.

III.7.3. Planning Target Volume (PTV):

PTV is a geometric concept that is defined to select appropriate beam arrangements and sizes taking into account all possible variations to ensure that the prescribed dose at the CTV corresponds to the delivered dose.

III.7.4. Organs at risk (OAR):

must be defined in order to determine the effect of the planning geometry on them. Planning should be done in such a way as to limit the dose to the organs at risk at least so that they do not receive a dose that could lead to serious complications.

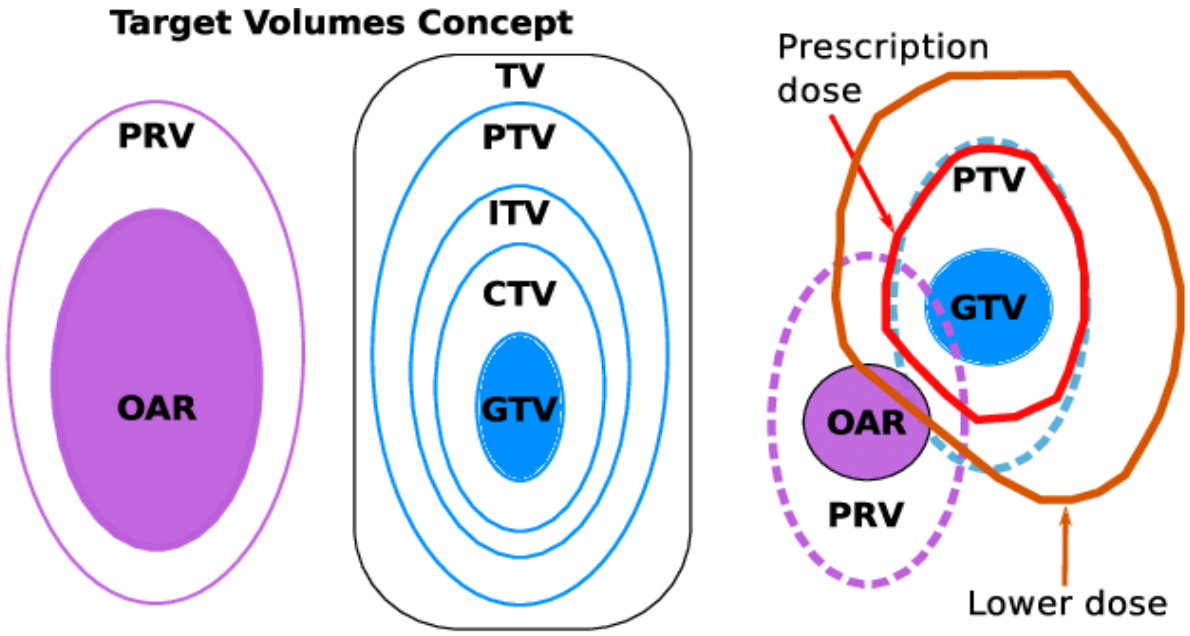

Figure III. 7. Target volumes concept [28].

The gross tumor volume (GTV) regions are the fundamental regions used to determine the clinical target volumes (CTVs) and planning target volume (PTV). The accuracy of the GTVs may affect tumor control and adverse events related to organs at risk or normal tissue. The PTV is the volume that includes the CTV plus CTV-to-PTV margin including the internal margin (IM) and the setup margin (SM).

III.7.5. Dose-related volumes

- **Processed volume**

it is a volume surrounded by an isodose surface specified by the radiotherapist, corresponding to a minimum dose level enabling the treatment goal to be achieved.

- **Irradiated volume**

This is the volume of tissues receiving a dose considered significant with respect to the tolerance of healthy tissues.

III.8. Treatment Planning System

The Treatment Planning System (TPS) is the process that allows radiation physicists and dosimetrists to reconstruct, model, predict and optimize the total radiation dose of a tumor and minimize the doses delivered to the organs at risk in the periphery. It is used to calculate the patient's treatment plan. These calculations are based on dose measurements made in a water tank for each beam size and each possible energy.

The physicist imports the digitized sections relating to patient data generally coming from CT sections taken under positioning conditions corresponding to those of irradiation. Then, it transfers these data to the TPS, which allows the conversion of these values into electronic density. The resulting advantage is the calculation of heterogeneity. Dose calculations are performed by overlay algorithms.

III.9. Evolution of external radiotherapy techniques

There are different techniques of external radiotherapy. Technological advances have made it possible to better protect healthy tissues and organs at risk while delivering the optimal therapeutic dose to treat the target volume.

III.9.1. 3D Conformal Radiation Therapy (CRT)

This technique makes it possible to match as precisely as possible (to conform) the volume on which the rays will be directed, to the volume of the tumor.

It uses 3D images of the tumor and surrounding organs obtained by CT scan, sometimes combined with other imaging exams (MRI, PET, etc.). Software makes it possible to simulate virtually, still in 3D, the shape of the irradiation beams and the distribution of the doses. With the use of volumetric images and the gradual improvement in image quality, it has become

possible to distinguish the extension of diseased tissues in the 3 directions of space and therefore to delineate them. Without these contours, the RC3D would not exist since it is a question of conforming the beams on the diseased volumes, while limiting the exposure of the healthy tissues.

The fine conformation of the beams is now mainly achieved using a multi-leaf collimator MLC (Multi Leaf Colimator). It is made up of 2 banks of symmetrical slats, each slat of the same bank being associated in a slot with its neighbors in order to reduce radiation leakage between them. this collimator is used to conform more exactly to the target volume.

III.9.2. Intensity Modulated Radiotherapy

Intensity-modulated conformal radiotherapy (IMRT) is an evolution of 3D conformal radiotherapy, it is a modern technique of high-precision external radiotherapy, in which the dose of irradiation delivered by each of the beams is not homogeneous. , but three-dimensionally modulated to deliver a higher dose to the tumor while minimizing radiation exposure to surrounding healthy tissue.

IMRT, combined with inverse planning software, provides new methods for delivering or shaping an inhomogeneous dose distribution that is virtually impossible to achieve with conventional radiation techniques. It is a system which proposes a dosimetric answer to the problem of irradiation which one posed to him through the planimetric constraints. The number of beams, the angle, and the energy are predetermined by the radiation therapist. The software will determine: the shape of the beams according to the shape of the contours of the PTV and the "fluence" according to the dosimetric constraints and the weightings fixed to these constraints. This system therefore requires new generation accelerators and high-performance calculation software.

Chapter IV

Published Articles

Chapter IV : Published articles

The work is divided into three main parts. The first part represents a dosimetric survey conducted in 5 Moroccan hospitals, focusing on routine diagnostic radiology examinations with the aim of determining the local dose reference levels based on the collection of patient data by calculating the ESD and ED numbers. In the second part, the verification of IMRT treatment plans is focused on the linear gas pedal and in particular the MLC. The aim is to evaluate and compare the parameters of the treatment plans delivered by the linear gas pedal with those planned. Complex treatment plans such as those developed in IMRT cannot be controlled by in vivo dosimetry. To control these types of treatments, more complex solutions are implemented, based on the use of a fixed or rotating Octavius 4D PTW phantom. In this case, it is a 4D system that is used to verify the treatment plans. This system has the particularity of allowing a fast and direct analysis. The verification of the treatment plans is divided into two main parts. First, there is the verification of the superposition of isodoses and profiles. Secondly, there is the Gamma index analysis comparing the calculated and measured dose distribution. These two steps will be described in detail in this part.
The third study was focused on evaluation of planning target volume (PTV) margins for two different locations using an electronic portal imaging device (EPID) to ensure that the correct radiation dose is delivered to the tumour when using intensity-modulated radiation therapy (IMRT).

IV.1. Article 1: Getting started with medical physics in Morocco via the introduction of local dose reference levels and international bench marking.

IV.1.1. Introduction

Ionizing radiation is widely used in medicine for diagnosis and treatment. The number of people exposed to low doses of radiation used in diagnostic radiology far exceeds the number of patients at higher doses used in radiotherapy [29]. This leads to actions in different contexts to prevent the risks of exposures involving many people. Indeed, low dose ionizing radiation for diagnostic use has great medical benefits; however, its widespread use has also

raised concerns about the harmful the inducted effects. The biggest preoccupation with ionizing radiation is the increased risk of cancer, especially after childhood exposures [30].

The general principle of ALARA radiation protection [31] indicates that exposures should be kept as low as reasonably achievable by reducing doses to patients. This means that special attention must be paid to each medical exposure. Every exposure to radiation must be carried out with great vigilance. If the necessary measures are not considered, exposure to X-rays can cause damage to the body, thus inducing certain types of cancers [32].

In addition to the rules established to protect the population against ionizing radiation, the standardization of radiological practices remains a challenge to overcome. This implies that certain measures to optimize radiological parameters and practices are necessary.

The radiographic image quality is the main element to be taken with great regard. To obtain a good image, certain measures concerning the quality of the equipment as well as radiological practices, must be followed. The European guidelines [33] give an example of good radiographic techniques by which diagnostic requirements and dose criteria can be achieved. This is in line with the optimization of medical exposure, where quality criteria must go hand in hand with a low dose of radiation. These provisions will protect the patient and staff from unnecessary exposure to radiation. The establishments of diagnostic reference levels (DRLs) can help to intervene if certain aberrations are noted. They are defined for typical examinations for standard size patient groups or standard phantoms for defined types of equipment. These levels should not be exceeded for standard procedures when good normal practice in diagnostic and technical performance is applied. This was adopted by The Council of the European Union adopted the concept of DRL in the Medical Exposure Directive (MED) 97/43/EURATOM [34]. The International Atomic Energy Agency (IAEA) advice on the use of DRLs in radiology, in the International Basic Safety Standards [35]. This concept was introduced by ICRP publication 73 (ICRP, 1996) which introduced the term "Diagnostic Reference Level", developed the recommendation from ICRP publication 60. The main objective is advisory to identify the examinations delivering doses systematically exceeded or below a dose of radiation insufficient to obtain an appropriate medical image. The diagnostic reference levels do not represent a dose constraint, and not linked to limits. The main goal is ensuring the adoption of the DRLs into national legislation and regulations concerning radiation protection [36]. The countries where DRLs are well established for radio diagnostic examinations and interventional radiology procedures require that these should be reviewed regularly and used for optimization purposes [33].

In our case, the national diagnostic reference levels are not yet adopted and even less used as

a reference, to review radiological procedures and equipment when large dose differences are mentioned. The present work is part of the 'Radiology as a Steward for Quality in Moroccan Health Care' (RASQUAM) of the VLIRUOS (Flanders, Belgium) to contribute to the establishment of national diagnostic reference levels. The study was performed in Moroccan hospitals and focused on some common diagnostic radiology examinations such as (Chest, Skull, cervical, Lumbar).

The aim of this work is to estimate the Entrance Skin Dose (ESD) and the Effective Dose (ED) for patient exposure to x-rays and to compare these results with other data published in previous studies.

IV.1.2. Material and methods

The data were collected in six conventional radiology rooms of five hospitals, in the cities of Rabat, Ouezzane and Tantan. For the sake of confidentiality, the rooms are randomly identified as A, B, C, D, E and F. The examinations included Chest, Cervical spine, Skull and Lumbar spine. The technical parameters used (x-ray tube voltage kV, milliamperage mAs and the focus Skin distance FSD) and patient data (age, sex, weight), were collected at the time of the examination. These values are used to calculate the dose using the DoseCal software that provides the Entrance Skin Dose (ESD) and the Effective Dose (ED) for adults. Once the potential of the tube, the tube current, the exposure time and the focus-skin distance are known, the ESD value is given by the following expression used by Ofori, et al. [37].

Where:

- BSF is backscattering factor.
- Output (in mGy / mAs): is the output of the x-ray tube at 1 m normalized to 32 mAs;
- mAs: is the product of the tube current (in mA) and the exposure time (in seconds),
- FSD: is the distance between the x-ray source and the skin (in cm);

The tube output (in mGy / mAs) of all x-ray machines was measured using a PTW ionization chamber.

The doses were calculated first by the last relation considering the output of each X-ray tube, then by the software. The results were comparable with an average accuracy of 5% (Table IV.1).

Table IV. 1. X-ray machine characteristics

Hospital	**A**	**B**	**C**	**D**	**E**	**F**
Tube	Stefanix evidence	Siemens Luminos RF classic 150/40/80HC	Siemens	-------	Comet DX81HS-28/70-150	Siemens R202 MLP/B
Manufacture date	-------	2012	2004	-------	September 2001	2001-05
Inherente filtration (mmAl/ kV)	-------	1.5 /80	1.5/80	-------	0.9/70	1/75
Add. filtration (mmAl)	-------	1	1	-------	2	2.5

Table IV. 2. Number of patients for all the hospitals

Exam	Projection	Hopital	Number of patients	Age (mean)
CHEST	PA	Room 1	10	36
		Room 2	16	63
		Room 3	42	52
		Room 4	19	51
		Room 5	32	48
		Room 6	20	47
	AP	Room 1	10	59
		Room 2	14	67
Skull	Face	Room 1	19	35
	Lat	Room 1	21	35
cervical	Face	Room 1	10	50
		Room 2	6	49
	LAT	Room 1	18	41
		Room 2	6	49
lumbar	Face	Room 1	7	37
		Room 2	12	50
	LAT	Room 1	7	37

IV.1.3. Results and Discussion

Tables (IV.2,IV.4) summarize the number of patients by examination and the radiological parameters kv, mAs and FSD for the examinations carried out, for the 6 rooms of the 5 hospitals. The kV varies, depending on the type of examination, from 100 to 110 kV for PA projection of Chest examination in hospital A and from 102 to 125 in hospital B and from 53 to 100 kV and 96 to 125 kV for the projection of AP, respectively in hospitals A and B. In (Table IV.5) are presented skin entrance doses and the effective doses. The skin entrance doses and the effective doses calculation (Tables IV.5 and IV.6) show that the values vary according to the examinations as well as the hospitals where the data were collected. In hospital E, where examinations are carried out by analog (silver) radiology, a reduction in PA

chest examination dose (Table IV.5) is observed. This is linked to good radiological practice due to the experience of the radiology technician of this department. In fact, the average value of mAs is significantly lower than that of hospitals A, B, C and D (Table IV.3). For the PA chest examination, (Table IV.5) shows that, A and B rooms presents higher ESD values than the recommended ones (300 µSv) [36].For the skull face examination, the mean values of the ESD (Table IV.6) correspond to the recommended one (5000 µSv) [36]. Some differences in radiological practices were noted across the rooms where the data were taken. For the chest examination projection PA; the lowest ESD median values (Table IV.5) were observed; except in rooms A and B; mainly due to the adequate radiological used. Indeed; the median charge were less than 3 mAs (equal to 2 mAs in room E) and the FSD is greater than 120 cm: The voltage varying between 100 and 120 kV (Table IV.3). In room A; a large fluctuation for the mAs values was noted with a maximum of 10 mAs and a median of 5 mAs. This remark is also valid for the AP projection (Table IV.4).

Table IV. 3. Technical radiological parameters for chest PA for all the rooms

Exam	Rooms		Mean	Max	Min	Median
Chest PA	A	kV	104	110	100	103.5
		mAs	4.98	10	2.5	5
		FSD	123.98	127	122	122.1
	B	kV	113.06	125	102	113
		mAs	4.03	5.06	3.24	3.63
		FSD	123.38	127	120	123
	C	kV	119.93	120	117	120
		mAs	2.89	4.01	2.2	3.2
		FSD	126.7	143	111	127
	D	kV	119.21	120	114	120
		mAs	2.86	3.2	2.42	3.1
		FSD	129.31	137	113	132
	E	kV	110.31	117	104	110
		mAs	2.06	3.2	1.6	2
		FSD	1320.3	147	109	132.5
	F	kV	99.05	111	78	101
		mAs	4.55	2.5	3	3
		FSD	123.77	127	122.99	123

Table IV. 4. Technical parameters for chest, scull, cervical and lumbar examinations for rooms A and B

Rooms		A						B					
position		AP			LAT			AP			LAT		
Exam		kV	mAs	FSD	kV	MAs	FSD	kV	mAs	FSD	kV	mAs	FSD
Chest	mean	92.1	5.11	85.14	-------	-------	-------	112.43	4.19	92.66	-------	-------	-------
	max	109	8	97	-------	-------	-------	125	8.07	97	-------	-------	-------
	min	60	2.5	73	-------	-------	-------	96	3.23	88	-------	-------	-------
	Median	100	5	85.85	-------	-------	-------	113	3.82	93	-------	-------	-------
Skull	mean	60.7	46.42	76	60.81	45.81	80.27	65	32.32	90.9	-------	-------	-------
	max	65	63	78	65	63	80.6	70	75.08	91.6	-------	-------	-------
	min	60	32	76	60	32	80	60	14.06	90.9	-------	-------	-------
	Median	60	50	77	60	50	80.5	65	20.06	91.6	-------	-------	-------
Cervical	mean	60.15	30.3	78.83	58.92	35.67	83.25	66.83	29.36	93.67	66.83	29.36	99.2
	max	61.5	50	91.9	70	56	84.4	75	36.05	94	75	36.04	99.4
	min	60	16	76.9	50	16	81.3	60	22.05	92	60	22.05	99
	Median	60	30	76.9	59.5	36	83.1	66.5	28.53	94	66.5	28.52	99.2
Lumbair	mean	80.64	64.14	74.91	80.64	70.57	69.31	79.21	51.25	116.05	-------	-------	-------
	max	99	90	77	99	125	72.4	87.5	71	125	-------	-------	-------
	min	52	36	74	52	36	68.7	70	22	89.6	-------	-------	-------
	Median	86	63	74.2	86	63	68.7	81	50	125	-------	-------	-------

Table IV. 5. ESD and ED for CHEST PA projection for all rooms

	Rooms	A	B	C	D	E	F
ESD	Min	0.18	0.36	0.19	0.19	0.11	0.14
	Median	0.46	0.38	0.29	0.24	0.15	0.28
	Mean	0.43	0.43	0.3	0.25	0.16	0.29
	Max	0.88	0.66	0.48	0.36	0.22	0.42
	75^{th} percentile	0.5	0.46	0.35	0.28	0.18	0.35

ED	Min	0.02	0.03	0.02	0.02	0.01	0.01
	Median	0.03	0.04	0.03	0.02	0.02	0.03
	Mean	0.04	0.04	0.04	0.03	0.02	0.03
	Max	0.07	0.06	0.07	0.05	0.03	0.04
	75^{th} percentile	0.06	0.05	0.04	0.03	0.02	0.04

Table IV. 6. ESD for the other examinations for rooms A and B

Examen		Room	ESD				
			Min	Median	Mean	Max	75^{th} percentiel
Chest	AP	A	0.35	0.55	0.67	1.11	0.83
		B	0.55	0.75	0.75	1.16	0.77
Skull	AP	A	1.96	3.06	2.95	3.92	3.23
		B	0.61	1.15	1.98	5.01	2.35
	LAT	A	4.65	7.28	6.91	9.28	7.37
Cervical	AP	A	1	1.75	1.71	2.38	2.07
		B	1.1	1.45	1.66	2.51	2.07
	LAT	A	0.99	1.77	2.07	4.03	2.75
		B	1.11	1.5	1.67	2.62	1.96
Lumbar	AP	A	4.6	8.08	8.91	14.13	11.47
		B	1.3	3.45	3.33	5.61	3.96
	LAT	A	2.7	5.01	4.92	8.95	5.83

Table IV.7 representing a comparison of the ESD values relatively to previous studies, reveals that the results comply with the international recommendation. The values are in accordance with those of international recommendations and, with the exception of those of UK and Canada, are in the range found by most previous studies and sometimes lower. This conclusion is also deducted from (Table IV.8) regarding the effective dose results. The dose to the organ has been detailed in (Table IV.9). It is noted that rooms E and D have the lowest values, due to the appropriate choice of radiological parameters. The values are in accordance with international standards and comparable to those of most of the studies considered for examinations and projections used; except for skull LAT. The chest PA DRLs of the present study are of the same order as those of Slovenia and Brazil, whereas they are lower than those of India and Iran and that they are obviously higher than those the UK and Canada and Japan; while being within the range of values proposed by the European community. The DRLs of the other examinations are on the whole comparable to most of the previous studies (Table IV.7).

Table IV. 7. Mean DRL and ESD (mGy)

ESD (mGy)									
Examen		Chest		Skull		Cervical		Lumbar	
Projection		PA	AP	Face	Lat	Face	Lat	Face	Lat
Present study	Mean	0.31	0.68	2.47	6.91	1.69	1.87	6.12	4.92
	DRL	0.35	0.81	2.79	7.37	2.07	2.36	7.72	5.83
EU RP 109 [37]	Mean	-------	-------	-------	-------	-------	-------	-------	-------
	DRL	0.3	-------	5	3	-------	-------	10	30
Canada 2013 [38]	Mean	0.14	------	1.67	0.76	0.62	0.44	3.72	6.28
	DRL	-------	------	-------	-------	-------	-------	-------	-------
Slovenia 2006 [39]	Mean	0.29	0.32	2.2	1.73	1.4	1.4	-------	-------
	DRL	0.35	0.35	2.54	2.02	1.73	1.83	-------	-------
India 2009 [40]	Mean	0.53	0.38	-------	4.11	-------	-------	7.3	14.19
	DRL	0.68	0.47	-------	5.16	-------	-------	8.39	15.66
UK 2005 [41]	Mean	0.1	0.13	1.54	1.07	-------	-------	3.86	8.03
	DRL	0.14	0.15	2.04	1.34	-------	-------	5.06	11.2
UK 2019 [41]	Mean	-------	-------	-------	-------	-------	-------	-------	-------
	DRL	0.15	0.2	1.8	1.1	-------	-------	5.7	10
France 2012 [42]	Mean	-------	-------	-------	-------	-------	-------	-------	-------
	DRL	0.4	-------	4.8	2.6	-------	-------	10	26
Iran 2016 [43]	Mean	0.49	-------	1.47	1.01	0.67	0.79	2.81	4.28
	DRL	0.7	-------	2.55	1.42	1.07	1.17	3.55	4.69
B razil 2009 [44]	Mean	0.3	0.4	2.8	2.04	0.52	0.77	5.4	11.2
	DRL	0.35	0.5	3.28	2.14	0.72	1.2	6.6	16.2
Ghana 2014 [45]	Mean	0.27	-------	-------	-------	1.05	0.45	3.25	------
	DRL	-------	-------	-------	------	-------	-------	-------	-------
Japan 2019 [46]	Mean	0.17	0.17	1.3	1	0.45		2.3	6.5
	DRL	0.2	0.2	1.6	1.4	0.6		2.9	8.9

Table IV. 8. Mean effective dose ED

Studies	Chest PA	Chest AP	Skull AP	Cervical AP	Cervical Lat	Lumb AP
Present study	0.03	0.19	0.03	0.08	0.03	0.45
Canada 2013 [38]	0.0204	-----	0.0202	0.023	0.0025	0.38
Bangldesh 2018 [47]	0.011	0.022	-----	-----	-----	0.133
Serbia Montenego 2005 [48]	0.05	-----	0.03	0.09	0.02	0.8
Ghana 2014 [45]	0.02	-----	-----	0.05	0.03	0.41
Metaxas2018 Greece [49]	0.01	-----	0.02	0.03	0.03	0.26
UK 2008 ICRP 60 [50]	0.014	-----	0.022	0.018	0.012	0.409
UK 2008 ICRP 103 [51]	0.014	-----	0.033	0.018	0.012	0.389

Table IV. 9. Body mean dose organ (mGy) for Exam Chest PA

Organs	Room A	Room B	Room C	Room D	Room E	Room F	Values reported in literatures (mGy) UK [52]
Adrenal glands	0.12	0.13	0.1	0.13	0.05	0.06	0.052
Breast glands	0.03	0.03	0.03	0.02	0.01	0.01	------
Lungs	0.12	0.13	0.11	0.14	0.05	0.08	0.046
Spleen	0.08	0.09	0.07	0.05	0.03	0.04	0.043
Thyroid	0.07	0.07	0.06	0.05	0.03	0.05	------

IV.1.4. Conclusion

This preliminary study was carried out in five radiology departments to estimate the local diagnostic reference levels, considering the most used examinations. The overall DRLs values were in accordance with international recommendations, although some rooms had higher values mainly due to an increase in the X-ray tube load because of to the variability of radiological practices. These results may lead to awareness raising relating to the optimization of radiological practices and consequently of the doses received by patients. A broader investigation targeting more radiology departments across the country should be undertaken to determine the national DRLs. In addition, training of radiology technicians is necessary and mminent for the following investigation to be beneficial and fruitful.

IV.2. Article 2: Combined analysis of breast morphometry, compression and volumetric breast density: valuable input to improve mammography screening using international bench marking.

IV.2.1. Introduction

Mammography is an effective exam for the early detection of breast cancer. As the glandular tissue in the female breast is considered a radiosensitive organ, the mammographic exam should be associated with the lowest achievable dose to the patient, usually expressed in terms of mean glandular dose (MGD) which is considered to be the most important quantity to estimate the risk of radiation-induced carcinogenesis [53, 54].

The distribution of adipose and fibroglandular breast tissue is variable and strongly correlated with age: in older women, breast density generally tends to decrease [55].

Breast density is a radiological entity representing the amount of radiopaque or dense

mammary structures known as fibroglandular tissue, relative to radiolucent tissue such as fatty tissue [56]. This has an impact on the description of mammography's ability to detect lesions: the denser the breast, the lower the sensitivity of the mammogram. In addition, the high density is responsible for a higher rate of interval cancers and false positives [57].

Several studies evaluating the relationship between breast density and breast cancer have shown a significant increase in cancer risk for women with dense breasts. In fact, mammography is less efficient for detecting cancers in dense breasts. Dense breast shots are more difficult to read and can also lead to additional exams [58, 59]. High density is an appreciable predictor of the risk of missing cancer detection at mammography. Density varies especially with age, but is also influenced by hormonal treatment and is seen only on mammograms. Quantitatively, volume breast density (VBD) can be measured from digital images with a proper algorithm.

The breast parenchyma structure depends strongly on the proportion of its different tissue components. It can be quite dense and can consequently mask the presence of a tumor [60]. The breast density, representing an important expression of the amount of fibroglandular tissue, is related to breast cancer risk [61]. Many studies have focused on this topic, especially regarding the relationship between density and breast cancer risk, which clearly seem to be correlated.

Already in 1976, Wolfe investigated a relationship between mammographic parenchyma (functional tissue of a glandular organ) and the risk of breast cancer. The results showed four classifications: N1, P1, P2 and DY with a gradual progression of risk. N1 corresponds to a radiologically transparent mammary parenchyma, very low density, with the lowest risk and DY indicates a breast where the parenchyma is represented by diffuse or nodular densities and where the risk of cancer is the highest. P1 and P2 refer to densities associated with intermediate degrees of risk [62].

Later, N.F Boyd et al shown that mammographic densities are an important indicatorof breast cancer risk [63]. They determined a quantitative classification of densities indicating higher risk gradients in general than other risk factors for breast cancer, using radiological and computer-assisted methods.

Giske Ursin et al [61] investigated the percent and absolute mammographic density of patients aged 35–64 years, from three different ethnic groups, using a computer-assisted method. The breast cancer risk increased with increasing percent mammographic density, for the three ethnic groups without noting a significant difference depending on the ethnicity. The impact of percent density on risk was stronger for older than for younger women.

Cancer risk prediction approaches, taking density into account, improve the predictive risk level. This is of great benefit for high-risk women as well as in screening strategies and diagnostic procedures [64].

Proper radiographic technique, applied on excellent technical performance of the x-ray device are crucial to minimize the dose and optimally visualize all the glandular tissue. Especially important in this regard is breast compression [65].

In mammography, it is important to exert a compression force on the breast in order to spread the gland, reduce breast thickness and thus obtain a better image of the inner breast inside [66]. This compression permits to separate the superimposed structures increasing the precision of the details [67].

However, the compression force cannot be fixed to a constant value. It is largely determined by the large variability in the pain threshold of the patient and the experience and training of the mammography practitioners [68, 69].

Ioannis et al [65] mentioned that there are no quantitative guidelines for the compressive force that should be applied for an adequate mammogram. Indeed, previous studies have concluded that there is great variability in the compressive force depending on screening centers and radiographers, and countries [66]. Other studies have shown [67] that several women complain of pain which may discourage them from participating in screening. Whelehan P et al even suggested reducing the compressive force in order to encourage them to undergo mammographic exams during screening companions [68].

The effectiveness of a mammographic screening program is the best implement for early-stage detection of breast cancer and can potentially reduce the risk of death from breast cancer [69].

Breast screening is well established thanks to numerous measurement campaigns and global investigations across the countries of the European Union. Thus, in order to reduce the mortality rate due to this disease, systematic early detection by screening, effective diagnostic methods and optimal treatment were necessary [70]. National standards help to optimize the quality of screening programs and develop coordination between national, regional and European programs [70].

Special attention should therefore be devoted to a complete investigation and a combined analysis of all mammographic parameters to correctly apply the results to the local population at the beginning of a new screening program. Focused on this direction, this study will contribute to developing the screening methodology and will therefore increase its effectiveness in our country.

Previous studies concluded that a program to promote early detection of breast cancer needs to be tailored to the particular circumstances of each country, because of important differences between and within different populations. For instance, ShivaaniMariapun et al have pointed out a lower precision on mammographic results [71] due to the difficulty of visualizing mammographic details in the Chinese small breasts. A study carried out on the Lebanese population [72] showed that the distribution of breast density is similar to that of Western society and that a high breast density was statistically linked to breast cancer, especially in elderly and menopausal women.

This is why the first step of the study was to check whether there is a resemblance between the compression parameters evolution with the results of previous work based on European standards to be able to apply the same guidelines

In the second part, an analysis of the combined compression parameters was proposed in order to extract possible suggestions relative to the compression range to adopt to guide practitioners when taking a mammographic image. For this; an attempt to identify possible relationships between compression parameters and mammographic density was suggested.

IV.2.2. Material and Method

The present investigation was conducted in a mammography unit of a Moroccan university hospital where a full-field digital mammography system is used. In Table IV.10 the main technical characteristics of the system are summarized. The system was used in Automatic Exposure Control mode (AEC).

Table IV. 10. Technical characteristics of the equipment

System	Detector type pixel and matrix size	Characteristics	X-ray system target/filter
Siemens Mammomat Inspiration (2013)	24 x 30 cm Direct Ray A-Se 85µm 2816*3584	SID =65 cm	Mo/Mo Mo/Rh W/Rh

The study considered DICOM data from 250 patients recorded during mammographic exposures. In this study, the images were taken by several radiologists (non-tecihnicians). The main technical and compression parameters were collected for each mammogram. For each breast, the CC and the MLO images were analyzed.

The Relationship's direction among the breast parameters was expressed by the Spearman correlation coefficient (Rs or ρ). All bivariate correlation analysis expresses the strength of association between two variables in a single value, which varies between -1 and +1. The

sign of the coefficient Rs shows the direction of the correlation. A negative Rs means that the variables are inversely related. The strength of the correlation increases both from 0 to 1, and from −1 to 0. Zero means that there is no correlation [73].

IV.2.3. Results

In the first part of this study we focused on the different mammographic factors, as thickness, glandularity and density related to patient's age.

The average and median values of breast glandularitywere 17.8% and 21.8% respectively (Table IV.11). It was also pointed out that the sample was composed of women in the 29-88 years age range (Figure IV.1) candidate for diagnosis examinations.

Table IV. 11. Overall statistics on patients of all age groups, breast characteristics and compression parameters.

Parameters	Mean ± SD	Median	Range
Age (y)	52±10	51	29-88
CBT(mm)	53.1±11.5	53	22-103
Breast volume (cm^3)	851.3±406.7	804.4	103-2342
Absolute dense volume (cm^3)	66.6±38.7	55.7	12-286
Volumetric breast density (%)	9.3±6	7.3	2.2-38.6
Glandularity (%)	17.8±11.4	14.5	4.3-73.6
Compression force (N)	70.7±14.8	73	28-128
Compression pressure (kPa)	7.9±3.5	7.1	2-25.8

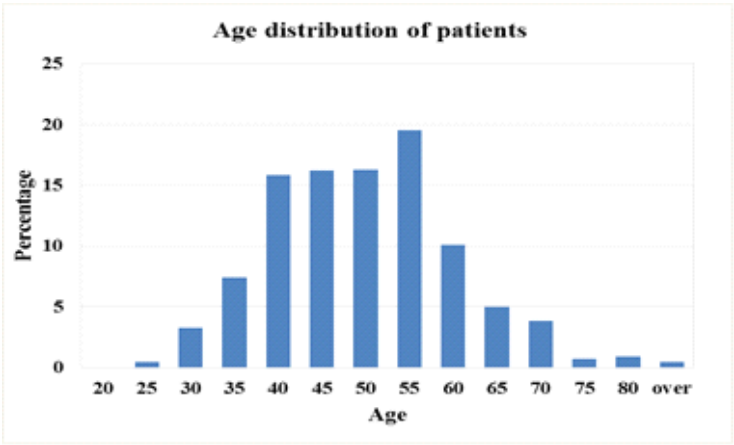

Figure IV. 1. Age distribution of the patients' database

The variation of mean glandularity depending on breast thickness for two groups of age (40-49y and 50-64y) is shown in figure IV.2. Results were compared to those reported by Dance et al [74]. The general trend is similar to that of Dance, but with much smaller amplitudes.

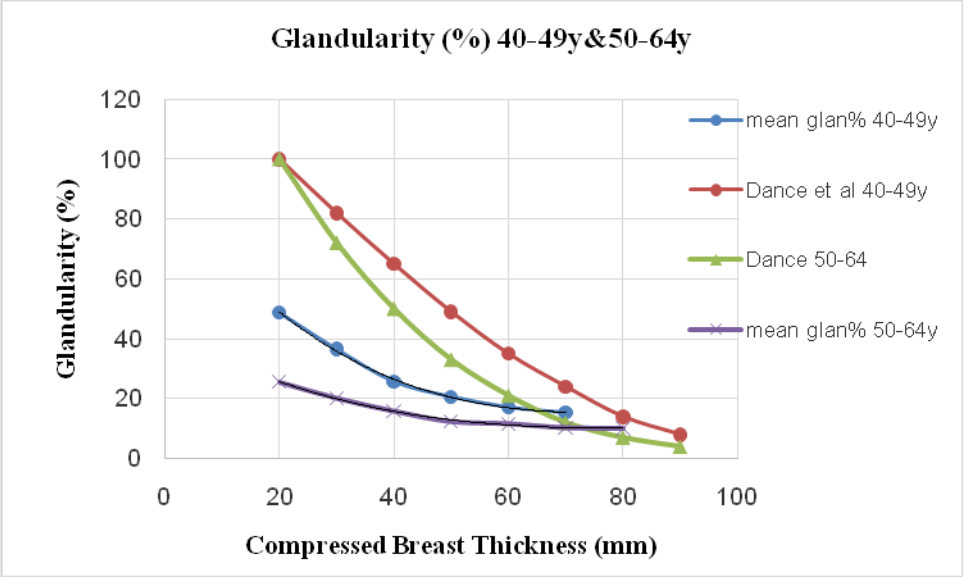

Figure IV. 2. Comparison of glandularity's evolution with Dance results concerning two age groups

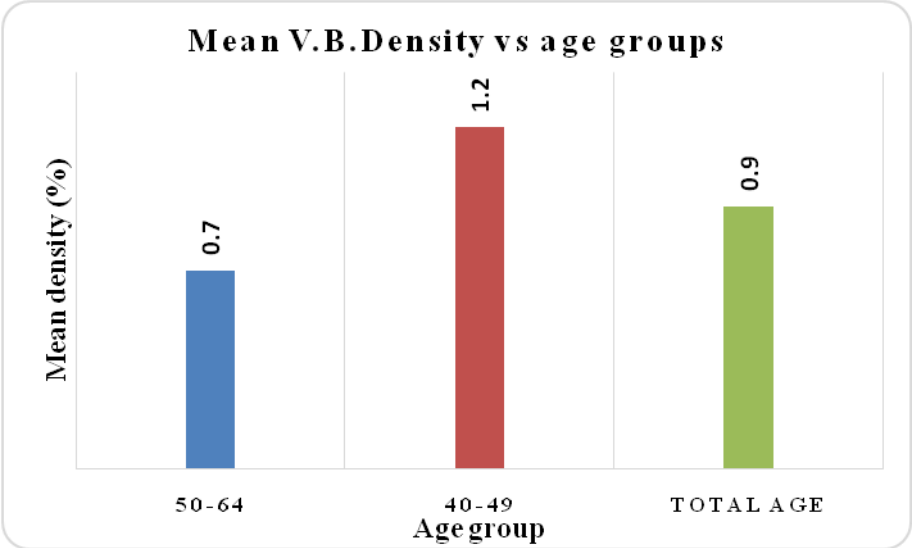

Figure IV. 3. Variation of Volumetric Breast Density with age groups

Figure IV.3 displays the variation of themean volumetric breast density in two age groups. As expected, the density is generally higher for the younger people: the VBD for the 40-49y age range and the 50-64y age range varies up to 12% and about 7%respectively.

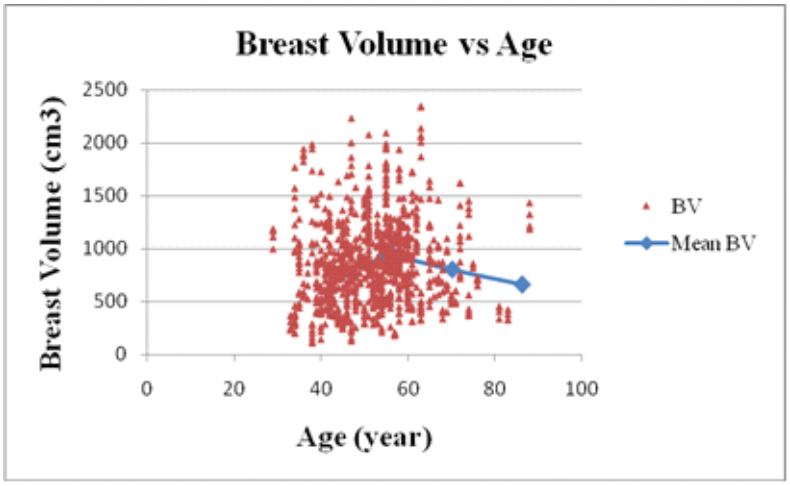

Figure IV. 4. Variation of Breast volume versus age

Figure IV.4 shows that the values vary around an average of 850 cm^3 and that they decrease from about 60 years. A previous study [75] indicated that the average breast volume increases with age and then decreases from a certain age.

The sample taken into consideration in the present part of study was 235 patients, of which the age was greater than or equal to 50 years. The analysis of the latter data was compared with those 250 patients from Leuven University Hospital, taken during a screening campaign. Figure IV.5 giving the average of the volumetric breast density in Morocco and Belgium, shows that the tendency of the two curves is exactly the same with a slight increase in for Belgian patients for small breast sizes. In addition, figure IV.6 shows that the values range of the compressive force is higher for the Belgian data relatively to the breast density and the breast volume respectively. It varies from 40 to about 100N for Moroccan patients while began from about 100N for Belgian population and can reach 160N.

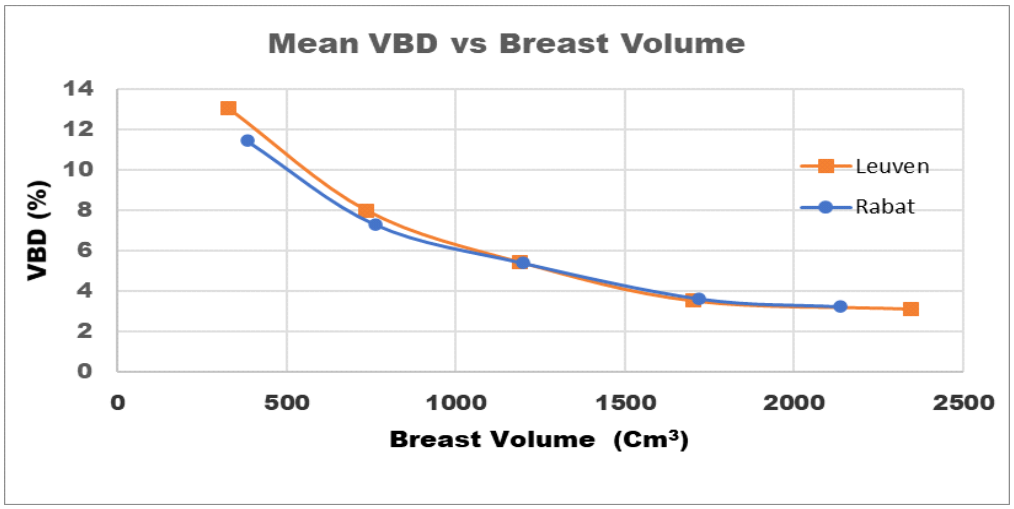

Figure IV. 5. Variation of volumetric breast density versus breast volume for Moroccan and Belgian populations.

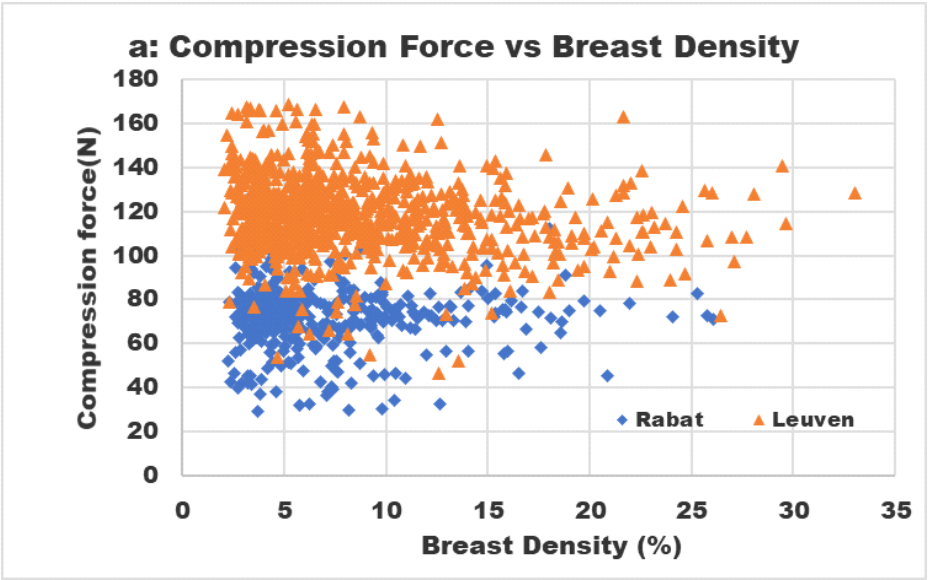

Figure IV. 6. Variation of compression force with breast density for Moroccan and Belgian populations.

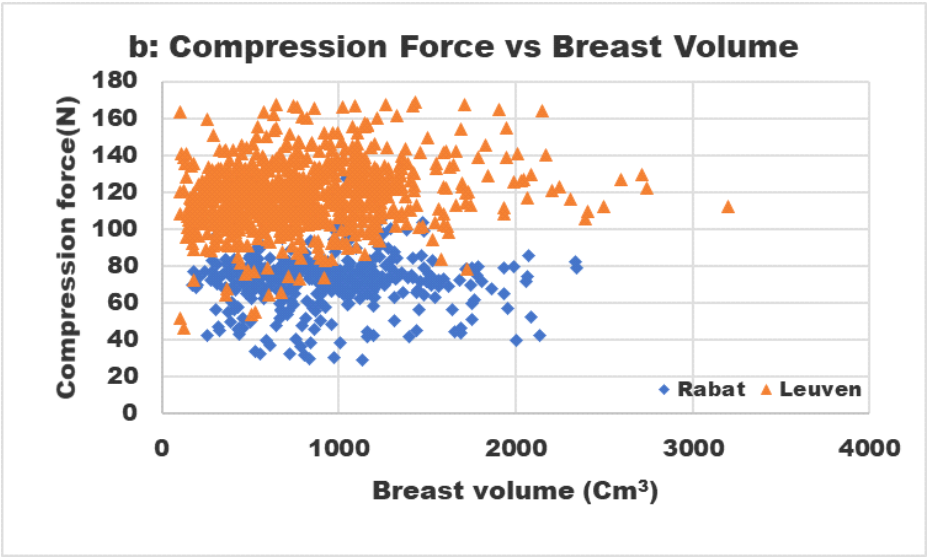

Figure IV. 7. Variation of compression force with breast volume for Moroccan and Belgian population

It is noted that the results are conform to those established by Dance regarding the evolution of glandularity versus the women age groups. In addition, comparison with Belgian results where guidelines in the domain are used, gives similar conclusion. These directives can also be applied for our results, as in our country there are no guidelines yet to assess the results of this study.

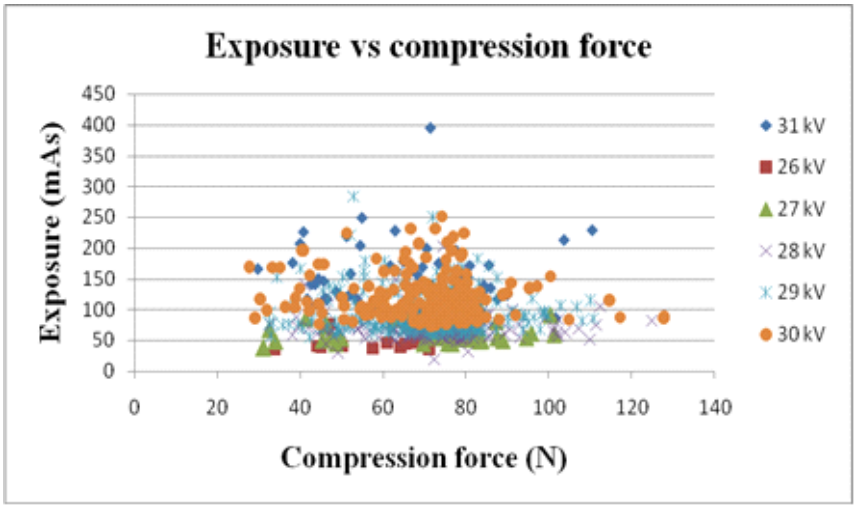

Figure IV. 8. Variation of exposure versus compression force for different tube tension

For all the kV values used, the compressive force is generally between 25 and 80 N (figure IV.8). It is noted that for 26, 27, and 28 kV, the exposure is relatively low and less than 100 mAspermitting thus administered dose reduction.

Several previous studies showed that breast density is related to breast cancer incidence [62.63], mainly because of the possible difficulty to visualize the fine details in mammogram. Precisely, when the breast is dense, it is more difficult to visualize the small details if the compressive force applied is not adequate in order to properly flatten the breast and consequently visualize the small details.

Compression in mammography represents the force exerted on the breast to flatten it by reducing its thickness. Although it has no explicit limitations and this practice can have a significant impact on the quality and visibility of the image. The same compression force may have different pain effects felt by the patient, depending on the size of the breast.

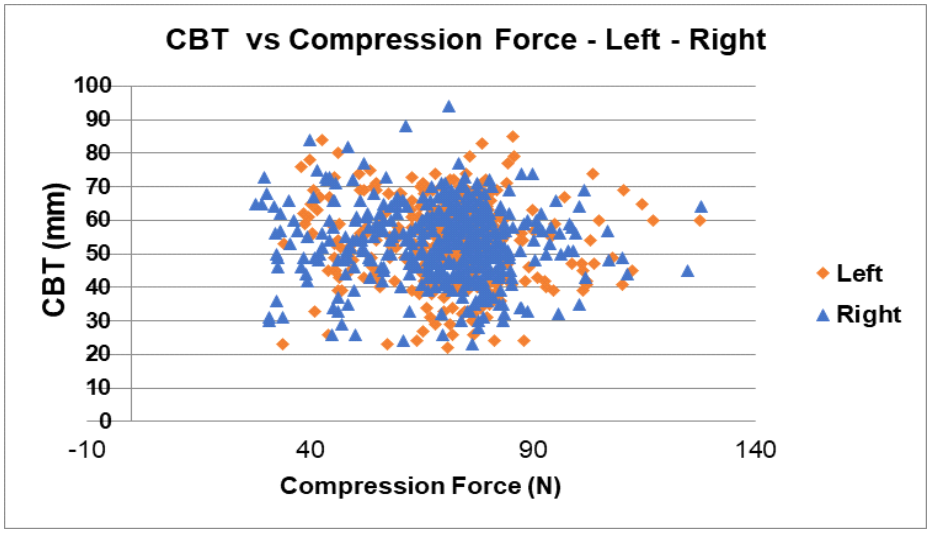

Figure IV. 9. CBT vs compression force for left and right breast side.

The CBT variation vs compression force (figure IV.9), for left and right breast sides are similar and the Rs factor calculation indicates that relationship is poor between these two parameters (Rs=-0,11 left value and Rs= 0,10 right value). CC and MLO left and right.

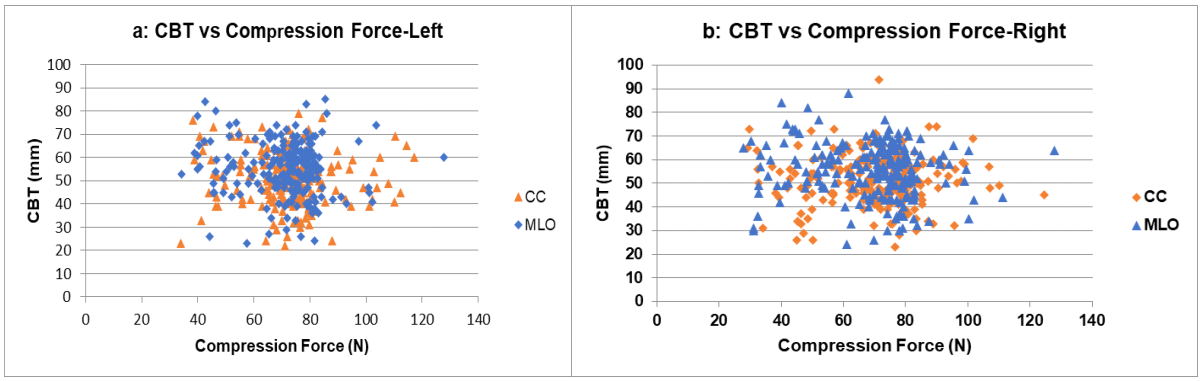

Figure IV. 10. CBT vs compression force CC and MLO; a: left and b: right

Figure IV.10 shows that the point cloud is concentrated between 20 and 80 N for the CC and the MLO projections and for left and right breasts.

In this part, combined analysis of breast compression, breast morphometry, and VBD were investigated to search the relationship between these imaging parameters**.**

Figure IV.11 shows that compression force values used for imaging are included between about 30 and 80N (81%) varying around an average of 75 N (rarely exceeding 100 N). Compression force did not exceed 80 N for volumes larger than 1500cm^2.

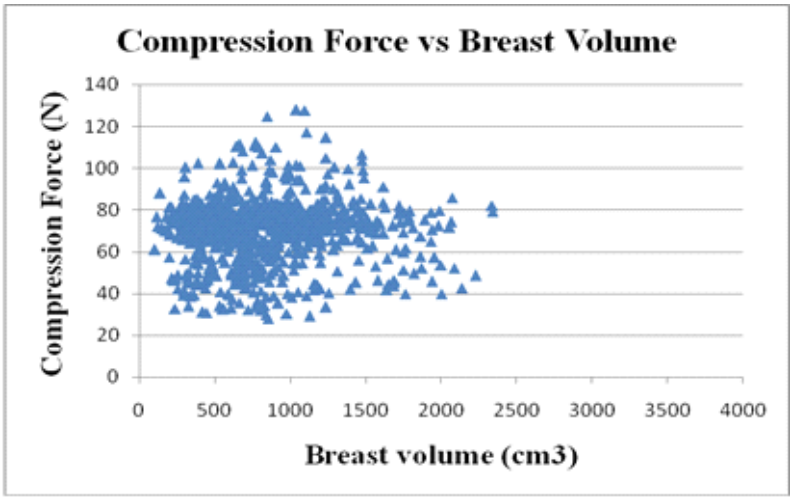

Figure IV. 11. Variation of compression force versus breast volume

Figure IV.11 points out that a broad range of compression values is used for the same breast volume ranging from 30 up to 120N, but the large volumes are visualized with compression forces less than 80 N.

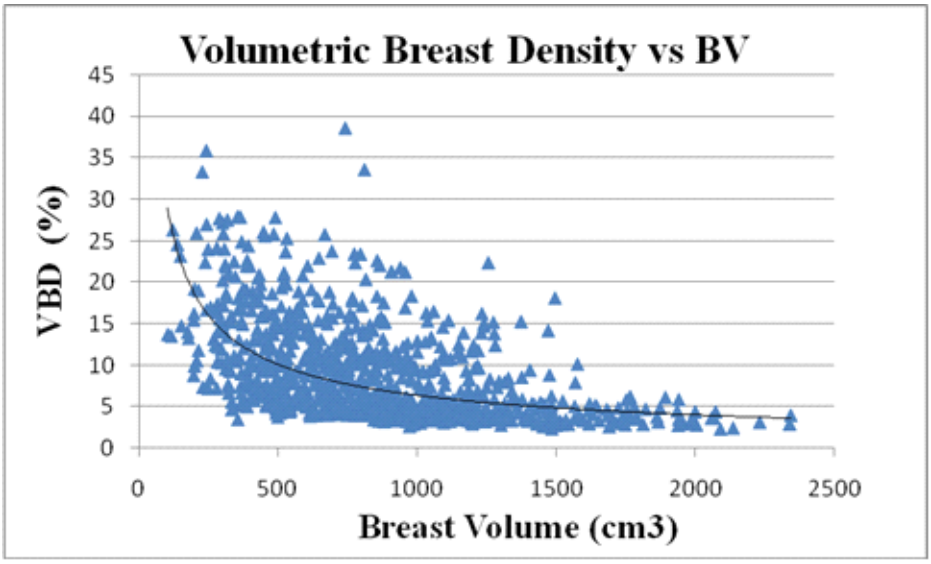

Figure IV. 12. Variation of VBD versus breat volume

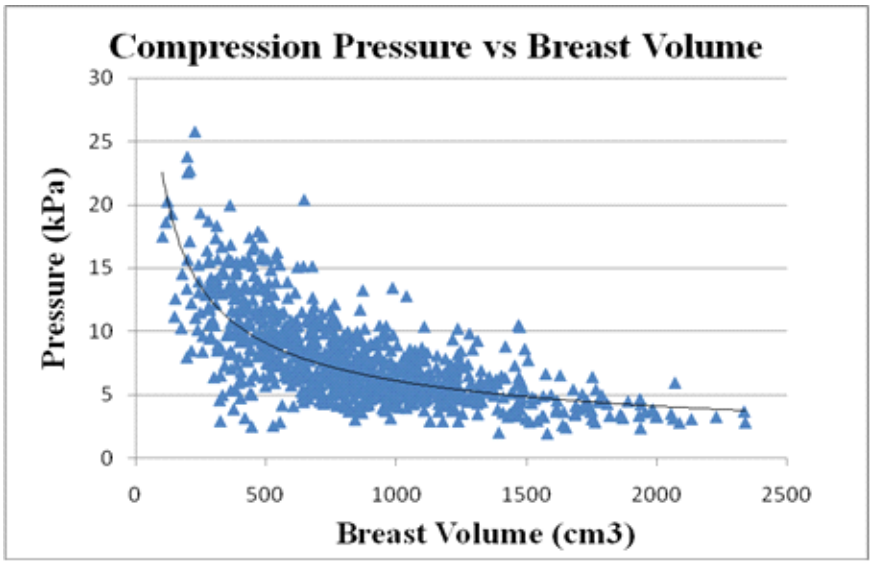

Figure IV. 13. Variation of compression pressure versus breast volume

Figures IV.12 and IV.13 show that the density decreases with increasing volume and the lowest compression pressures correspond to large volumes.

It is observed that larger breasts are imaged using lower pressure (Figure IV.13) and the small volumes correspond to higher pressures. A negative moderate correlation was observed between these parameters (Rs=-0,689). This trend was also emphasized by Holland et al [65]. These authors also suggest that additional research is needed to confirm the potential effects of pressure on mammographic performance and that greater attention should be considered to achieve a significant standardization of compression levels that could improve mammography in the future. The statistical results did not permit to clearly distinguish the relations between the pressure and the density but the calculation showed that there is a fair

tolerable relationship between breast volume density and compressive pressure (Rs = 0.46).

Our results pointed that the lower pressures correspond to higher breast volumes and consequently to the higher contact areas. Figure IV.14a represents the variation of compression pressure versus the contact area, evince that effectively higher pressures are needed to display small breasts (small contact area). Figures IV.14a and IV.14b show that the pressure is all the higher as the contact surface is small and that for a given value of the contact surface several values of this one are used. This once again confirms the great variability of this parameter during mammographic examinations.

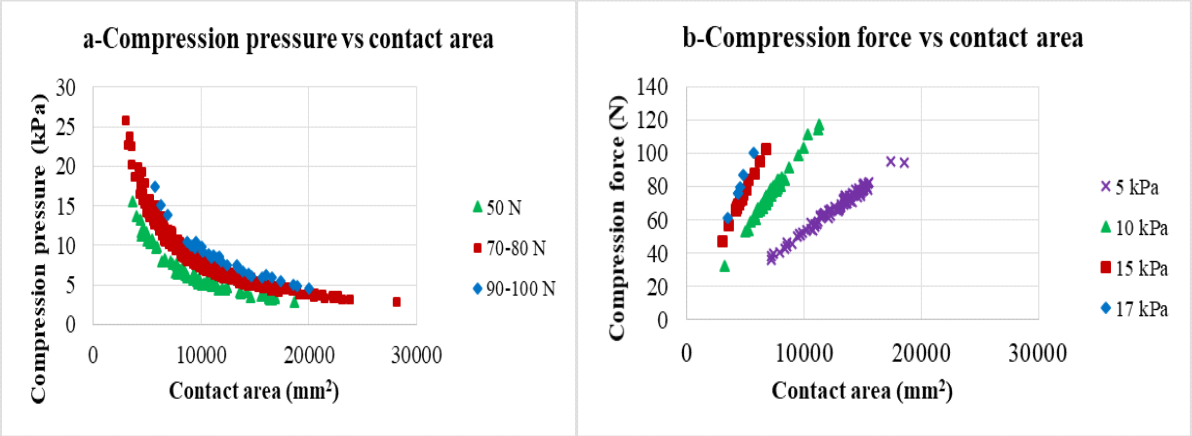

Figure IV. 14. Variation of –a-compression pressure –b-compression force versus contact area.

Figure IV.14 gives interesting indications since it shows the implication of two compression parameters at the same time, according to the volume of the breast.

IV.2.4. Discussion

The variation of glandularity according to age and breast size shows that it is higher for young patients and for compressed breast thickness (CBT) less than about 45 mm. This agrees well with the results of the dance (Figure IV.2).

The direct comparison of the evolution of the compression parameters between the Moroccan and Belgian populations (Figure IV.7), leds to a good similarity. It was also noted that the two populations had the same range of breast size. Moreover, for the same volume of breast, the density is lower in Moroccan patients probably due to the greater proportion of adipose tissue relative to fibrous one. This suggests that the guidelines already established in European countries can be used to carry out a mammography screening examination in our country, while waiting to develop our own.

Among the objectives of this investigation was to try to find correlations between

compression parameters and mammographic and technical parameters, as there is not yet quantified limit for compression force.

Results analysis considered hypothesis testing ie: paired samples t-test to determine if compression vs left and right was different. A poor negative correlation was noted between CC and MLO (Rs=-0.11, Rs=-0,1) left, and right respectively.

The study pointed also out that there is no correlation between age and compression force (Rs=0.006). It was noted that coefficient Rs= -0.208 indicated that there is a negative poor correlation between age and compression pressure.

It was recorded that breasts with the same volume are imaged using a wide range of compressions (from about 30 up to 120 N), while for the large volumes forces less than 80N were applied. This can be explained by the fact that exerting a compressive force on a breast means flattening it; this does not mean changing its volume.

Strong negative correlation was identified between compression pressure and breast volume (Rs= -0.689), and a moderate negative correlation was identified between BVD and breast volume (Rs= -0.57).

This trend was also observed by Moshina et al [76], except for the large breasts that were visualized using higher compression forces than used in this study. Indeed, an earlier study demonstrated a significant difference in the average compression used by different practitioners. This factor was applied in three groups: low, medium, or high compression with no significant difference in average compression in each group. The compression has varied considerably for a given volume and the general trend has been the application of higher compression to larger breast volumes by the three groups of practitioners [77]. This study highlighted variation in the application of compression by practitioners and encouraged further investigations in order to facilitate a new perspective on the analysis of compression variables in mammography

A wide spectrum of compression forces is generally used, depending on radiological practices in the mammography centers. This was noted in different previous works pointing out the absence of indications to follow for this parameter. According to European recommendations [78] it's denoted that, to have good image quality, the breast must be sufficiently compressed but no more than necessary, without giving a quantitative indication. Figure IV.11 showing the variation of compression force with breast volume indicates a similar trend between our results and those of recent work [65].

The similarity of the mammary characteristic’s evolution according to the age, the breast thickness, and the compression parameters of the Moroccan population and the Western

population was clearly exhibited. This was also exposed by a direct comparison of Moroccan and Belgian patient data. The European guidelines can then be extrapolated to the Moroccan population.

Furthermore, previous studies have shown that there is still no quantified limitation of the application of the compression force in mammography and that there is great variability in the values used depending on the collection centers of data[65, 66].

It was then necessary to study this parameter through the data collected in our population and to try to find out whether correlations are possible between the force used and the mammographic parameters. This is the subject of the second part of this work.

The compression forces applied in present investigation's hospital are generally weak compared to those described in previous works [76, 65]. It seems that the range depends on strategies adopted by the mammography service. Indeed, a comparative study between Netherland and in the USA, employing the same strategy, investigating the variation of compression force versus contact surface [66]concluded that the evolution trend of the two studies was similar but the compression forces range used clinically by each study was different; the values were lower for the US population. They were concentrated between 50 and 150 N for the US and between 100 and 200 for the Netherlands. Thus, the authors called for a need of mechanical standardization for breast compression.

The results of our work led to the same conclusions but using the lowest compression forces, than those of these studies, rarely exceeding 80 N.

A recent study [Egyptian journal 2022] investigated the relationship between volumetric density grade (VDG) and risk of breast cancer in premenopausal and postmenopausal age groups for Indian women. The authors suggested a positive association between high VDG and cancer risk in premenopausal and postmenopausal women.

Sham CBT was positively correlated with breast volume ($r > 0.868$) and negatively correlated with VBD ($r < –0.338$). The results of this study provide a topic-specific, evidence-based suggestion of mammographic compression force for radiographers with consideration of image quality and patient comfort. The authors concluded that there is a positive association between high VDG and cancer risk in both age groups.

In a study developed by Tien-Yu Chang et al [Electronic 2022] based on the construction of specific breast models concluded that a personalized and evidence-based compression force suggestion can be provided to radiographers taking into account the quality image, patient comfort and radiation dose.

The technologist must adjust the force of compression according to the size of the breasts,

their composition and the patient's tolerance to pain. Work habits mean that the compression is more or less strong depending on the region of the globe, ranging from less than 3 kilopascals (kPa) to more than 30 kPa.

A literature review was conducted by Elizabeth Serwan et al [compression practices] to explore existing breast compression force and pressure standardization protocols in clinical application. The authors suggest that the synthesis of published studies in the field may lead to the implementation of mechanically standardized mammographic compression pressure as a feasible tailored approach for clinical practice. They also conclude that as a suggested mammographic guideline, compression pressures of approximately 10 kPa contribute to the reproducibility of image acquisition; pain levels decrease, with minimal variations in breast thickness, mean glandular dose, and image quality.

IV.2.5. Conclusion

The patients considered in this investigation were a sample of Moroccan women, characterizing the population presented to a diagnostic mammography examination at a hospital that receives a large number of women enrolled in the breast screening program.

The similarity of the mammary characteristic's evolution (Volumetric breast density VBD, of the glandularity, …) according to the age, the breast thickness, and the compression parameters of the Moroccan population and the Western population was clearly exhibited. This was also exposed by a direct comparison of Moroccan and Belgian patient data and Dance's investigation. The European guidelines can then be extrapolated to the Moroccan population.

In previous studies there is a significant variability in the compression force use, noting an absence of range limit values. In this work, we tried to figure out whether there are correlations between the compression parameters and the technical and mammographic parameters. This was the subject of the second part of the investigation.

Strong negative correlation was identified between compression pressure and breast volume and a moderate negative correlation was identified between BVD and breast volume, without, however, giving an explicit range of values to be applied during radiological examinations.

After this preliminary study, it would be interesting to include a larger number of establishments and equipment, to have a more complete idea of the exposure parameters used in Moroccan hospitals. The next step will be to provide education to radiographers and see the impact on new data analyses.

IV.3. Article 3: Validation and comparison of intensity modulated radiation therapy patient plans with Octavius 4D Phantom using the Gamma Index analysis in 2D and 3D.

IV.3.1. Introduction

Intensity Modulated Radiotherapy (IMRT) by modulating the beam intensity across each treatment field allows for better dose conformation particularly to concavely shaped contours of the target volume which is enough to control tumour cells, while reducing doses to normal tissues by modulating photon beam intensities by varying the Multi-Leaf Collimator (MLC) positions [79]. IMRT can produce highly conformal radiation dose distributions and enhance treatment localization. These complex treatment techniques also place higher demands on delivering dose treatment in terms of both accuracy and verification of treatment plans [80]. The verification of treatment plans in Intensity Modulated Radiation Therapy (IMRT) is focused on the linear accelerator and in particular the MultiLeaf Collimator (MLC). It involves evaluating and comparing the parameters of the treatment plans delivered by the linear accelerator with those planned. Complex treatment plans such as those developed in IMRT cannot be controlled by in vivo dosimetry. Verification in IMRT consisted mainly of the use of 2D measurements, but technological advances in medical physics have led to the use of new 3D measurement phantoms [79-81].

To control these types of treatments, more complex solutions are implemented, based on the use of a PTW Octavius 4D phantom by checking a Gamma index (γ) introduced by Low et al. [82]. In this case, a 4D system is used to carry out the verification of the treatment plans. The special feature of this system is that it allows a quick and direct analysis. The verification of the 3D measurement is an extension of the 2D measurement with another dimension, allowing later on an evaluation and verification of the volumetric distribution of the dose along the x, y and z axes to be taken into account by verifying the superposition of isodoses and profiles. In this work we compared the measured dose distribution with the calculated dose distribution, the γ assessment method is adopted in this study, which quantifies both the absolute Dose Difference (DD) and the Distance-to-Tolerance Criteria (DTA) [83]. The DD represents the positional deviation between the two calculated and measured dose matrices [84]. DTA is used to compare doses in areas of high gradients, where only a deviation is of little interest, because a small positional deviation results in a large dose difference.

The γ Index analysis is based on DTA and DD, and is designed to check regions of low and

high dose gradient. This test is only successful when the DD and DTA criteria are all valid. This index is formulated so that when the value ≤ 1, the patient's plan is accepted and when the γ value is greater than one, the plan is rejected [85-86]. Thus, the γ index is a measure of the quality of the treatment plan that presents the percentage of dose points that meet the acceptance criteria [87].

The aim of this study is to ensure the quality of treatment plans by the IMRT using sophisticated analysis software such as Verisoft which offers many options such as γ index comparison.

IV.3.2. Materials and Methods

We studied 10 patients from two localizations Head and Neck (HN) and Prostate treated at the Department of Radiotherapy, University Hospital Hassan II Fez in Morocco. HN localization was stabilized in supine position, with thermoplastic mask attached at five fixation points to a carbon-fiber plate support (CIVCO Radiotherapy Coralville, Iowa, USA). For Prostate cancer, we used a knee and foot support as immobilization device. CT simulation was performed in 3 mm slices using Siemens Somatom Sensation Open CT (Siemens, Erlangen, Germany). In this work all the treatments were carried out with a Varian 2300 DHX linear accelerator (Varian, Palo Alto, CA, USA) equipped with a dynamic MLC, with a width of 1 cm projected at the isocentre. Two energies are available in the photon mode (6 MV and 18 MV). For the IMRT, 6 MV X-photons were used for Head and Neck tumours and prostate tumours. The calculation and optimisation of the dose were performed by an Eclipse treatment planning system using the Analytical Anisotropic Algorithm (AAA) (v.10.0.28).

The quality control checking the fluence is carried out with the help of an Octavius 4D phantom by PTW. This is a 2D matrix of ionisation chambers, which is inserted into a motorised homogeneous cylindrical phantom. The cylindrical phantom is made of acrylic with a density of 1.05 g/cm3 . The system rotates synchronously with the rotation of the accelerator arm by using an inclinometer attached to the accelerator. This ensures that the beam incidence is always perpendicular to the plane detector inserted in the phantom (Figure IV.15).

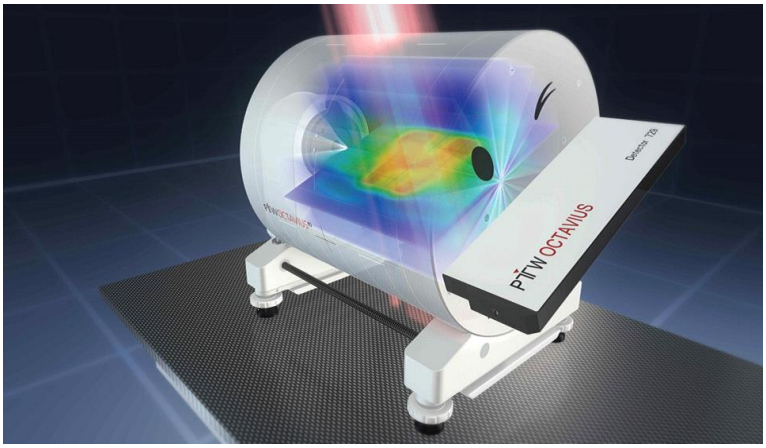

Figure IV. 15. The OCTAVIUS 4D system.

The detector panel 2D is inserted in a cylindrical phantom that rotates synchronously with the gantry. The detector 2D Array This matrix is composed of 1500 ionisation chambers with a size of (4.4 × 4.4 × 3) mm3, whose centres are separated two by two by 7.07 mm. The matrix therefore has 27 rows of 27 chambers ([105] Phantom Octavius Linac and Octavius CT).
Two types of phantoms are used for the quality assurance of the treatment plans shown in Figure IV.16 by a slice section to observe their internal structure.

The CT phantom: This is a cylindrical phantom made of plastic materials equivalent to water with a density of 1.05 g/cm3. It has a rectangular opening and has a detector array or perforated inserts that can accommodate one or more cylindrical chambers.

The LINAC phantom: Also a cylindrical phantom with the same characteristics as the CT phantom with the difference that it also has a semi-cylindrical air cavity in its lower part to correct the non-water equivalence of the matrix.

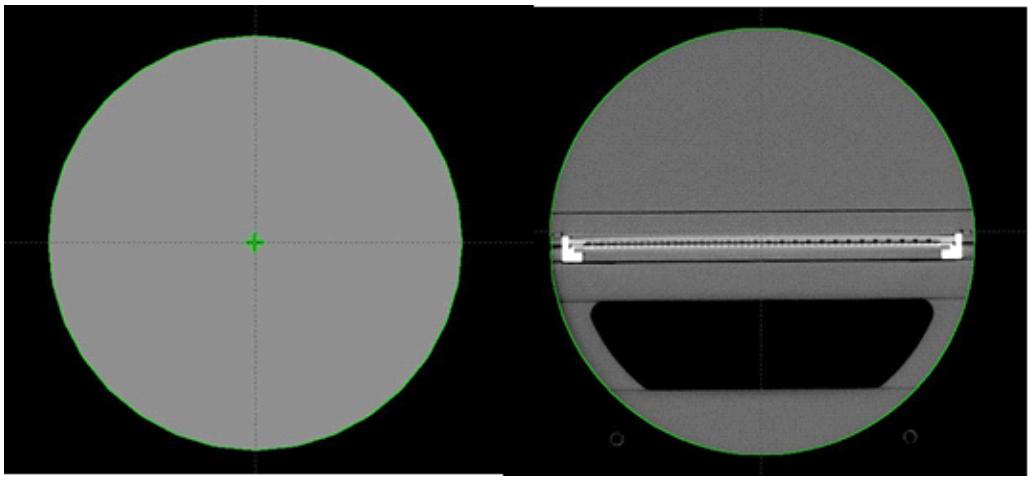

Figure IV. 16. Internal view of the CT and LINAC phantoms

The measurements are taken and sent to PTW's analysis software Verisoft V4.1. Calculation-

measurement consistency is evaluated by the γ index test, proposed by Low, et al. [82] to perform a global analysis of a dose distribution. This γ index combines Dose Difference (DD) in % for low gradient areas and distance Distance-to-Tolerance criteria (DTA) in mm for high gradient areas.

Gamma index The γ index is a comparison tool that takes into account both the difference in dose as well as the difference in distance between the two distributions. The principle is as follows: the calculated dose/measured dose difference is evaluated for each point. A deviation of less than 3% is considered acceptable. However, if the deviation is greater than 3%, the measurement software searches around the point in question for points that receive the same dose. If the distance between these points is less than 3 mm, this is considered correct. Overall, 95% of the pixels must meet these criteria for the treatment plan to be validated by the physicist (Figure IV.17). It gives a picture of the physical differences between the calculated and measured dose distributions [82, 88-90]. The definition of the γ index is defined by the following equation:

$$\Gamma(r_m, r_c) == 1$$

$$\gamma = \min \Gamma(r_m, r_c)$$

• ΔDmax is the criterion that represents the maximum accepted dose difference in percentage (applied to regions with a low dose gradient).

• DTA (Distance-To-Agreement) is the criterion that represents the maximum accepted distance difference (applied to regions with a high dose gradient) in mm.

• Δr, the distance between the reference point and the measured point in mm.

• ΔD, the dose difference between the reference point and the measured point in %.

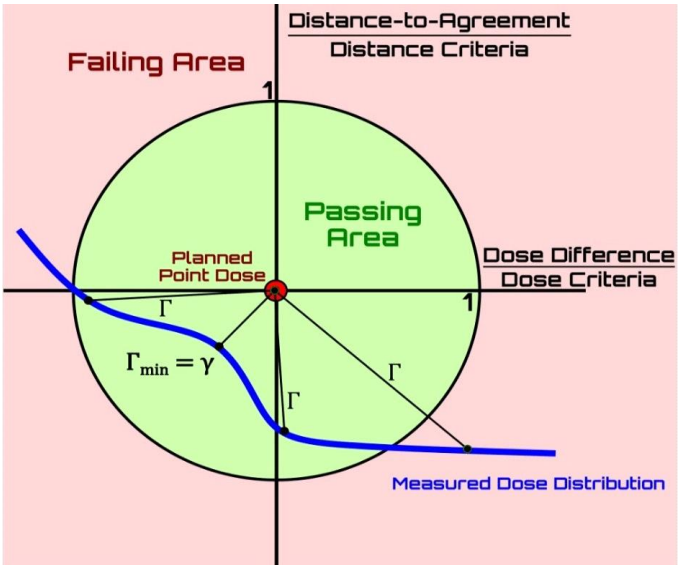

Figure IV. 17. Evaluation principle of the Gamma function[106]

IV.3.3. Results

The validation of treatment plans requires the comparison of calculating and measured dose distributions. Displaying a two dimensional distribution is the most commonly used methods. Qualitative validation is usually performed by superposing calculated and measured isodoses and profiles. Currently, analyses are performed on computers with sophisticated software called Verisoft, which offers many options such as γ index comparison. Superposition of isodoses: For the comparison of calculated and measured isodoses, it seems difficult to establish a quantitative verification criterion, so the results are quite qualitative. However, the superposition of the isodose lines was carried out by the dotted calculation and the measurement, which allows an immediate overview of the similarity of the two isodoses (calculation and measurement) with the help of verisoft software. The tools at our disposal allow us to superpose the results obtained in the three directions (Transversal, sagittal and coronal). In addition, the results of the comparison of isodose lines are shown in Figure IV.18

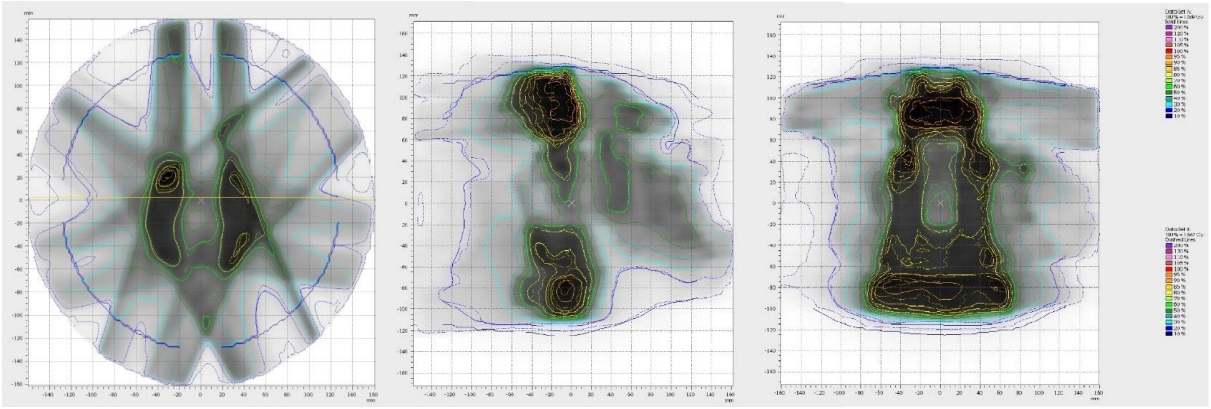

Figure IV. 18. Comparison of calculated and measured isodose lines for the Transverse, Sagittal and Coronal planes

This strictly visual study makes it possible to show the good general correlation between the calculated and measured dose plans. Thus, deviations could be observed for certain isodoses (calculation and measurement) during the verification of superposition. These differences were due to a problem of dose rates. Sometimes, the speed of leafs failed to meet the modulation constraints imposed on the accelerator. This parameter is therefore to be considered if the correspondence is not adequate. Superposition of profiles: Several profiles were measured by our Octavius 4D phantom to compare the profiles in order to validate treatment plans. Whatever the technique, the profiles measured in the transverse, sagittal, coronal and also diagonal planes are globally superposable with the calculated profiles.

Our objective in this study was to show the capacity of the machine during the delivery of the treatment, but also to prove the feasibility of the controls with the Octavius 4D phantom. To illustrate this, below the dose profiles are presented comparing the calculation and the measurement profiles as shown in Figure IV.19.

NB: Calculated profile in blue and the measured profile in orange.

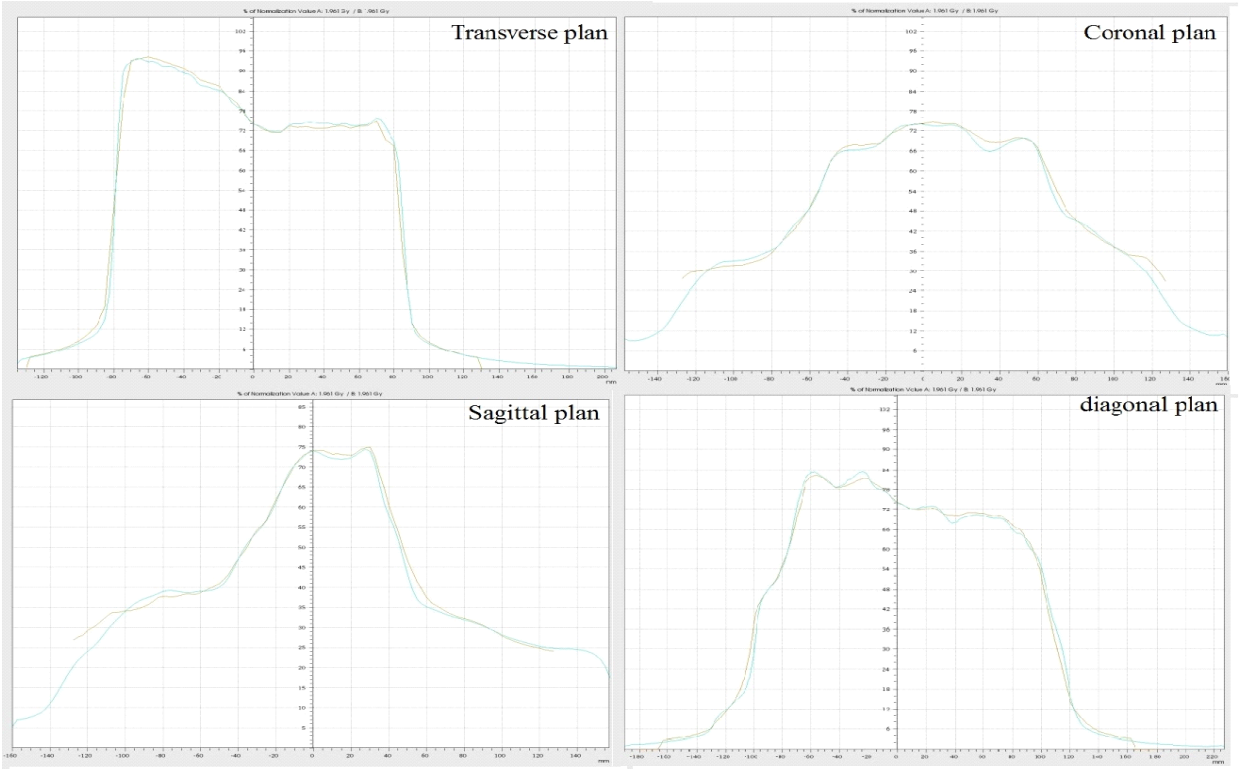

Figure IV. 19. Dose profiles for the transverse, coronal, sagittal and diagonal planes

Overall, the calculated dose distribution is accurately measured with the Octavius 4D phantom. However, there may be differences between the calculated and measured profiles in several directions. It is therefore possible to quickly identify the areas most affected by significant errors. Above all, it is possible to differentiate the observed differences according to whether they appear in a high or low dose area or whether they are contained in high or low gradient. In this way the planning console calculates a smooth profile, which is certainly less correct than the measurement that it represents high gradients. Also on the superposition of two dose profiles, one can identify deviations in amplitude and deviations in distance. In this case, always check for resetting and normalization. If a discrepancy persists, then the Multi Leaf Collimator may be involved as shown in figure IV.20. Other causes may be involved: the direction of movement of the blades, at the junction between two leaves, discrepancies are often observed between the calculation and the measurement. These

differences are certainly due to the modelling of the leakage between leaves in the calculation algorithm.

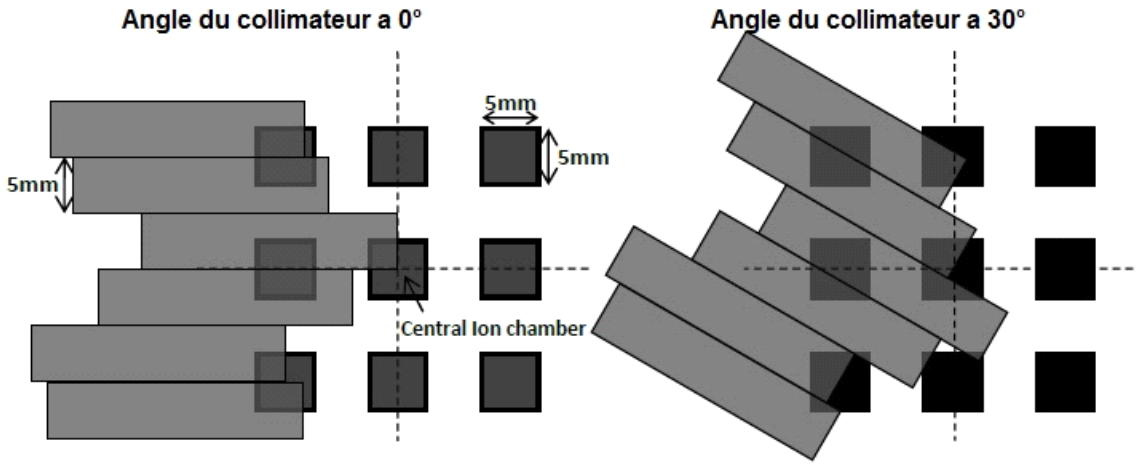

Figure IV. 20. Diagram of the overlap between the MLC of 5 mm and the ionisation chambers of the 2D-Array matrix for a collimator rotation of 0° and 30° degrees. The dotted line indicates the central axis.[107]

Study of the Gamma (γ) index The γ index provides a quantitative study or analysis of the correlation between the calculated and measured dose, the calculation of this index is based on the concept of Low [82]. Tables IV.12 and IV.13 show the results obtained in a population of ten patients planned with a 2D and 3D analysis. As an example, figure IV.21 shows the results of the γ index analysis for the pass/fail test. This test displays images of the three planes (Transverse, Sagittal and Coronal) in which pixels with γ less than 1 are shown in green and pixels with γ greater than 1 in red and blue.

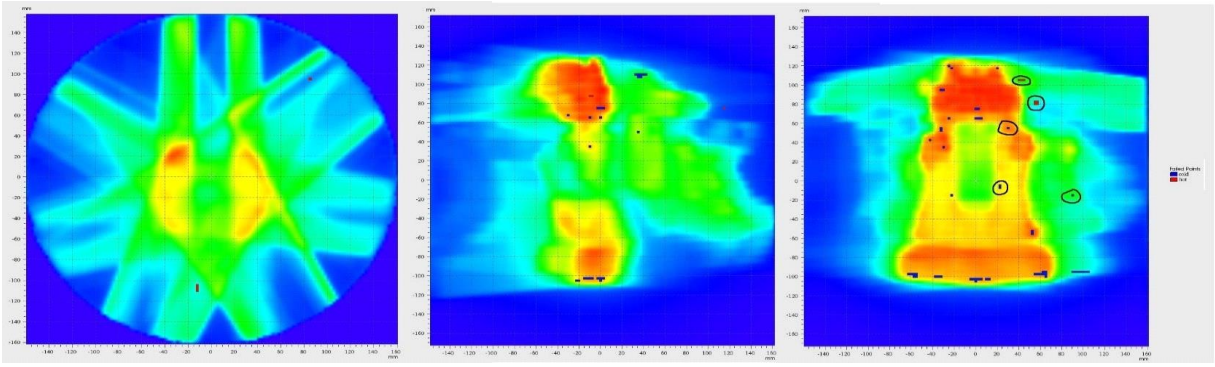

Figure IV. 21. Results of a pass/fail test for the calculation of the γ index in a transverse, sagittal and coronal planes

We performed a comparison of the DD as well as the DTA for our 10 patients with malignant

neoplasms using different criteria: 3%/3 mm, 3%/2 mm and 2%/2mm DD/DTA. The choice of these criteria was made to obtain and observe as much information as possible about the correlation between the calculated and measured dose plans. We then evaluated the DD between the doses delivered by the Varian machine and the dose predicted by the TPS. When analysing the γ index for the pass/fail test, we obtained the following results for the 3%/3mm criterion: 97.11% and 99%. For the 3%/2mm criterion, the γ index results were 95.42% and 96.81%. For the last criterion of 2%/2mm, we found 92.01% and 93.66% of accepted points for 2D and 3D analysis respectively as shown in Tables IV.12 and IV.13. For all 10 patients considered, the γ index varied between 0.13 and 0.46; between 0.13 and 0.46; between 0.17 and 0.62 for the 3%/3mm, 3%/2mm and 2%/2mm criteria respectively as shown in Table IV.13. These results show that quantitatively, the use of the Octavius 4D Phantom allows a better comparison between calculation and measurement. Indeed, the results obtained with the 3%3mm criterion are perfectly comparable to those obtained with the TPS.

When analysing the γ index for the pass/fail test, we obtained the following results for the 3%/3mm criterion: 97.11% and 99%. For the 3%/2mm criterion, the γ index results were 95.42% and 96.81%. For the last criterion of 2%/2mm, we found 92.01% and 93.66% of accepted points for 2D and 3D analysis respectively as shown in Tables IV.12 and IV.13. For all 10 patients considered, the γ index varied between 0.13 and 0.46; between 0.13 and 0.46; between 0.17 and 0.62 for the 3%/3mm, 3%/2mm and 2%/2mm criteria respectively as shown in (Table IV.13). These results show that quantitatively, the use of the Octavius 4D Phantom allows a better comparison between calculation and measurement. Indeed, the results obtained with the 3%3mm criterion are perfectly comparable to those obtained with the TPS.

Table IV. 12. Results of the γ-index success rate for a sample of 10 patients in our centre in 2D analysis

	γ-index passing rates (%)								
	3%/3mm			3%/2mm			2%/2mm		
P	Trans	Sagi	Coro	Trans	Sagi	Coro	Trans	Sagi	Coro
1	98,2	96,9	97,5	98,8	94,6	95,7	96,7	91,7	92,1
2	98,6	96,4	97,2	98	93,3	94	94,5	87,7	89,5
3	97,8	97,7	97,8	95,2	94,2	95,4	90,5	89,1	91,2
4	99	98,7	98,4	98,6	97,6	96,3	96,8	94,1	93,7
5	98,7	97,7	97,4	97,3	94,2	93,8	94,1	87,4	89,6
6	98,2	98,2	98,3	96,5	95,7	95,9	93,3	90,9	91,6
7	98,7	98,8	98,9	98,1	98,2	98,8	96,8	97,8	98,1
8	98	97,6	97,6	91,4	93,1	94,2	92,1	90,4	91,2
9	98,5	97,3	96,7	96,1	94,7	92,9	91,5	91,5	89,5

10	99	99	98,9	99	98,8	97,2	97,4	97,5	97,2
M	98,47	97,83	97,87	96,9	95,44	95,42	94,37	91,81	92,37
ET	0,41	0,85	0,73	2,30	2,06	1,77	2,49	3,65	3,08
M		98,06			95,92			92,85	

Table IV.13: Results of the success rate in % and the γ-index values obtained when comparing the calculated and measured plans for a sample of 10 Patients in our center with 3D analysis.

	γ-index passing rates (%)					
P	3%/3mm	Indice γ	3%/2mm	Indice γ	2%/2mm	Indice γ
1	98,7	0,276	96,4	0,276	91,9	0,410
2	97,3	0,397	93,9	0,400	87,7	0,568
3	98,3	0,424	95,2	0,427	89 ,9	0,600
4	99,6	0,340	98,1	0,386	95,1	0,550
5	99,1	0,456	95,9	0,460	91,3	0,624
6	99,4	0,379	97,2	0,380	93,4	0,548
7	99,8	0,085	99,4	0,085	98,8	0,105
8	99,1	0,317	96,1	0,318	92,6	0,472
9	98,9	0,284	96,7	0,284	93,7	0,426
10	99,8	0,127	99,2	0,127	98,4	0,168
M	99	0,31	96,81	0,31	93,28	0,45
ET	0,77	0,12	1,73	0,13	3,48	0,18

IV.3.4. Discussion

In this study, a criterion of 3%/3mm was established as a standard for verification of intensity modulated treatment plans based on a γ index [91-93]. We presented the results of the γ index assessment for IMRT treatment, according to the 3%/3mm, 3%/2mm and 2%/2mm criteria. The γ assessment with 3%/3mm has been successfully applied for patient-specific quality assurance before treatment in our institution for two years. Several studies have recently shown that the percentages of accepted points in the 2D γ Index test are not relevant, in contrast to the 3D dose parameters [94,95]. The information from the 2D γ assessment is not sufficient to detect errors in the administered doses that are 3D in the patient's body [96]. Furthermore, γ evaluation is a comprehensive tool for checking the whole plan and not the doses delivered to each organ individually, the accuracy of dose delivery to each structure, including target volumes and OAR, cannot be checked individually with γ evaluation [97]. However, as initial measurements and quality assurance of the treatment plans showed that the MLC movements were larger than expected, it is necessary to find conditions that meet the standard γ index criterion in line with other studies that have analyzed the sensitivity of

IMRT with γ indices of 3%/3 mm, 3%/2 mm and 2%/2 mm [98].

Thus, the various DD and DTA controls were performed to see to what extent the criteria could be reduced to simultaneously achieve a success rate of more than 97% for IMRT treatments and still be strict enough to allow for the containment of execution errors of plans that do not meet the selected γ index criteria. In the present study, we compared the results of the 2D and 3D analysis for a variety of DD and DTA criteria. For all parameters assessed, the differences between the 2D and 3D results were slightly different. In terms of average, in all conditions evaluated in this study, the percentage of success for a 3D analysis was 99% compared to 2D which was 97.11% of pixels for the γ index. On the other hand, larger analysis errors were expected in the 2D results than in 3D because the 2D analysis is more sensitive to dose gradients perpendicular to the measurement plane (as there is no data above and below the plane to allow for a DTA analysis to compensate for these errors in that dimension). This would result in an even greater difference between the γ index in 2D and 3D, as shown by Sanghangthum, et al. [99] for IMRT treatment plans. Although the literature and current clinical practice indicate that γ measurement success rate, whether in 2D or 3D form, is commonly used for routine IMRT QA, it should be noted that the literature raises the question of whether or not γ measurement success rate alone is useful in IMRT QA for detecting plan errors. Indeed, two independent studies by Kruse [100] and Nelms, et al. [101] have shown that 2D γ measurement has a low sensitivity for detecting clinically relevant plan errors.

Our study also shows another problem with current QA practices in IMRT, namely the higher γ index success rate associated with the low dose thresholds commonly used by the medical physics community. A survey of QA practices in IMRT by Nelms and Simon [102] showed that all responding facilities used a low dose threshold between 0 and 15%, most commonly a low dose threshold of 5-10%. These low-dose thresholds include a large number of low-dose pixels, which may result in an inflated pass rate when assessed using an overall dose difference criterion. This is consistent with our results which showed an increasing pass rate for 2D and 3D γ with a decreasing low dose threshold (2D and 3D being 95.2% and 97.1% with a low dose threshold of 15%, compared to 98.06% and 99% with a threshold of 5%). In general, there are many differences between planar and volumetric analysis for checking treatment plans. Individual plans in 2D analysis may miss problems that would be identified with 3D analysis, but may also highlight areas where problems exist.

IV.3.5. Conclusion

Before the start of treatment of each new patient with intensity modulated conformal radiotherapy, a time slot is set aside to validate the dosimetry, and to ensure a good correlation between calculation and measurement [103]. Based on the results of the evaluation, we conclude that the Octavius 4D System is a suitable device for patient-specific quality assurance. The ability of the system to reconstruct the volumetric dose distribution in the phantom provides additional information compared to conventional 2D detectors [104]. The results obtained confirm its ability to assure the quality of intensity modulated beams. The results of the correlation between the calculated and measured planes, i.e. the γ analysis results, indicate that the Octavius 4D Systems has a better correlation between the planes (calculated and measured)

as well as with the volumetric γ analysis pass rates. This system allows for a quantitative assessment of design complexity and can provide more information on treatment delivery and control of beam parameters such as arm rotation and blade speed. This could be useful throughout the treatment planning and quality assurance process. Finally, it appears that the Octavius 4D is fast and reliable and still has a very important role to play in patient management.

IV.4. Article 4: Evaluation of PTV margins in IMRT for head and neck cancer and prostate cancer

IV.4.1. Introduction

The delivery of a homogeneous high dose to the tumour region has been one of the cornerstones of radiotherapy (RT) treatment since its early days. According to the organ type and to cancer histology, different doses are required to inactivate malignant cells, thus stopping proliferation. However, radiation-induced cell killing is a stochastic process. Tumour control probability (TCP) models have been developed to assign a success rate to a given RT treatment. At the same time, there is a need to keep the risks of normal tissue toxicity at an acceptable level. Normal tissue complication probability (NTCP) models provide a means of doing this.1 Intensity-modulated RT (IMRT) is an approach of delivering non-uniform radiation beam fluences to produce a uniform dose distribution that maximises dose-to-tumour volume while minimising dose-to-normal tissue and critical structures. To clinically implement such a treatment modality, three systems are needed: a treatment planning computer system that can calculate non-uniform fluence maps from multiple beam

directions, a radiation delivery system capable of delivering such beam fluences, most often employed by a linear accelerator, and a quality assurance system to verify planned dose distributions. IMRT can generate dose distributions superior to 3D conformal treatments in several situations, including concave target volumes where multiple organs at risk (OARs) are close to the target volume, and for producing multiple dose levels in the target volume similar to boost therapy.2 IMRT can lead to improved conformity of the high-dose region to the tumour and requires more accurate delineation of both tumour and normal tissue than conventional RT. Additional normal tissue often has to be delineated because a tissue that is not specified can receive unexpected high doses. Patient positioning and localisation become even more important due to the reduced margins, which increase the risk of tumour miss. Furthermore, the true extent of disease and motion of delineated structures (both intra and inter fractions) cannot be fully accounted for using CT-based treatment plans. To mitigate the limitations in disease extent and motion, positron emission tomography (PET/CT) and treatment console station (4DTC; v.10, Varian, CA, USA) are often employed, respectively, within the treatment planning process.3 Through image-guided radiation therapy (IGRT) methods, the target and normal structures can be localised at the time of treatment to assure precise and accurate placement of the radiation, thereby pursuing highly conformal dose distributions, higher dose prescriptions and shorter fractionation schedules. IGRT techniques can substantially reduce geometric positioning errors that can occur between treatment planning and delivery. These include the reduction in 'systematic' errors that would otherwise persist over the entire course of therapy, as well as 'random' errors that vary from fraction to fraction.4 The purpose of this work is to quantify the random and systematic errors by using an electronic portal imaging device (EPID) for setup accuracy to evaluate the adequacy of the imperial planning target volume (PTV) margin employed for IMRT for two different locations: head and neck (HN) cancer and prostate cancer. These two locations were selected due the local regional anatomy and their proximity to surrounding critical organs. Uncertainties in the planning phase are influenced by patient setup, data acquisition, image registration, contouring and dosimetric planning. If present throughout the complete fractionation schedule, they become systematic errors. They can be omitted using appropriate wide margins and setting up control procedures. The uncertainties in the treatment in phase are influenced by patient setup, data acquisition for control, image registration and dose delivery. When restricted to a single fraction throughout the complete fractionation schedule they become random errors (often they called day-to-day variations). This study was conducted to assess the setup errors for patients being treated with IMRT and to determine

the optimal PTV margin specific to our centre.

IV.4.2. Materials and Methods

Forty consecutive patients presenting with advanced tumours of the nasopharynx, oropharynx and hypopharynx and low-risk prostate cancer were randomly selected for this retrospective study. All patients were treated in an RT department of a university hospital with IMRT. In this study, the position for HN patients was immobilisation in the supine position using a thermoplastic mask attached at five fixation points to a carbon-fibre plate support (CIVCO Radiotherapy Coralville, IA, USA). For prostate cases, immobilisation was achieved using knee and foot support as immobilisation device. The urologist places three fiducial markers around the prostate before the CT scan. CT simulation was performed in 3-mm slices using Siemens Somatom Sensation Open CT (Siemens, Erlangen, Germany). Target volumes and OARs were delineated using Varian SOMAVISION Focal workstations v.10.0.28 (Varian). Radiation fields were simulated and optical field projection was marked on the thermoplastic mould for subsequent positioning and treatment. The anterior, left lateral, right lateral and posterior simulator images were transferred to DICOM (Digital Imaging and Communications in Medicine) (4DTC; v.10, Varian). These served as reference images for comparison with images taken by the EPID.5 Treatment position verification using EPID to measure setup errors is accepted in standard practice.6 Digitally reconstructed radiographs (DRR) of the treatment fields were used as reference images. DRRs were imported from the treatment planning station (Eclipse v.10) to the treatment machine and compared online on the 4DTC screen or offline (Offline Review program v.10) with the EPID protocol as detailed in this section. Our objective was to evaluate EPID images for each patient. Four images (anterior, left lateral, right lateral and posterior) were performed for the setup fields on day 1 and two images (anterior, left lateral or right lateral) on day 2. After that, two images (anterior and lateral) were performed weekly.

For treatment planning and delivery technique, Varian Clinac 2300 DHX (Varian Medical System, CA, USA), a linear accelerator equipped with an 80-leaf dynamic multileaf collimator, was used. Clinac 2300 DHX was equipped with an MV EPID for the image system. Treatment techniques used in this study were IMRT. Eclipse 10 (Varian Medical System) was used as the treatment planning system (TPS). Radiation was delivered to the tumour at a dose rate of 400 MU/min with a photon energy of MV [6]. Evaluation protocol was an offline review procedure. Images were evaluated by two observers on the same day independently. The Offline Review program was used for EPID evaluation. DRR images

were compared to the EPID, and differences between EPID and DRR using bony landmarks (HN and prostate) and fiducial markers (prostate) were measured for each direction: lateral (X), cranio-caudal (Y), antero-posterior (Z). If the difference in the measurements between the two observers was 3 mm, the mean of the two measurements was taken [114].

In this study, we aimed to calculate and analyse PTV margins from the clinical target volume (CTV), and a formula was used to analyse setup errors for random (σ) and systematic (Σ) errors in the patient setup correction :

• To determine setup margin, ICRU 628 recommends the quadratic combination of random and systematic errors as shown in Equation (1)

$$\text{ICRU 62 formula} = \sqrt{\sum^{2} + \sigma^{2}} \qquad (1)$$

The margin recipes of Stroom et al.[116] assumed a 95% dose to 99% of the CTV on average based on tests of realistic plans as shown in Equation (2):

$$\text{Stroom et al.'s formula} = 2\sum + 0{\cdot}7\sigma \qquad (2)$$

The margin recipes of Parker et al.[117] assumed a 95% minimum dose and 100% dose for 95% of the volume. Probability levels were not specified as shown in Equation (3):

$$\text{Parker et al.'s formula} = \sum + \sqrt{\sum^{2} + \sigma^{2}} \qquad (3)$$

Van Herk et al.[118] assumed minimum dose to CTV to be 95% for 90% of patients. Analytical solution for a perfect conformation is shown in Equation (4) :

$$\text{Van Herk et al.'s formula} = 2,5\sum + 0{\cdot}7\sigma \qquad (4)$$

Van Herk et al.[119] assumed a Monte-Carlo-based test of 1% TCP loss due to geometric errors for the prostate. Their formula is defined as:

$$\text{Van Herk et al.'s formula} = 2,5\sum + 0{\cdot}7\sigma - 3\,\text{mm}$$

IV.4.3. Results

Seven hundred twenty images were analysed for HN and prostate cancers, and setup uncertainty was calculated aligning the setup images relatively to DRR images. The mean displacement in X, Y and Z directions was 0·73, 0·43 and 0·08 mm for HN and 0·16, 0·11 and 0·27 mm for prostate.

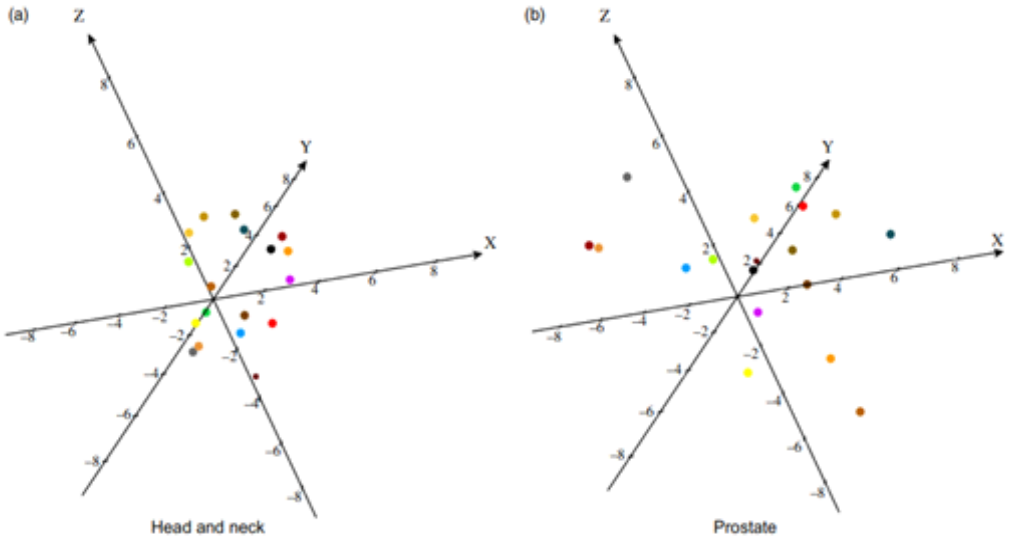

Figure IV. 22. Displacement of patients along the X, Y and Z axes for HN and prostate cases

As shown in Figure IV.22 , displacements of PTV in patients who had an HN immobilisation system tended to be localised in a small area offset from the centre (systematic error), but with a certain dispersion (random error), and a large deviation occurred in patients with prostate cancer who used a knee and ankle support as an immobilisation device. This variation in mean displacement may be explained by several reasons, first by the variation in patient positioning and mechanical uncertainties of the equipment. Another cause may be the patient's marking procedures, which are performed with a permanent marker whose thickness could lead to the radiation therapist to have some uncertainty in positioning the patient daily. Figures IV.23 and IV.24 indicate the setup variations with means and standard deviations (SD) in X, Y and Z dimensions for the 40 patients under both HN and prostate treatment. After the calculation of mean displacement, we calculated systematic and random setup uncertainties for each location as shown in Table IV.14. PTV margins were calculated for HN and prostate using ICRU Report 62, Stroom's, Parker's and Van Herk's formulas (Table IV.15). This margin in the X, Y and Z directions was 1·91, 2·16 and 2·11 mm, respectively. The corresponding values were 3·61, 3·93 and 4·00 mm with Stroom's formula; 3·78, 3·84 and 3·92 mm with Parker formula; and 4·27, 4·62 and 4·74 mm with Van Herk's formula. On the other hand, the results of prostate were calculated and presented in the same order: 3·73, 3·17 and 3·34 mm for ICRU Report 62 formula; 7·02, 5·75 and 6·80 mm with Stroom's formula; 5·02, 4·47 and 5·18 mm with Parker formula; and 8·31, 6·76 and 8·17 mm with Van Herk's formula.

IV.4.4. Discussion

Optimal IMRT requires more accurate delineation of both tumour and normal tissues compared with conventional RT because of the resulting steeper absorbed dose gradients, and PTV margin determination is crucial to control the dose in normal tissues, which might cause unacceptable complications. This work evaluated the setup accuracy in patients receiving IMRT for HN and prostate cancer using EPID. We found the PTV margin around CTV to be ranging between 2–4·3, 2·2–4·6 and 2·1–4·7 mm in X, Y and Z directions, respectively, for HN cases. Similarly, the prostate site was 3·7–8·3, 3·2–6·8 and 3·3–8·2 mm in X, Y and Z directions, respectively. At our centre, a margin of 10 mm is currently used for prostate cancer and 5 mm for HN location in all directions. All these results are similar with other studies,13,14 although there are differences between tumour location, OAR volume, RT indication (adjuvant/radical) and immobilisation systems. Table IV.15 summarises the margins found using the various formulas quoted above, suggesting that the values using the ICRU formula are the lowest for the three directions (X, Y and Z) for HN and prostate. In contrast, the Van Herk formula gives a fairly broad margin, allowing a better TCP.15 For the prostate, Wortel et al.[123] estimated a margin at 10 mm, whereas we found the value lying between those reported in Table IV.16 . In addition, the lowest values of Y and Z are those reported by this study. Margins do not differ significantly in the case of HN.

Table IV.14: Systematic error (Σ) and random error (σ) for HN and prostate sites

	HN			Prostate		
Direction	X	Y	Z	X	Y	Z
Σ	1.33	1.39	1.47	2.57	2.02	2.73
σ	1.37	1.65	1.52	2.71	2.45	1.93

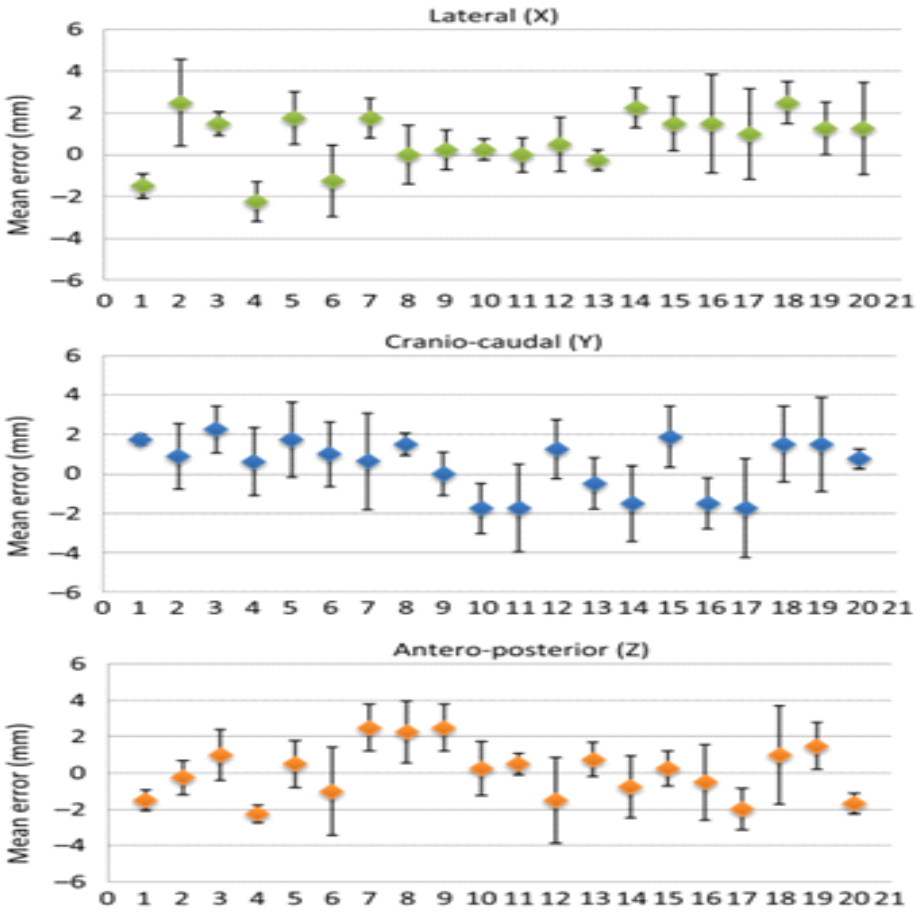

Figure IV. 23. Mean with error bars showing an SD of individual patient setup error alongthe lateral (X), cranio-caudal (Y) and anterior-posterior (Z) directions for 20 patients of the HN site.

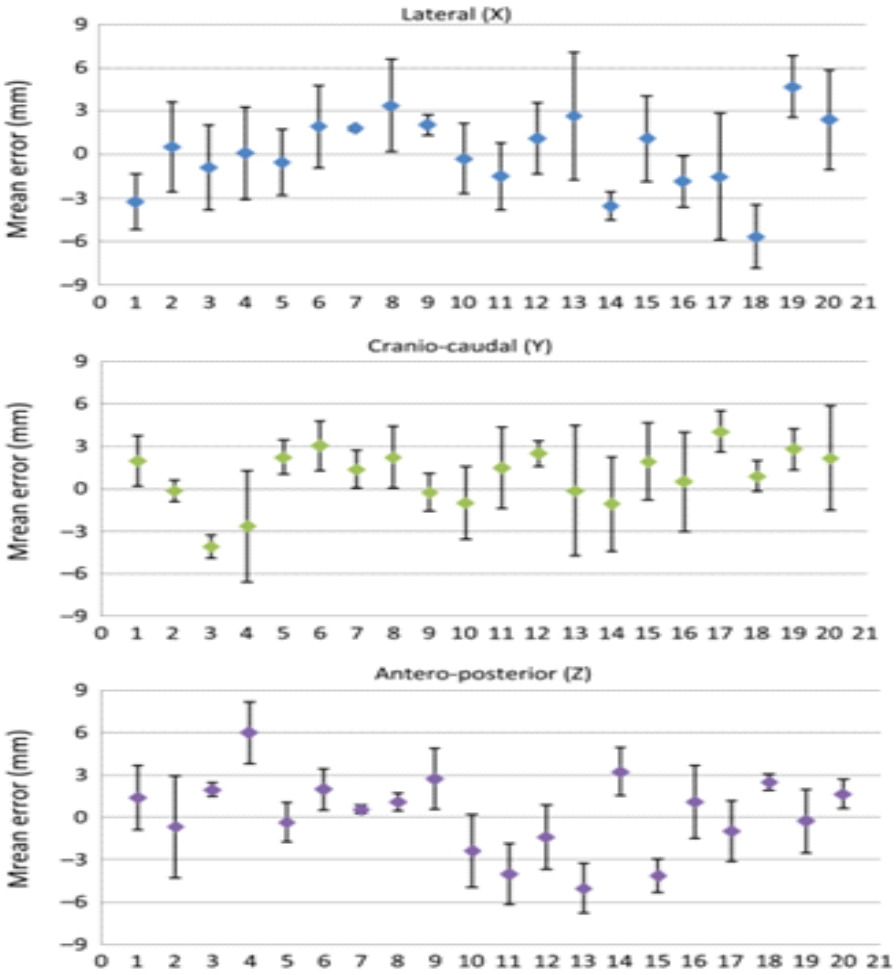

Figure IV. 24. Mean with error bars showing an SD of individual patient setup error along the lateral (X), cranio-caudal (Y) and anterior-posterior (Z) directions for 20 patients of the prostate site.

Also in Perera et al.'s trial, this was below 10 mm may result in a marked decrease in TCP. Hence, the use of 10 mm margin, rather than those calculated, will allow a reduction in dose to critical structures while maintaining an acceptable TCP. The results of previous works 16,19–22 are comparable to those reported in our study. In contrast, the estimated values of Y and Z are, on average, lower than those found by the works cited in Table IV.16 . The implications of this study on our practice are to ensure better coverage of target volumes. We adopted a PTV margin of 5 mm for HN PTVs and 10 mm for prostate PTVs in our department. Limitations of the Study Our results can serve as a good estimate of the appropriate margin to be taken and will contribute to the optimisation of treatments for HN and prostate cancers using the equipment available in our department. In addition, these results can be improved by a CT-based clinical assessment at the time of dose volume

histogram analysis, based on accurate dose calculations. This study does not deal with rotations or pitch. Prostate deformation or evaluation of volume reductions was not included. Currently, in our institution, EPID and DRR images are manually matched. This may result in low variability by observers, but staffs are trained in the use of common stable anatomical points, and all disagreements are averaged and should generally not exceed 0·1 mm.

Table IV.15: CTV–PTV margins (mm) using different formulas: ICRU 62, Stroom, Parker and Van Herk

	HN				Prostate			
Direction	ICRU 62	Stroom	Parker	Van Herk	ICRU 62	Stroom	Parker	Van Herk
X (mm)	1·91	3·61	3·78	4·27	3·73	7·02	5·02	8·31
Y (mm)	2·16	3·93	3·84	4·62	3·17	5·75	4·47	6·76
Z (mm)	2·11	4·00	3·92	4·74	3·34	6·80	5·18	8·17

Table IV.16: Results of applying Van Herk formula on HN and prostate CTV–PTV margins for some studies compared with our study

CTV–PTV margins (mm)				
Series	Location	X	Y	Z
Graf[19]		7·0	9·5	9·5
Beltran[20]	Prostate	7·3	8·1	10·5
Wortel[16]		10	10	10
Present study		8·31	6·76	8·17
Suzuki[21]		5	5	5
Gilbeau[22]	HN	4·5–5·5	4·5–5·5	4·5–5·5
Present study		4·27	4·62	4·74

Future studies involving a larger population of patients would allow for better variety and, therefore, a more accurate representation of a given population.

IV.4.5. Conclusion

The present investigation focused on evaluating the setup accuracy of patients treated for HN and prostate cancers by IMRT. Results were compared with similar published studies. We found that margins found by using the Van Herk formula were close to those adopted at our centre (5 mm for HN and 10 mm for prostate), permitting a good compromise between the margins and TCP to ensure that a correct radiation dose is delivered to the tumour by IMRT. Thus, weekly setup verifications that use EPID are very useful for evaluating setup uncertainties and determining setup margins for HN and prostate cancers.

Conclusion

At present, medical physics is a very fertile and developing field of research. It is characterized by its rapid evolution and development which requires scientific researchers to give interest to this discipline. The work of this thesis is aimed at the optimization of the fields of radiology and radiotherapy, of which we have presented some contributions such as:
Contribution to the start of medical physics in Morocco by introducing local dose reference levels and an international reference. This preliminary study was carried out in five radiology departments in order to estimate the local diagnostic reference levels, considering the most used examinations. The overall DRLs values were in accordance with international recommendations, although some rooms had higher values mainly due to an increase in the X-ray tube load because of to the variability of radiological practices. These results may lead to awareness raising relating to the optimization of radiological practices and consequently of the doses received by patients. A broader investigation targeting more radiology departments across the country should be undertaken to determine the national DRLs. In addition, training of radiology technicians is necessary and imminent for the following investigation to be beneficial and fruitful.
In the second contribution, we selected parameters from a combined analysis of breast compression, breast morphometry and volumetric breast density, and applied these investigations to a Moroccan population at the start of new breast cancer screening. breast, it was for the purpose of justifying the use of international standards for our screening program, as these have not yet been developed in our country. The results show a correlation between compression force and breast density. Volumetric breast density (VBD) decreases with compressed breast thickness (CBT) and age. The overall analysis and the comparison of the mammographic parameters showed a good similarity between the Moroccan population and the population of previous studies.
The third contribution was focused on the verification of IMRT treatment plans. The objective is to evaluate and compare the parameters of the treatment plans delivered by the linear gas pedal with those expected. Before the start of treatment of each new patient with intensity modulated conformal radiotherapy, a time slot is set aside to validate the dosimetry, and to ensure a good correlation between calculation and measurement. Based on the results

of the evaluation, we conclude that the Octavius 4D System is a suitable device for patient-specific quality assurance. The ability of the system to reconstruct the volumetric dose distribution in the phantom provides additional information compared to conventional 2D detectors. The results obtained confirm its ability to assure the quality of intensity modulated beams. The results of the correlation between the calculated and measured planes, i.e. the γ analysis results, indicate that the Octavius 4D Systems has a better correlation between the planes (calculated and measured) as well as with the volumetric γ analysis pass rates. This system allows for a quantitative assessment of design complexity and can provide more information on treatment delivery and control of beam parameters such as arm rotation and blade speed. This could be useful throughout the treatment planning and quality assurance process. Finally, it appears that the Octavius 4D is fast and reliable and still has a very important role to play in patient management.

In the fourth contribution we presented the evaluation of PTV margins in IMRT treatment for Head & Neck and Prostate cancer. IMRT of HN and Prostate cancers has several difficulties because the organs at risk in vicinity of the tumor, a high geometrical accuracy is required. This is why EPID is used to check the patient's setup error in order to determine the optimal PTV. The present study is a work to evaluate the set-up accuracy of patients receiving IMRT head, neck and prostate radiotherapy that compares well with published set-up error data.Thus, daily setup verifications that use EPID are very useful for evaluating the setup uncertainties and determining the setup margin for Head & Neck and this on one hand, and on the other hand IGRT is the easy way to determine the optimal PTV for the prostate.

References

References

[1] Aubert, B., et Bridier, A. Histoire de la radiophysique médicale, IRSN, Club Histoire SFRP, 2012

[2] Miller, D. L., Schauer, D. The ALARA principle in medical imaging, philosophy, 2015; 44, 595-600.

[3] Hendry, J. H., Simon, S. L., Wojcik, A., Sohrabi, M., Burkart, W., Cardis, E., Laurier, D., et al. Human exposure to high natural background radiation: what can it teach us about radiation risks. Journal of Radiological Protection, 2009; 29(2A), A29.

[4] Ryan, J. L., Ionizing radiation: the good, the bad, and the ugly. Journal of Investigative Dermatology,2012; 132(3), 985-993.

[5] De la santé, Organisation Mondiale. Rayonnements ionisants, effets sur la santé et mesures de protection. Repéré à http://www. who. int/mediacentre/factsheets/fs371/fr, 2016.

[6] Özkaya, U., Seyfi, L., & Yaldız, E. Analysis of Electromagnetic Radiation in Daily Life. In SETSCI Conference Indexing System, 2018 ; Vol. 3, pp. 505-509.

[7] Macana, R. J., Moirangthem, T. T., et Baik, O. D. Shielding effectiveness of electromagnetic energy from 50-ohm radio frequency heating system for disinfestation of stored grains. American Society of Agricultural and Biological Engineers, 2018; p.1.

[8] Connor, N. What is Linear and Mass Attenuation Coefficient – X-rays – Definition, 2019

[9] Introduction à la dosimétrie, INFO-0827, commisssion canadienne de sureté nucleaire, Fevrier 2012.

[10] Herres, D., X-rays and ionizing radiation, 2015

[11] Tao, S. Rigid motion correction for head CT imaging, 2018

[12] MUHAMMAD, W., HUSSAIN, A., & MAQBOOL, M. Basic Concepts in Radiation Dosimetry. An Introduction to Medical Physics. Springer, Cham, 2017; p. 9-41.

[13] Piotrowski, T., Tefelski, D., Polański, A., & Skubalski, J. Monte Carlo simulations for optimization of neutron shielding concrete. Open Engineering, 2012; 2(2), 296-303.

[14] Catuzzo, P., Aimonetto, S., Zenone, F., Fanelli, G., Marchisio, P., Meloni, T., & Tofani, S. Population exposure to ionising radiation from CT examinations in Aosta Valley between 2001 and 2008. The British Journal of Radiology, 2010; 83(996), 1042-1051.

[15] INRS , Réglementation et démarche de prévention, santé et securité de travail,2022

[16] Hunter, J. Nucléaire - Indemnisation : le millisievert de la discorde, 2019

[17] REHEL, J. L., ROCH, P. Les niveaux de reference, Unité d'Expertise en radioprotection Médicale, Module national d'enseignement de radioprotection du DES de Radiologie, 2010.

[18] Choi, L. MD, Karmanos Cancer Center, Breast Cancer, 2022

[19] EINSMANN, S. Mammogram more like mammogreat. Thèse de doctorat. Southern New Hampshire University, 2021.

[20] Bluegyn spip, Classification ACR BI-RADS, 2006

[21] Anjali, S. Mammography, 2016

[22] Luiten, J. D., Voogd, A. C., Luiten, E. J., Broeders, M. J., Roes, K. C., Tjan-Heijnen, V. C., & Duijm, L. E. Recall and outcome of screen-detected microcalcifications during two decades of mammography screening in the Netherlands National Breast Screening Program. Radiology, 2020 ; 294, 528-537.

[23] Waqar, M., Abro, M. N., Soomro, Q., Shahban, M., & Khatoon, S. Retrospective incidence analysis of head and neck cancer patients in rural areas of Sindh, Pakistan. Jundishapur Journal of Chronic Disease Care, 2019 ; 8(4).

[24] Ping, H. S. Minimizing skin toxicity in intensity modulated radiotherapy of head and neck, Conference: Annual Scientific Congress Malaysian Oncological Society, 2009

[25] National cancer institute. Prostate cancer treatment, Health Professional Version, 2021

[26] Mayo Clinic Family Health. External beam radiation for prostate cancer, 2021

[27] HILT, G. THESE, Vérification automatique de la position d'un patient pendant les en radiothérapie externe par recalage d'images, 2000

[28] Schlachter, M., Raidou, R. G., Muren, L. P., Preim, B., Putora, P. M., & Bühler, K. State-of-the-Art Report: Visual Computing in Radiation Therapy Planning. In Computer Graphics Forum, 2019 (Vol. 38, No. 3, pp. 753-779).

[29] Aubert, B., Biau, A., Derreumaux, S., Etard, C., Rannou, A., et al. Radiological Protection in Medicine. ICRP Publication 105. 2008;37:1-71.

[30] Directive C. 97/43/Euratom of 30 June 1997 on health protection of individuals against the dangers of ionizing radiation in relation to medical exposure, and repealing Directive 84/466/Euratom. Off J Eur Communities L. 1997; 180:07.

[31] Hendee, W. R., & Edwards, F. M. ALARA and an integrated approach to radiation protection. In Seminars in nuclear medicine. WB Saunders. 1986; 16(2), pp. 142-150.

[32] González A. B., & Darby S. Risk of cancer from diagnostic X-rays: estimates for the UK and 14 other countries. Lancet. 2004; 363:345-351.

[33] European Commission. Council Directive 2013/59/Euratom of 5 December 2013 laying down basic safety standards for protection against the dangers arising from exposure to ionizing radiation, and repealing Directives 89/618/ Euratom, 90/641/Euratom, 96/29/Euratom, 97/43/Euratom and 2003/122/ Euratom. Official J. 2014; 13:1-73.

[34] Directive C. 97/43/Euratom of 30 June 1997 on health protection of individuals against the dangers of ionizing radiation in relation to medical exposure, and repealing Directive 84/466/Euratom Off. J. Eur. Communities L. 1997; 180:07.

[35] Radiation Protection and Safety of Radiation Sources: International Basic Safety Standards. Int at energy agency. 1996.

[36] Guidance on diagnostic reference levels (DRLs) for Medical Exposures. Luxembourg: Eur. Communities.1999.

[37] Carmichael, J. H. European guidelines on quality criteria for diagnostic radiographic images. Off. Off. Publ. Eur. Communities; 1996.

[38] Osei, E.K., Darko, J. A. Survey of organ equivalent and effective doses from diagnostic radiology procedures. Int Sci Res Not. 2013.

[39] Škrk, D., Zdešar, U., Žontar D. Diagnostic reference levels for X-ray examinations in Slovenia. Radiol Oncol. 2006;40.

[40] Sonawane AU, Shirva VK, Pradhan AS. Estimation of skin entrance doses (SEDs) for common medical X-ray diagnostic examinations in India and proposed diagnostic reference levels (DRLs). Radiat prot dosim. 2010; 138:129-36.

[41] Hart D, Hillier M, Shrimpton P. Doses to patients from radiographic and fluoroscopic x-ray imaging procedures in the UK. Chilton: Health Protection Agency Centre for Radiation. Chem Environ Hazards. 2010.

[42] Roch P, Aubert B. French diagnostic reference levels in diagnostic radiology, computed tomography and nuclear medicine: 2004–2008 review. Radiat prot dosim. 2013; 154:52-75.

[43] Khoshdel-Navi D, Shabestani-Monfared A, Deevband MR, Abdi R, Nabahati M. Local reference patient dose evaluation in conventional radiographyin mazandaran, Iran. J biomed phys eng. 2016; 6:61-70.

[44] Freitas MB, Yoshimura EM. Diagnostic reference levels for the most frequent radiological examinations carried out in Brazil. Rev. Panam Salud Pública. 2009; 25:95-104.

[45] Ofori K, Gordon SW, Akrobortu E, Ampene AA, Darko EO. Estimation of adult patient doses for selected X-ray diagnostic examinations. J Radiat Res Appl Sci.2014; 7:459-462.

[46] Asada Y, Ono K, Kondo Y, Sugita K, Ichikawa T, et al. Proposal for local diagnostic reference levels in general radiography in Japan. Radiat prot dosim. 2019; 187:338-344.

[47] Rubai SS, Rahman MS, Purohit S, Patwary MK, Moinul AK, et al. Measurements of Entrance Surface Dose and Effective Dose of Patients in Diagnostic Radiography. Biomed J. 2018;12.

[48] Ciraj O, Markovic S, Kovacevic M, Kosutic D. A survey of patient doses from conventional diagnostic radiology examinations: first results from Serbia and Montenegro. A Survey of Patient Doses from Conventional Diagnostic Radiology Examinations. 2005;21:159 163.

[49] Metaxas VI, Messaris GA, Lekatou AN, Petsas TG, Panayiotakis GS. Patient doses in common diagnostic X-ray examinations. Radiat prot dosim. 2019;184:12-27.

[50] Recommendations of the international commission on radiological protection. ICRP publication 60. 1990

[51] Recommendations of the international commission on radiological protection. ICRP publication 103. 2007

[52] Wall BF, Haylock R, Jansen JTM, Hillier MC, Hart D et al, Radiation Risks from Medical X-ray Examinations as a Function of the Age and Sex of the Patient, Health Protection Agency, Centre for Radiation. Chem Environ Hazards.2011.

[53] BOYD, N. F., DITE, G. S., STONE, J., et al. Heritability of mammographic density, a risk factor for breast cancer. New England Journal of Medicine, 2002, vol. 347, no 12, p. 886 894.

[54] WOLFE, J.N. Breast patterns as an index of risk for developing breast cancer. American Journal of Roentgenology, 1976, vol. 126, no 6, p. 1130-1137.

[55] KOPANS, D. B. The positive predictive value of mammography. AJR. American journa of roentgenology, 1992, vol. 158, no 3, p. 521-526.

[56] LESUR, Anne et TRISTANT, Henri. Pour en finir avec la densité mammaire et le traitement hormonal substitutif de la ménopause. Reproduction humaine et hormones, 2002, vol. 15, no 5, p. 341-345.

[57] TARDIVON, A. Quels risques, pour quelles femmes? Densité mammaire et cancer du sein. In: Prévention du cancer du sein. 2008. p. 93-101.

[58] STINÈS, J. La densité mammaire: un concept radiologique.26es journées de la SFSPM, Nancy, novembre 2004.

[59] SÉRADOUR, B. Impact de la densité mammaire sur le dépistage. 26es journée de la SFSPM, Nancy, novembre 2004.

[60] ASSI, V., WARWICK, J., CUZICK, J., et al. Clinical and epidemiological issues in mammographic density. Nature reviews Clinical oncology, 2012, vol. 9, no 1, p. 33-40.

[61] URSIN, Giske, MA, Huiyan, WU, Anna H., et al. Mammographic density and breast cancer in three ethnic groups. Cancer Epidemiology and Prevention Biomarkers, 2003, vol. 12, no 4, p. 332-338.

[62] WOLFE, John N. Risk for breast cancer development determined by mammographic parenchymal pattern. Cancer, 1976, vol. 37, no 5, p. 2486-2492.

[63] BOYD, Norman F., GUO, Helen, MARTIN, Lisa J., et al. Mammographic density and the risk and detection of breast cancer. New England journal of medicine, 2007, vol. 356, no 3, p. 227-236.

[64] O'LEARY, D., GRANT, T., et RAINFORD, L. Image quality and compression force: the forgotten link in optimisation of digital mammography?. Breast Cancer Research,

2011, vol. 13, no 1, p. 1-13.

[65] HOLLAND, Katharina, SECHOPOULOS, Ioannis, MANN, Ritse M., et al. Influence of breast compression pressure on the performance of population-based mammography screening. Breast cancer research, 2017, vol. 19, no 1, p. 1-8.

[66] BRANDERHORST, Woutjan, DE GROOT, Jerry E., HIGHNAM, Ralph, et al. Mammographic compression–a need for mechanical standardization. European journal of radiology, 2015, vol. 84, no 4, p. 596-602.

[67] DAVEY, Belinda. Pain during mammography: possible risk factors and ways to alleviate pain. Radiography, 2007, vol. 13, no 3, p. 229-234.

[68] WHELEHAN, Patsy, EVANS, Andy, WELLS, Mary, et al. The effect of mammography pain on repeat participation in breast cancer screening: a systematic review. The Breast, 2013, vol. 22, no 4, p. 389-394.

[69] WÜBKER, Ansgar. Explaining variations in breast cancer screening across European countries. The European Journal of Health Economics, 2014, vol. 15, no 5, p. 497-514.

[70] EUREF4, European guidelines for quality assurance in breast cancer screening and diagnosis Fourth edition.

[71] KARTHIK, L., KUMAR, Gaurav, KESWANI, Tarun, et al. Protease inhibitors from marine actinobacteria as a potential source for antimalarial compound. PloS one, 2014, vol. 9, no 3, p. e90972.

[72] SALEM, C., ATALLAH, D., SAFI, J., et al. Breast density and breast cancer incidence in the Lebanese population: results from a retrospective multicenter study. BioMedresearch international, 2017, vol. 2017.

[73] AKOGLU, Haldun. User's guide to correlation coefficients. Turkish journal of emergency medicine, 2018, vol. 18, no 3, p. 91-93.

[74] DANCE, D. R., SKINNER, C. L., YOUNG, K. C., et al. Additional factors for the estimation of mean glandular breast dose using the UK mammography dosimetry protocol. Physics in medicine & biology, 2000, vol. 45, no 11, p. 3225.

[75] ALONZO-PROULX, O., JONG, R. A., et YAFFE, M. J. Volumetric breast density characteristics as determined from digital mammograms. Physics in Medicine & Biology, 2012, vol. 57, no 22, p. 7443.

[76] MOSHINA, N., ROMAN, M., WAADE, G. G., et al. Breast compression parameters and mammographic density in the Norwegian Breast Cancer Screening

Programme. European radiology, 2018, vol. 28, no 4, p. 1662-1672.

[77] MERCER, C. E., HOGG, P., LAWSON, R., et al. Practitioner compression force in mammography: a preliminary study. The British journal of radiology, 2013, vol. 86, no 1022, p. 20110596.

[78] PERRY, Nicholas, BROEDERS, Mireille, DE WOLF, Chris, et al. European guidelines for quality assurance in breast cancer screening and diagnosis.-summary document. Oncology in Clinical Practice, 2008, vol. 4, no 2, p. 74-86.

[79] Elmpt W, Sebastiaan N, Mijhnheer B, Dekker A, Lambin P. "The next in patient specific QA: 3D dose verification of conformal and intensity-modulated RT based on EPID dosimetry and Monte Carlo dose calculations," Radiother Oncol. 2008; 86:86-92.

[80] Ansbacher W ."Three-dimensional portal image-based dose reconstruction in a virtual phantom for rapid evaluation of IMRT plans". Med Phys.2006; 33:3369-3382.

[81] Mans A, Remeijer P, Olaciregui-Ruiz I, Wendling M, Sonke J, et al. "3D dosimetric verification of volumetric-modulated arc therapy by portal dosimetry." Radiat Oncol. 2010;94:181-187.

[82] Low DA, Harms WB, Mutic S, and Purdy JA. "A technique for the quantitative evaluation of dose distributions," Med Phys. 1998;25:656- 661.

[83] Mijheer B, Georg D. Guidelines for the verification of IMRT. Brussels, Belgium. ESTRO; 2008.

[84] Depuydt T, Van Esch A, Huyskens DP. A quantitative evaluation of IMRT dose distributions: refinement and clinical assessment of the gamma evaluation. Radiother Oncol. 2002;62:309-319.

[85] Tonigan JR. Evaluation of intensity modulated radiation therapy (IMRT) delivery error due to IMRT treatment plan complexity and improperly matched dosimetry data. MSc Thesis. The University of Texas. Houston, Texas. 2011.

[86] Varatharaj C, Ravikumar M, Sathiyan S, Supe s, Vivek TR, et al. Dosimetric verification of brain and head and neck intensity-modulated radiation therapy treatment using EDR2 films and 2D ion chamber array matrix. Cancer Res Ther. 2010;6:179-184.

[87] Stasi M, Bresciani S, Miranti A, Maggio A, Sapino V, et al. Pretreatment patient specific IMRT quality assurance: A correlation study between gamma index and patient clinical dose volume histogram. Med Phys. 2012;39:7626-7634.

[88] Harms W, Low D, Wong J, Purdy JA. A software tool for the quantitative evaluation of 3D dose calculation algorithms. Med Phys. 1998;25:1860- 1866.

[89] Stock M, Kroupa B, Georg D. Interpretation and evaluation of the gamma index and the gamma index angle for the verification of IMRT hybrid plans. Phys Med Biol. 2005; 50:399 411.

[90] Depuydt T, Van Esch A, Huyskens D. A quantitative evaluation of IMRT dose distributions: refinement and clinical assessment of the gamma evaluation. Radiother Oncol. 2002;62;309-319.

[91] Korreman S, Medin J, Kjaer-Kristoffersen F. "Dosimetric verification of RapidArc treatment delivery." Acta Oncol. 2009; 48:185-191.

[92] JBedford JL, Warrington AP. "Commissioning of volumetric modulated arc therapy (VMAT)." Int. J Radiat Oncol Biol Phys. 2009; 73:537-545.

[93] Iftimia I, Cirino ET, Xiong L, Mower HW. "Quality assurance methodology for Varian RapidArc treatment plans." J Appl Clin Med Phys. 2010; 11:130-143.

[94] Jin X, Yan H, Han C, Zhou Y, Yi J, et al. Correlation between gamma index passing rate and clinical dosimetric difference for pre-treatment 2D and 3D volumetric modulated arc therapy dosimetric verification. Br J Radiol. 2015; 88:20140577.

[95] Nelms BE, Zhen H, Tome WA. Per-beam, planar IMRT QA passing rates do not predict clinically relevant patient dose errors. Med Phys. 2011; 38:1037-1044.

[96] Kim JI, Choi CH, Wu HG, Kim JH, Kim K, et al. Correlation analysis between 2D and quasi-3D gamma evaluations for both intensity-modulated radiation therapy and volumetric modulated arc therapy. Oncotarget. 2017; 8:5449-5459.

[97] Park JM, Park SY, Kim H. Modulation index for VMAT considering both mechanical and dose calculation uncertainties. Phys Med Biol. 2015; 60:7101-7125.

[98] Yan G, Liu C, Simon TA, Peng LC, Fox C, et al. "On the insensitivity of patient-specific IMRT QA to MLC positioning errors." J Appl Clin Med Phys. 2009; 10:120-128.

[99] Sanghangthum T, Suriyapee S, Srisatit S, Pawlicki T, "Statistical process control analysis for patient-specific IMRT and VMAT QA." J Radiat Res. 2013; 54:546-552.

[100] Kruse J. "On the insensitivity of single field planar dosimetry to IMRT inaccuracies." Med Phys. 2010; 37:2516-2524.

[101] Nelms BE, Zhen H, Wolfgang T, "Per-bam planar IMRT QA passing rates do not predict clinically relevant patient dose errors." Med Phys. 2011; 38:1037-1044.

[102] Nelms BE, Simon JA, "A survey on planar IMRT QA analysis." J Appl Clin Med Phys. 2007; 8:76-90.

[103] Marcié S, Aletti P, Lefkopoulos P, Tomsej M, Participation of physicists. Quality assurance program for intensity-modulated radiotherapy (IMRT) treatments of head and neck carcinomas. Cancer Radiother. 2003; 7:172- 178.

[104] Dhanabalan R, Prakash J, Prabakar S, Rangnathan A, Johnjothi S, et al. A study on the correlation between plan complexity and gamma index analysis in patient specific quality assurance of volumetric modulated arc therapy. Rep Pract Oncol Radiother. 2014;20:57-65

[105] B. Allgaier, E. Schüle, J. Würfel, Dose reconstruction in the OCTAVIUS 4D phantom and in the patient without using dose information from the TPS, PTW-Freiburg. 2013

[106] Dyk, J., Barnett, R., Cygler, J., & Shragge, P. (1993). Commissioning and quality assurance of treatment planning computers. International Journal of Radiation Oncology Biology Physics, 26(2), 261–273

[107] Hussein M, Elizabeth J Adams, Thomas J Jordan, Catharine Clark, Andrew Nisbet, A critical evaluation of the PTW 2D-ARRAY seven29 and OCTAVIUS II phantom for IMRT and VMAT verification, Applied Clinical Medical Physics, VOLUME 14, NUMBER 6, 2013

[108] Tommasino F, Nahum A, Cella L. Increasing the power of tumour control and normal tissue complication probability modelling in radiotherapy: recent trends and current issues. Transl Cancer Res 2017; 6 (S5): 807–821.

[109] Khan F M. The Physics of Radiation Therapy: Lippincott Williams & Wilkins, 4th edition. Minneapolis, MN, USA: University of Minnesota Medical School, 2009.

[110] ICRU: Prescribing, Recording, and Reporting Photon-Beam Intensity-Modulated Radiation Therapy (IMRT). ICRU Report 83, J. ICRU, Volume 10(1). Oxford University Press, Oxford, UK, 2010.

[111] Jaffray D A, Katja L, Mageras G et al. Assuring safety and quality in image guided delivery of radiation therapy. Practical Radiat Oncol 2013; 3: 167–170.

[112] Tejpal G, Supriya C, Avinash K et al. Assessment of three-dimensional set-up errors in conventional head and neck radiotherapy using electronic portal imaging device. Radiat Oncol 2007; 2: 44–51.

[113] Langmack K A. Portal imaging. Br J Radiol 2001; 74: 789–794.

[114] Evrim B, OZlem A, Münir K, Fadime A. How to determine margins for planning target volume (PTV): from 2D to 3D planning in radiotherapy for head and neck cancer.Portal imaging assessment for set-up errors.Turkish J Oncol 2010; 25:104–110.

[115] International Commision on Radiation Units and Measurements: Prescribing, recording and reporting photon beam therapy (Supplement to ICRU report 50). In ICRU Report, 62. Bethesda, MD: ICRU Publications, 2000.

[116] Stroom J C, de Boer H C, Huizenga H et al. Inclusion of geometrical uncertainties in treatment planning by means of coverage probability. Int J Radiat Oncol Biol Phys 1999; 43: 905–919.

[117] Parker B C, Shiu A S, Maor M H et al. PTV margin determination in conformal SRT of intracranial lesions. J Appl Clin Med Phys 2002; 3: 176–189.

[118] Van Herk M, Remeijer P, Rasch C, Lebesque J V. The probability ofcorrect target dose: dose population histograms for deriving treatment margins in radiotherapy. Int J Radiat Oncol Biol Phys 2000; 47: 1121–1135.

[119] Van Herk M. Errors and margins in radiotherapy. Semin Radiat Oncol 2004;14: 52-64.

[120] Bel A, Keus R, Vijlbrief R E, Lebesque J V. Setup deviations in wedged pair irradiation of parotid gland and tonsillar tumors, measured with an electronic portal imaging device.Radiother Oncol 1995; 37: 153–159.

[121] Boer H C, de Koste J R V S, Creutzberg C L et al. Electronic portal image assisted reduction of systematic set-up errors in head and neck irradiation. Radiother Oncol2001; 61:299–208.

[122] Van Herk M, Remeijer P, Lebesque J V. Inclusion of geometric uncertainties treatment plan evaluation. Int J Radiat Oncol Biol Phys 2002; 52:1407–1422.

[123] Wortel R C, Incrocci L, Pos F J et al. Acute toxicity after image-guided intensity modulated radiation therapy compared to 3D conformal radiation therapy in prostate cancer patients. Int J Radiat Oncol Biol Phys 2015; 91: 737–744.

[124] Perera, T., Moseley, J., Munro, P. Subjectivity in interpretation of portal films. Int J Radiat Oncol Biol Phys 1999; 45: 529–534.

[125] Skarsgard, D., Cadman, P., El-Gayed, A. et al. Planning target volume margins for prostate radiotherapy using daily electronic portal imaging and implanted fiducial markers.Radiat Oncol 2010 Jun 10; 5: 52–62.

[126] Graf, R., Wust, P., Budach, V., Boehmer, D. Potentials of on-line repositioning based on implanted fiducial markers and electronic portal imaging in prostate cancer radiotherapy. Radiat Oncol 2009; 4: 13–21.

[127] Beltran, C., Herman, M., Davis, B. Planning target margin calculations for prostate radiotherapy based on intrafraction and interfraction motion using four localization methods. Int J Radiat Oncol Biol Phys 2008 Jan 1; 70 (1): 289–295.

[128] Suzuki, M., Nishimura, Y.,Nakamatsu, K. et al. Analysis of interfractional set-up errors and intrafraction organ motions during IMRT for head and neck tumors to define anappropriate planning target volume (PTV)- and planning organs at risk volume (PRV)-margins. Radiother Oncol 2006; 78: 283–290.

[129] Gilbeau, L., Octave-Prignot, M., Loncol, T. et al. Comparison of set up accuracy of three different thermoplastic masks for the treatment of brain and head and neck tumors. Radiother Oncol 2001; 58: 155–162.

Appendices

Appendices: List of publications and communications

Articles :

Article 1: Getting started with medical physics in Morocco viathe introduction of local dose reference levels and international bench marking

Oncology
and Radiotherapy ©
Vol.16 Iss.1:1-6 • Research Article

Getting started with medical physics in Morocco via the introduction of local dose reference levels and international bench marking

Sanae Douama[1], Youssef Bouzekraoui[1], Imane Ou-Saada[1], Hilde Bosmans[2], Lesley Cockmartin[3], Rachid Errifai[1,4], Zaama Lahoucine[1], M Ouahman[1], Farida Bentayeb[1]

[1] Faculty of Sciences, Laboratory of high energy physics Modelisation Simulation, University Mohammed V, Rabat, Morocco
[2] Faculty of Medicine, Department of Imaging and Pathology, Medical Physics and Quality Assessment, Catholic University of Leuven, Belgium
[3] Department of Radiology, University Hospital Leuven, UZ Leuven, Belgium
[4] Sheikh Zaid International University Hospital, Rabat, Moroccoa

SUMMARY

Introduction and purpose: The present work is part of the 'Radiology As A Steward For Quality In Moroccan Healthcare' (RASQUAM) of the VLIRUOS (Flanders, Belgium). Patient dose measurement campaigns were considered the best first initiative to promote medical physics Quality Assurance activities and to prepare the roll-out of a patient dose management system. The study in 5 Moroccan hospitals focused on common diagnostic radiology examinations. Patient doses were expressed as Entrance Skin Dose (ESD) and the Effective Dose (ED). The aim of the study was to calculate the local Dose Reference Levels (DRL), to compare dose data results with international literature and to plan subsequent actions.

Material and methods: The work was carried out in six conventional radiology rooms of five hospitals, designated by A, B, C, D, E and F. The examinations included Chest, Cervical spine, Skull and Lumbar spine, for lateral and Postero Anterior (PA) or Antero Posterior (AP) projections. Technical parameters (kV, mAs, FFD) and patient data (age, sex, weight) were collected at the time of the examination. Patient dose estimates were obtained with the DoseCal software that provides ESD and E for adults.

Results and discussion: The radiological parameters vary depending on the examination, projection types and rooms. The Local Diagnostic Reference Levels (IDRL) in terms of ESD are 0.35mGy for Chest PA, 0.8 mGy for Chest AP, 2.79mGy for Skull AP, 2.07 mGy for cervical spine AP, 2.36 mGy for cervical spine LAT and 2.72 mGy for lumbar AP spine. The local DRLs comply with international recommendations and their comparison with previous studies was satisfactory.

The average effective doses were: 0,03 mSv for the Chest PA, 0,07 mSv for the cervical spine AP, 0.03 mSv for the cervical spine LAT, 0.45 mSv for Lumbar AP, 0.66 mSv for the lumbar LAT, 0.03 mSv for the Skull AP and 0.01 mSv for the scull LAT.

Conclusion: The local DRLs are promising preliminary results that should be worked out up to the level of national DRLs. Medical physicists can now start with quality optimization strategies.

Key words: dose, radiologic x ray, body organ dose

INTRODUCTION

Ionizing radiation is widely used in medicine for diagnosis and treatment. The number of people exposed to low doses of radiation used in diagnostic radiology far exceeds the number of patients at higher doses used in radiotherapy [1]. This leads to actions in different contexts to prevent the risks of exposures involving many people. Indeed, low dose ionizing radiation for diagnostic use has great medical benefits; however, its widespread use has also raised concerns about the harmful the inducted effects. The biggest preoccupation with ionizing radiation is the increased risk of cancer, especially after childhood exposures [2].

The general principle of ALARA radiation protection [3] indicates that exposures should be kept as low as reasonably achievable by reducing doses to patients. This means that special attention must be paid to each medical exposure. Every exposure to radiation must be carried out with great vigilance. If the necessary measures are not considered, exposure to X-rays can cause damage to the body, thus inducing certain types of cancers [4]. In addition to the rules established to protect the population against ionizing radiation, the standardization of radiological practices remains a challenge to overcome. This implies that certain measures to optimize radiological

Article 2: Validation and comparison of intensity modulated radiation therapy patient plans with Octavius 4D Phantom using the Gamma Index analysis in 2D and 3D

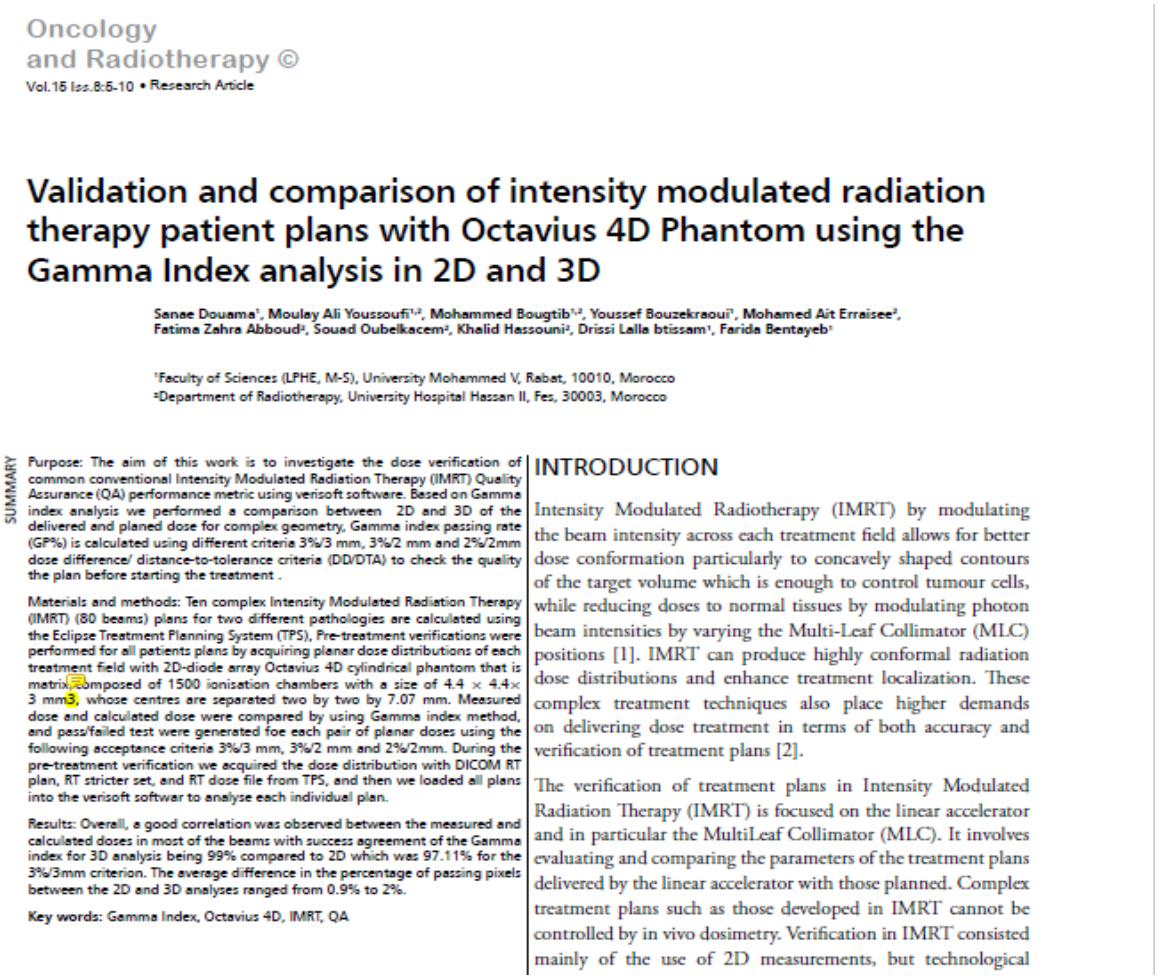

Oncology
and Radiotherapy ©
Vol.16 Iss.8:5-10 • Research Article

Validation and comparison of intensity modulated radiation therapy patient plans with Octavius 4D Phantom using the Gamma Index analysis in 2D and 3D

Sanae Douama[1], Moulay Ali Youssoufi[1,2], Mohammed Bougtib[1,2], Youssef Bouzekraoui[1], Mohamed Ait Erraisse[2], Fatima Zahra Abboud[2], Souad Oubelkacem[2], Khalid Hassouni[2], Drissi Lalla btissam[1], Farida Bentayeb[1]

[1]Faculty of Sciences (LPHE, M-S), University Mohammed V, Rabat, 10010, Morocco
[2]Department of Radiotherapy, University Hospital Hassan II, Fez, 30003, Morocco

SUMMARY

Purpose: The aim of this work is to investigate the dose verification of common conventional Intensity Modulated Radiation Therapy (IMRT) Quality Assurance (QA) performance metric using verisoft software. Based on Gamma index analysis we performed a comparison between 2D and 3D of the delivered and planed dose for complex geometry, Gamma index passing rate (GP%) is calculated using different criteria 3%/3 mm, 3%/2 mm and 2%/2mm dose difference/ distance-to-tolerance criteria (DD/DTA) to check the quality the plan before starting the treatment .

Materials and methods: Ten complex Intensity Modulated Radiation Therapy (IMRT) (80 beams) plans for two different pathologies are calculated using the Eclipse Treatment Planning System (TPS), Pre-treatment verifications were performed for all patients plans by acquiring planar dose distributions of each treatment field with 2D-diode array Octavius 4D cylindrical phantom that is matrix composed of 1500 ionisation chambers with a size of 4.4 × 4.4× 3 mm3, whose centres are separated two by two by 7.07 mm. Measured dose and calculated dose were compared by using Gamma index method, and pass/failed test were generated foe each pair of planar doses using the following acceptance criteria 3%/3 mm, 3%/2 mm and 2%/2mm. During the pre-treatment verification we acquired the dose distribution with DICOM RT plan, RT stricter set, and RT dose file from TPS, and then we loaded all plans into the verisoft softwar to analyse each individual plan.

Results: Overall, a good correlation was observed between the measured and calculated doses in most of the beams with success agreement of the Gamma index for 3D analysis being 99% compared to 2D which was 97.11% for the 3%/3mm criterion. The average difference in the percentage of passing pixels between the 2D and 3D analyses ranged from 0.9% to 2%.

Key words: Gamma Index, Octavius 4D, IMRT, QA

INTRODUCTION

Intensity Modulated Radiotherapy (IMRT) by modulating the beam intensity across each treatment field allows for better dose conformation particularly to concavely shaped contours of the target volume which is enough to control tumour cells, while reducing doses to normal tissues by modulating photon beam intensities by varying the Multi-Leaf Collimator (MLC) positions [1]. IMRT can produce highly conformal radiation dose distributions and enhance treatment localization. These complex treatment techniques also place higher demands on delivering dose treatment in terms of both accuracy and verification of treatment plans [2].

The verification of treatment plans in Intensity Modulated Radiation Therapy (IMRT) is focused on the linear accelerator and in particular the MultiLeaf Collimator (MLC). It involves evaluating and comparing the parameters of the treatment plans delivered by the linear accelerator with those planned. Complex treatment plans such as those developed in IMRT cannot be controlled by in vivo dosimetry. Verification in IMRT consisted mainly of the use of 2D measurements, but technological

Article 3: Combined analysis of breast morphometry, compression and volumetric breast density: valuable input to improve mammography screening using international bench marking

Iranian Journal of
Medical Physics

Home Browse Journal Info Guide for Authors Submit Manuscript Reviewers Contact Us

Combined analysis of breast morphometry, compression and volumetric breast density: valuable input to improve mammography screening using international bench marking

Document Type : Original Paper

Authors
Youssef Bouzekraoui [1]; sanae Douama [2]; imane Ou-saada [3]; Hilde Bosmans [4]; Lesley cockmartin [5,6]; Mauro campoleoni [7]; FARIDA BENTAYEB [8]

[1] Hassan First University of Settat, High Institute of Health Sciences, Laboratory of Sciences and Health Technologies, Settat, Morocco
[2] Laboratory of high energy physics Modelisation Simulation, Faculty of Sciences, University Mohammed V, Rabat, Morocco
[3] Laboratory of high energy physics Modelisation Simulation, Faculty of Sciences, University Mohammed V, Rabat, Morocco.
[4] KU Leuven, Faculty of Medicine, Department of Imaging and Pathology, Medical Physics and Quality Assessment, Belgium.
[5] Universitair Ziekenhuis Leuven
[6] UZ Leuven · Department of Radiology, Belgium.
[7] association di fisica milan
[8] Departement of Physics, Laboratory of High Energy Physics, Modelling and Simulation, Faculty of Science, Mohammed V Agdal University, Rabat, Kingdom of Morocco

10.22038/IJMP.2022.59988.2008

Abstract

High-quality mammograms are a necessity for the adequate detection of breast cancer. Hence, quality is multifactorial, and includes successively breast positioning, technical image quality and radiological reading. The aim of this study was to select parameters from a combined analysis of breast compression, breast morphometry and volumetric breast density to apply these investigations on a Moroccan population at the start of new breast cancer screening activities.

The study was carried out in a university hospital, a candidate screening center in a newly established screening program in Morocco, provided with new technology equipment, qualified staff and doctors of different specialties. This hospital is frequented by patients from all Moroccan regions and also from some countries in the rest of Africa. There are seven radiologists that four of whom are permanent. Image acquisition was procured on a FFDM Siemens Inspiration system for 250 patients in diagnostic mammography and all patients' information was collected. The data about dose, compression

Article 4: Evaluation of PTV margins in IMRT for head and neck cancer and prostate cancer

Journal of Radiotherapy in Practice

cambridge.org/jrp

Technical Note

Cite this article: Youssoufi MA, Bougtib M, Douama S, Ait Erraisse M, Abboud FZ, Hassouni K, and Bentayeb F. (2020) Evaluation of PTV margins in IMRT for head and neck cancer and prostate cancer. *Journal of Radiotherapy in Practice* page 1 of 6.
doi: 10.1017/S1460396919000931

Received: 12 June 2019
Revised: 21 October 2019
Accepted: 24 November 2019

Key words:
electronic portal imaging device; head and neck; planning target volume; prostate

Author for correspondence:
F. Bentayeb, Department of Physics, Faculty of Sciences, B.P. 1014, 10000 Rabat, Morocco.
Tel: +00212 668460012.
E-mail: bentayebfr@yahoo.fr

Evaluation of PTV margins in IMRT for head and neck cancer and prostate cancer

M. A. Youssoufi[1,2], M. Bougtib[1,2], S. Douama[1], M. Ait Erraisse[2], F. Z. Abboud[2], K. Hassouni[2] and F. Bentayeb[1]

[1]Faculty of Sciences (LPHE, M-S), University Mohammed V, Rabat, Morocco and [2]Department of Radiotherapy, University Hospital Hassan II, Fes, Morocco

Abstract

Purpose: The aim of this study was to evaluate planning target volume (PTV) margins for two different locations using an electronic portal imaging device (EPID) to ensure that the correct radiation dose is delivered to the tumour when using intensity-modulated radiation therapy (IMRT).
Materials and methods: Setup data were collected from 40 patients treated with IMRT for head and neck cancer (HN) (20 patients) and prostate cancer (20 patients). Setup errors from 720 registration images were analysed to evaluate systematic and random errors. Thereafter, optimal PTV margins were calculated based on International Commission on Radiation Units and Measurements 62 (ICRU), Stroom and Parker formulas compared with the Van Herk's recipe.
Results: To calculate the margins around the PTV, several different formulas have been used. Setup margins ranged between 2–4·3, 2·2–4·6 and 2·1–4·7 mm in X, Y and Z directions, respectively, for HN cases. Similarly, for the prostate site, setup margins ranged between 3·7–8·3, 3·2–6·8 and 3·3–8·2 mm in X, Y and Z directions.
Conclusion: To ensure better coverage of target volume, we adopted a PTV margin of 5 mm for HN PTVs and 10 mm for prostate PTVs in our department.

Article 5: Collimator and Energy Window Evaluation in Ga-67 Imaging by Monte Carlo Simulation

Original Article
Mol Imaging Radionucl Ther 2020;29:118-123 DOI:10.4274/mirt.galenos.2020.21549

Collimator and Energy Window Evaluation in Ga-67 Imaging by Monte Carlo Simulation

Ga-67 Görüntülemede Monte Carlo Simulasyonu Kullanılarak Kolimatör ve Enerji Penceresi Değerlendirmesi

Mina Ouahman[1], Rachid Errtfai[1], Hicham Asmi[1], Youssef Bouzekraoui[1], Sanae Douama[1], Farida Bentayeb[1], Faustino Bonutti[2]

[1]Mohammed V-Rabat University Faculty of Science, Laboratory of High Energy Physics Modelisation Simulation, Rabat, Morocco
[2]Academic Hospital of Udine, Clinic of Medical Physics, Udine, Italy

Abstract

Objectives: Gallium-67 (Ga-67) imaging is affected by collimator penetration and scatter components owing to the high-energy (HE) gamma-ray emissions. The characterization of penetration and scatter distribution is essential for the optimization of low-energy high-resolution (LEHR), medium energy (ME), and HE collimators and for the development of an effective correction technique. We compared the image quality that can be achieved by 3 collimators for different energy windows using the SIMIND Monte Carlo code.

Methods: Simulation experiments were conducted for LEHR, ME, and HE collimators for Ga-67 point source placed at 12-cm distance from the detector surface using the Monte Carlo SIMIND simulation code. Their spectra point spread functions as well as the original, penetration, scattering, and X-rays curves were drawn and analyzed. The parameters full-width at half maximum and full-width at tenth maximum were also investigated.

Results: The original, penetration, and scatter curves within 10% for LEHR were 34.46%, 33.52%, 17.29%, and 14.72%, respectively. Similarly, the original, penetration, scatter, and X-rays within 10% for ME and HE were 83.06%, 10.25%, 6.69%, and 0% and 81.44%, 11.51%, 7.05%, and 0%, respectively. The trade-off between spatial resolution and sensitivity was achieved by using the ME collimator at 185 photopeak of Ga-67.

Conclusion: The Monte Carlo simulation outcomes can be applied for optimal collimator designing and for the development of new correction method in Ga-67 imaging.

Keywords: Ga-67 imaging, primary photons (original), penetration, scatter, SIMIND, sensitivity

Article 6 : Energy Window and Collimator Optimization in Lutetium‐177 Single‐photon Emission Computed Tomography Imaging using Monte Carlo Simulation

Original Article

Energy Window and Collimator Optimization in Lutetium-177 Single-photon Emission Computed Tomography Imaging using Monte Carlo Simulation

Abstract

Introduction: In lutetium-177 (Lu-177) single-photon emission computed tomography (SPECT) imaging, the accuracy of activity quantification is degraded by penetrated and scattered photons. We assessed the scattered photon fractions in order to determine the optimal situation and development of correction method. This study proposes to compare the image quality that can be achieved by three collimators. **Materials and Methods:** Siemens Medical System Symbia fitted with high-energy (HE), medium-energy (ME), and low-energy high-resolution collimators was simulated using the SIMIND Monte Carlo code simulation code. Counts were collected in three different main-energy window widths (20%, 15%, and 10%) for Lu-177 point source. Primary and scattered point spread functions and also geometric, penetration, scattering were drawn and analyzed. **Results:** In Lu-177 imaging, a 20% of main-energy window and ME collimator were found to be optimal. HE collimator can be used when the resolution is not required. **Conclusion:** These results provide the optimal energy window and collimator in Lu-177 SPECT imaging and will help the quantification of Lu-177.

Keywords: *Energy window, lutetium-177 imaging, penetration, primary, scatter, SIMIND*

Hicham Asmi, Farida Bentayeb, Youssef Bouzekraoui, Faustino Bonutti[1], Sanae Douama

Department of Physics, LPHE, Modeling and Simulations, Faculty of Science, Mohammed, V University, Rabat, Morocco, [1]Department of Medical Physics, Academic Hospital of Udine, Udine, Italy

Article 7: Detailed CT Dosimetry in 4 Moroccan Hospitals as a Preparation for the Development of National DRLs

Iranian Journal of Medical Physics

Home Browse Journal Info Guide for Authors Submit Manuscript Reviewers Contact Us Login Register

Detailed CT Dosimetry in 4 Moroccan Hospitals as a Preparation for the Development of National DRLs

Document Type : Original Paper

Authors

imane ou-saada [1]; sanae douama [1]; Youssef Bouzekraoui [2]; Hilde Bosmann [3]; Lesley cockmartin [4,5]; Mauro campoleoni [6]; FARIDA BENTAYEB [1]

[1] Laboratory of high energy physics Modelisation Simulation, Faculty of Sciences, University Mohammed V, Rabat, Morocco.
[2] Hassan First University of Settat, High Institute of Health Sciences, Laboratory of Sciences and Health Technologies, Settat, Morocco
[3] KU Leuven, Faculty of Medicine, Department of Imaging and Pathology, Medical Physics and Quality Assessment, Belgium.
[4] Universitair Ziekenhuis Leuven
[5] UZ Leuven - Department of Radiology, Belgium.
[6] Associazione Italiana di Fisica Medica (AIFM), Milan, Italy

10.22038/IJMP.2021.56076.1934

Abstract

Introduction: Diagnostic reference levels (DRLs) can prevent excessive, unnecessary radiation exposure to patients and reduce the dose variation during different practices. This study aims to establish local DRLs for computed tomography (CT) procedures corresponding to Head, Chest, and Abdomen-Pelvis examinations (single acquisition) in Moroccan hospitals.
Material and Methods: A total of 1917 diagnostic CT examinations were included in this study: head, chest, abdomen–pelvis, lumbar, cervical, chest-abdomen–pelvis (CAP), and scanopelvimetry. Firstly, we analyzed the CT dose indicators in terms of the Volume computed tomography dose index (CTDIvol) and the dose length product (DLP) of all the examinations collected. Local diagnostic reference levels were proposed just for the head, thorax, and abdomen-pelvis due to the lack of data for the other examinations. Furthermore, we calculated the effective dose for chest examination using CT-expo software to estimate the effective and organ dose for chest CT.
Results: The estimated local DRLs expressed as the 3rd quartile using $CTDI_{vol}$ were 48 mGy, 14 mGy, and 12 mGy for the head, chest, and abdomen-pelvis, respectively, and 986 mGy.cm, 496 mGy.cm, and 651 mGy.cm for DLP, respectively. Moreover, the proposed average effective dose for chest CT examinations was 6,3 mSv.
Conclusion: This work establishes local DRLs for CTDIvol and total DLP for head, chest, and abdomen-pelvis procedures and proposes effective doses for chest CT examinations in adult patients. The study shows that the results are conforming to the literature.

Volume 19, Issue 4
July and August 2022
Pages 241-249

Files
XML
PDF 1.32 M
History
Share
How to cite
Statistics
Article View: 407
PDF Download: 143

Oral communications:

"Getting started with medical physics in Morocco via the introduction of local dose reference levels and international bench marking" Annual congress of the Belgian hospital physicists association, 26-30 April 2021

"Radiation protection in a hospital setting" Doctoral days CPM-2016, 26,27,28 may 2016, faculty of sciences & scientific institute, Mohammed V university ,Rabat